



If you have discovered material in AURA which is unlawful e.g. breaches copyright, (either yours or that of a third party) or any other law, including but not limited to those relating to patent, trademark, confidentiality, data protection, obscenity, defamation, libel, then please read our [Takedown Policy](#) and [contact the service](#) immediately

To my family.

THE FATIGUE AGEING OF VULCANISED RUBBERS

by

JEFFREY PAUL MOLYNEUX

Submitted for the Degree of

DOCTOR OF PHILOSOPHY

of the University of Aston in Birmingham

July 1981

THE UNIVERSITY OF ASTON IN BIRMINGHAM

THE FATIGUE AGEING OF VULCANISED RUBBERS

JEFFREY PAUL MOLYNEUX

Submitted for the Degree of PhD

July 1981

S U M M A R Y

The cause of the respective rough and smooth fatigue failure surfaces of Neoprene GS : Neoprene W and Neoprene GS : natural rubber vulcanisates is investigated. The contrasting morphology of the vulcanisates is found to be the major factor determining the fatigue behaviour of the blends.

Neoprene GS and Neoprene W appear to form homogeneous blends which exhibit physical properties and fatigue failure surfaces intermediate between those of the two homopolymers.

Neoprene GS and natural rubber exhibit heterogeneity when blended together. The morphology of these blends is found to influence both the fatigue resistance and failure surface of the vulcanisates. Exceptional uncut and cut initiated fatigue lives are observed for blends having an interconnecting network morphology.

The network structure and cross-link density of the elastomers in the blends and the addition of carbon black and antioxidant are all found to influence the fatigue resistance but not the failure mechanism of the vulcanisate.

KEY WORDS

Fatigue
Blends
Network structure
Chlorprene rubber
Natural rubber

ACKNOWLEDGMENTS

I wish to express my thanks to Mr J E Stuckey for his advice and encouragement throughout the project. Also the staff and technicians at the University of Aston and Girling Limited for advice and practical help given.

I also wish to thank my wife Peggy for the support and understanding she has given throughout the writing of this thesis.

Finally, my appreciation goes to Maxine Husbands for the typing and final completion of the thesis.

LIST OF CONTENTS

| | <u>Page</u> |
|------------------|-------------|
| Dedication | i |
| Title Page | ii |
| Summary | iii |
| Acknowledgments | iv |
| List of Contents | v |
| List of Tables | xiii |
| List of Figures | xiv |
| List of Frames | xv |
| | |
| Chapter One | 1 |
| THEORY | |
| 1.1 | 1 |
| 1.2 | 3 |
| 1.2.1 | 3 |
| 1.2.2 | 3 |
| 1.2.3 | 4 |
| 1.2.4 | 5 |
| 1.2.5 | 7 |
| 1.3 | 9 |
| 1.4 | 12 |
| 1.5 | 13 |
| 1.6 | 16 |
| 1.6.1 | 18 |

| | | |
|-------------|---|----|
| 1.6.2 | Effect of Atmosphere on Fatigue | 19 |
| 1.6.3 | Oxygen | 19 |
| 1.6.4 | Ozone | 20 |
| 1.6.5 | Effect of Fillers on Fatigue | 24 |
| 1.6.6 | Effect of Cross-link Type | 24 |
| 1.7 | Effect of Fatigue on Network Structures | 25 |
| 1.8 | Elastomer Blends | 26 |
| 1.8.1 | Blend Morphology | 26 |
| 1.8.2 | Vulcanisation of Elastomer Blends | 29 |
| 1.8.3 | Interpolymer Formation | 30 |
| Chapter Two | EXPERIMENTAL THEORY | 32 |
| 2.1 | Introduction to Network Analysis | 32 |
| 2.2 | Measurement of the Degree of | |
| | Cross-linking | 32 |
| 2.2.1 | Introduction | 32 |
| 2.2.2 | Dry Extension | 33 |
| 2.2.3 | Swollen Compression | 35 |
| 2.2.4 | Equilibrium Volume Swelling | 39 |
| 2.2.5 | Calculation of the Degree of | |
| | Cross-linking | 40 |
| 2.3 | Network Structure Analysis | 42 |
| 2.3.1 | Chemical Probes | 42 |
| 2.3.2 | Methyl Iodide Probe | 43 |
| 2.3.4 | Thiol-amine Probes | 44 |
| 2.4 | Fatigue Testing | 46 |
| 2.4.1 | Introduction | 46 |

| | | |
|---------------|---|----|
| 2.4.2 | De Mattia Flex Tester | 46 |
| 2.4.3 | Flipper or Torrens | 46 |
| 2.4.4 | Du Pont Fatigue Tester | 47 |
| 2.4.5 | The Ross Flex Tester | 47 |
| 2.4.6 | The Monsanto Fatigue to Failure Tester | 48 |
| 2.5 | Phase Contrast Microscopy | 50 |
| 2.6 | The Monsanto Rheometer | 51 |
| Chapter Three | GENERAL EXPERIMENTAL | 53 |
| 3.1 | Fatigue Life Measurements | 53 |
| 3.1.1 | Sample Preparation | 53 |
| 3.1.2 | Operation of the Monsanto Fatigue to Failure Tester | 54 |
| 3.1.3 | Determination of Test Conditions for Fatigue Evaluations | 55 |
| 3.1.4 | Introduction | 55 |
| 3.1.5 | Method | 55 |
| 3.2 | Scanning Electron Microscopy | 57 |
| 3.2.1 | Introduction | 57 |
| 3.2.2 | The Scanning Electron Microscope | 57 |
| 3.2.3 | Preparation of Samples for Scanning Electron Microscopy | 59 |
| 3.3 | Preparation of Microtome Sections for Optical Microscopy | 59 |
| 3.4 | Phase Contrast Microscopy | 61 |
| 3.5 | Measurement of the Degree of Cross-linking | 62 |

| | | |
|--------------|---|----|
| 3.5.1 | Swollen Compression | 62 |
| 3.5.2 | Equilibrium Volume Swelling | 63 |
| 3.5.3 | Time to Equilibrium Swelling | 64 |
| 3.6.1 | Chemical Probes | 65 |
| 3.6.2 | Methyl Iodide | 65 |
| 3.6.3 | Methyl Iodide and Mercuric Iodide at 25°C | 65 |
| 3.6.4 | Methyl Iodide under Vacuum at 80°C | 66 |
| 3.6.5 | Determination of the Reaction Times for Methyl Iodide | 67 |
| 3.6.6 | Method | 67 |
| 3.6.7 | Propan-2-thiol/Piperidine | 68 |
| 3.6.8 | n-Hexan-thiol/Piperidine | 69 |
| 3.6.9 | Determination of Reaction Times for Thiol/Amine Reagents | 69 |
| 3.6.10 | Method | 70 |
| 3.7 | Interpolymer Formation | 70 |
| 3.7.1 | Introduction | 70 |
| 3.7.2 | Method | 71 |
| 3.7.3 | Preparation of Blends | 71 |
| 3.7.4 | Determination of Interpolymer Formation | 73 |
| 3.8 | Differential Scanning Calorimetry (DSC) | 73 |
| Chapter Four | EXPERIMENTAL | 75 |
| 4.1 | Experimental | 75 |
| 4.2.1 | Preparation of Gum Formulations | 75 |

| | | |
|-------|---|----|
| 4.2.2 | Preparation of Black Formulations | 78 |
| 4.2.3 | Curing of Formulations | 78 |
| 4.3 | Determination of Isostress Fatigue Conditions | 79 |
| 4.4 | Tear Strength Measurements | 79 |
| 4.5 | Network Analysis | 80 |
| 4.5.1 | Soxhlet Extractions | 80 |
| 4.5.2 | Calculation of χ | 80 |
| 4.6 | Evaluation of Original GS/W and GS/NR Formulations | 81 |
| 4.6.1 | Preparation of GS/W Formulations | 81 |
| 4.6.2 | Preparation of GS/NR Formulations | 81 |
| 4.6.3 | Testing of Original Formulations | 82 |
| 4.6.4 | Effect of Carbon Black Content on the Fatigue Behaviour of a 75 : 25 GS : W Vulcanisate | 83 |
| 4.7.1 | Effect of Blend Ratio on Fatigue | 83 |
| 4.7.2 | Effect of Morphology on Fatigue of GS/NR Blends | 83 |
| 4.7.3 | Effect of Interpolymer on the Fatigue Behaviour of GS/NR Blends | 84 |
| 4.8.1 | Network Structure Analysis | 85 |
| 4.8.2 | Determination of Cureatives for NR in Original GS/NR Blend | 85 |
| 4.8.3 | Effect of Neoprene GS on Cure of Natural Rubber | 85 |

| | | |
|--------------|--|----|
| 4.8.4 | Level of Sulphur in Neoprene GS and Neoprene W | 86 |
| 4.8.5 | Calculations from Preferential Swelling Measurements | 86 |
| 4.8.6 | Identification of Preferential Swelling Solvents | 88 |
| 4.8.7 | Preferential Swelling Measurements | 89 |
| 4.8.8 | Effect of Cure Time on Network Structure of Neoprene GS | 90 |
| 4.8.9 | Effect of Blending on GS and NR Network Structure | 90 |
| 4.8.10 | Effect of Fatigue on GS and NR Network Structure | 90 |
| 4.9.1 | Effect of Additional Cureatives on Fatigue Behaviour of a 50 : 50 GS : NR Blend | 91 |
| Chapter Five | DISCUSSION OF RESULTS | 93 |
| 5.1 | Effect of Compounding Ingredients on Fatigue Behaviour | 93 |
| 5.1.1 | Effect of Antioxidant Depletion on the Fatigue Behaviour of Filled GS : W and GS : NR Formulations | 93 |
| 5.1.2 | Effect of Black Content on the Fatigue Failure of a 75 : 25 GS : W Formulation | 95 |
| 5.2 | Effect of Elastomer Blend Ratio on Fatigue Behaviour | 97 |

| | | |
|-------|---|-----|
| 5.2.1 | Effect of Neoprene GS : Neoprene W Blend Ratio on Fatigue Behaviour | 97 |
| 5.2.2 | Effect of W : NR Blend Ratio on Fatigue Behaviour | 100 |
| 5.2.3 | Effect of GS : NR Blend Ratio on Fatigue Behaviour | 102 |
| 5.3.1 | Effect of the Morphology of GS : NR Vulcanisates on Fatigue Behaviour | 106 |
| 5.3.2 | Effect of Interpolymer on the Fatigue Behaviour of a 50 : 50 GS : NR Vulcanisate | 111 |
| 5.4.1 | Determination of the Cross-link Density of Natural Rubber and Neoprene GS in a 50 : 50 GS : NR Vulcanisate | 112 |
| 5.4.2 | Effect of Cure Time on the Network Structure of a Neoprene GS Vulcanisate | 115 |
| 5.4.3 | Effect of Blending on the Network Structure of Neoprene GS and Natural Rubber in a 50 : 50 GS : NR Vulcanisate | 117 |
| 5.4.4 | Effect of Fatigue on the Network Structure of Neoprene GS and Natural Rubber Vulcanisates | 119 |
| 5.5 | Effect of Additional Curatives on the Fatigue Behaviour of a 50 : 50 GS : NR Vulcanisate | 121 |

| | | |
|----------------|---|-----|
| 5.5.1 | Effect of Increasing Additions of Sulphur on the Fatigue Behaviour of a 50 : 50 GS : NR Vulcanisate | 121 |
| 5.5.2 | Effect of the Addition of CBS on the Fatigue Behaviour of a 50 : 50 GS : NR Vulcanisate | 122 |
| 5.5.3 | Effect of the Addition of TMTD on the Fatigue Behaviour of a 50 : 50 GS : NR Vulcanisate | 123 |
| Chapter Six | CONCLUSIONS AND SUGGESTIONS FOR FURTHER WORK | 125 |
| 6.1 | Summary | 125 |
| 6.2 | Conclusions | 126 |
| 6.3 | Suggestions for Future Work | 130 |
| Appendix One | Tables | 132 |
| Appendix Two | Figures | 184 |
| Appendix Three | Frames | 220 |
| References | | 226 |

LIST OF TABLES

| <u>Table</u> | <u>Page</u> | <u>Table</u> | <u>Page</u> |
|--------------|-------------|--------------|-------------|
| 1.1 | 133 | 4.11 | 159 |
| 3.1 | 134 | 4.12 | 160 |
| 3.2 | 134 | 4.13 | 161 |
| 3.3 | 136 | 4.14 | 162 |
| 3.4 | 137 | 4.15 | 163 |
| 3.5 | 138 | 4.16 | 164 |
| 3.6 | 139 | 4.17 | 165 |
| 3.7 | 140 | 4.18 | 166 |
| 3.8 | 141 | 4.19 | 167 |
| 3.9 | 142 | 4.20 | 169 |
| 3.10 | 143 | 4.21 | 170 |
| 3.11 | 144 | 4.22 | 171 |
| 3.12 | 145 | 4.23 | 172 |
| 3.13 | 146 | 4.24 | 173 |
| 3.14 | 147 | 4.25 | 174 |
| 3.15 | 148 | 4.26 | 175 |
| 4.1 | 149 | 4.27 | 176 |
| 4.2 | 150 | 4.28 | 177 |
| 4.3 | 151 | 4.29 | 178 |
| 4.4 | 152 | 4.30 | 179 |
| 4.5 | 153 | 4.31 | 180 |
| 4.6 | 154 | 5.1 | 181 |
| 4.7 | 155 | 5.2 | 181 |
| 4.8 | 156 | 5.3 | 182 |
| 4.9 | 157 | 5.4 | 183 |
| 4.10 | 158 | | |

LIST OF FIGURES

| <u>Figure</u> | <u>Page</u> | <u>Figure</u> | <u>Page</u> |
|---------------|-------------|---------------|-------------|
| 1.1 | 185 | 4.5 | 203 |
| 1.2 | 186 | 4.6 | 204 |
| 2.1 | 187 | 4.7 | 205 |
| 2.2 | 188 | 4.8 | 206 |
| 3.1 | 189 | 4.9 | 207 |
| 3.2 | 190 | 4.10 | 208 |
| 3.3 | 191 | 4.11 | 209 |
| 3.4 | 192 | 4.12 | 210 |
| 3.5 | 193 | 4.13 | 211 |
| 3.6 | 194 | 4.14 | 212 |
| 3.7 | 195 | 4.15 | 213 |
| 3.8 | 196 | 4.16 | 214 |
| 3.9 | 197 | 4.17 | 215 |
| 3.10 | 198 | 4.18 | 216 |
| 4.1 | 199 | 4.19 | 217 |
| 4.2 | 200 | 4.20 | 218 |
| 4.3 | 201 | 4.21 | 219 |
| 4.4 | 202 | | |

LIST OF FRAMES

| <u>Frame</u> | <u>Page</u> | <u>Frame</u> | <u>Page</u> |
|--------------|-------------|--------------|-------------|
| 5.1 | 221 | 5.8 | 223 |
| 5.2 | 221 | 5.9 | 223 |
| 5.3 | 222 | 5.10 | 224 |
| 5.4 | 222 | 5.11 | 224 |
| 5.5 | 222 | 5.12 | 225 |
| 5.6 | 222 | 5.13 | 225 |
| 5.7 | 223 | 5.14 | 225 |

CHAPTER ONE

THEORY

1.1 Introduction

Rubber brake hoses are used in cars to provide a flexible link between the rigid metal braking system attached to the car body and the brake assembly on the wheel of the car. They must, of necessity, be flexible so as to permit movement of the wheel relative to the chassis of the car. Since they are located on the underside of the vehicle, they are subjected to extremes in weathering conditions as well as continual cyclic deformations when the car is in motion. The outer protective cover must be highly resistant to the wide range of environments encountered and to fatigue failure under these conditions.

Polychloroprene rubbers (CR), because of their high resistance to weathering, appeared to be ideally suited for this application and had been extensively used by a specific company for many years in a blend with natural rubber. During this period, the formulation gave no serious failures and provided an adequate service life.

In 1972, however, the existing formulation was 'phased out' in favour of a new all chloroprene rubber hose cover formulation. The new formulation gave exceptional fatigue resistance on both

test rigs and during proof testing. It was also chosen for its ability to accept printing and for easier processing and handling. After minor alterations to antiozonant, hardness and plasticiser type, this new formulation was accepted and production of the earlier formulation was terminated.

After six to eight months, however, catastrophic failure of brake hose assemblies began to occur and immediate remedial action had to be taken. It was found that despite the good fatigue resistance of undamaged hose, a small cut in the sample lead to rapid failure characterised by the propagation of a single large crack. Fatigue failures of the chloroprene rubber/natural rubber formulation previously used took place much more slowly and was accompanied by a gradual and progressive increase in the number of surface crazes.

This research project was one of the investigations resulting from this situation; the objective being to optimise the fatigue resistance of both the chloroprene rubber and the chloroprene rubber/natural rubber blends. This included changes in formulation, vulcanisation and processing procedures with particular emphasis on gum stocks of the two blends. Attempts were made to relate the changes in fatigue behaviour with differences in the network structure and morphology of the vulcanisates.

1.2 Commercial Polychloroprenes

1.2.1 Introduction

Commercial polychloroprenes were introduced in 1934⁽¹⁻⁹⁾ and there are now twenty seven variations of solid polychloroprene polymers offered by the seven Western and Japanese suppliers under one hundred and eleven trade names or codes⁽¹⁰⁾.

Constant adaptation and modification of the base polymer and the ability to compound for specific durability properties⁽¹¹⁻¹⁴⁾ has encouraged its acceptance throughout the world.

1.2.2 Polymerisation of Chloroprene

The majority of commercial Neoprene polymers are prepared by the free radical emulsion polymerisation of chloroprene. Monomer droplets are dispersed in an aqueous phase using surfactants⁽¹⁵⁻¹⁹⁾ and polymerisation is generally carried out at a temperature of twenty to fifty degrees centigrade using a free radical polymerisation initiator⁽²⁰⁻²⁴⁾. Once the desired conversion is achieved, polymerisation is stopped by destroying the free radicals using short stopping or stabilising agents such as thiuram disulphide or phenolic antioxidants⁽²⁵⁻²⁸⁾. After removing unreacted monomer, the polymer is isolated by destabilising the colloidal mixture, separating the aqueous phase and freeze drying the polymer.

Chloroprene has a very high rate of polymerisation⁽²⁹⁻³¹⁾ and early attempts to prepare chloroprene rubber gave rise to a gelled, unprocessable polymer at conversions as low as thirty percent^(32,33). The techniques by which this problem was overcome led to the development of two general grades of polychloroprene rubber, namely:

- (i) sulphur modified polychloroprene (designated to the 'G' types), and
- (ii) mercaptan modified polychloroprenes (designated to the 'W' types).

1.2.3 Sulphur Modified Polychloroprenes

Sulphur modified polychloroprenes were the first chloroprene rubbers to be introduced commercially⁽⁶⁾. The polymerisation of chloroprene in the presence of sulphur produced a polymer containing di- or polysulphide segments in the main chain^(34,35). Post polymerisation reactions with thiuram disulphide or other thiophilic reagents were then used to cleave these groups. In this way, sufficient control of the molecular weight and molecular weight distribution was achieved to obtain a processable material.

The G type polychloroprenes have a molecular weight distribution ranging from 20,000 to 950,000, the greatest frequency occurring around 100,000⁽³⁶⁾. Because of the weaker

sulphur bonds in the main chain, they breakdown easily on milling. The masticated rubber is, therefore, tacky and has a low nerve and knits together well during moulding.

The high sulphur levels in the G types enables them to be cured rapidly without acceleration using metal oxides and vulcanisates of the sulphur modified grades exhibit good fatigue resistance and tear strength as a result of these labile polysulphide cross-links⁽³⁷⁾. Similarly, they have a slightly higher elongation and resilience than the W types and display better compatibility with natural rubber (NR) and styrene-butadiene rubber (SBR) substrates.

1.2.4 Mercaptan Modified Polychloroprenes

A wide variety of modifiers have been tested to control the molecular weight of polychloroprene during polymerisation^(20,38-40). Of these, the alkyl mercaptans have been the most successful⁽²⁰⁾. These materials prevent large scale combination of growing polymer chains during polymerisation by the chain transfer mechanism:



where P = polymer; M = monomer.

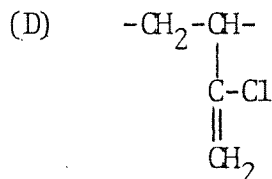
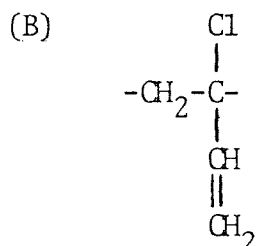
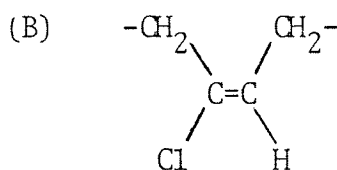
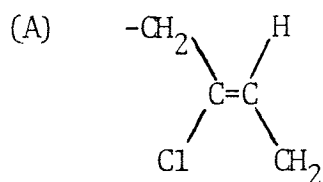
The use of alkyl mercaptans, therefore, enabled polymerisation of chloroprene to proceed to approximately sixty five percent conversion⁽⁴¹⁾ before branched or cross-linked structures were observed. The polymer obtained at this level of conversion contains only one or two sulphur atoms per polymer chain⁽³²⁾ and exhibits significantly different physical properties to the sulphur modified polychloroprenes.

The W types have a fairly narrow molecular weight distribution with the greatest frequency occurring between 180,000 and 200,000⁽⁴²⁾. As a result of having a low sulphur content in the main chain, they breakdown less in milling than the G types and are generally easier to process. Their low sulphur content also confers greater raw polymer stability than the G types, thus permitting longer storage times.

The lower sulphur content of the W types means they have acceptable curing characteristics and vulcanisate properties only if accelerators are used⁽⁵⁷⁾. The less labile ether cross-links and more stable polymer network of the W type vulcanisates, however, give superior compression set, heat resistance and tensile strength than the G types. Their narrower molecular weight distribution also reduces the level of crystallinity in the base polymer⁽⁴²⁾ and enables vulcanisates of lower hardness and modulus (for the same loading) and slightly higher electrical resistivity to be obtained.

1.2.5 Stereochemistry and Microstructure of Polychloroprene

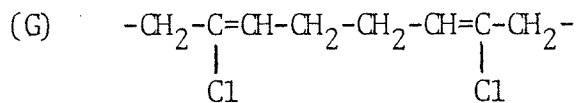
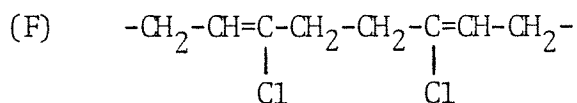
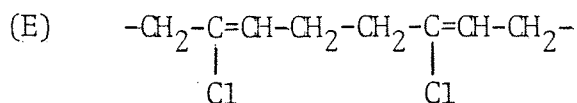
Maynard and Mochel⁽⁴³⁻⁴⁵⁾ established the basic aspects of the microstructure of polychloroprenes from analysis of their crystallisation behaviour and infra-red absorption spectra. They showed that it consisted primarily of linear sequences of (A) trans-2-chloro-2-butylene units and small portions of (B) cis-1,4-polymerisation, (C) 1,2-polymerisation and (D) 3,4-polymerisation.



Increasing polymerisation temperatures produce increasing amounts of (B), (C) and (D) linearly from a total of 5% at -40°C to approximately 30% at 100°C . The effect of these structural variations on the physical and chemical properties has also been determined⁽⁴³⁻⁴⁵⁾.

Other sequence isomers derived from head to tail (E), head to head (F) and tail to tail (G), 1,4-monomer additions have been identified by application of high resolution NMR

spectroscopy⁽⁴⁶⁾. Structures (F) and (G) account for 10-15% of the sequence distribution, regardless of the cis-trans isomer proportions.



The stereochemistry of polychloroprene has been further characterised by the unique synthesis of cis-1,4-polychloroprene⁽⁴⁷⁾ and by the preparation of a stereoregular trans-1,4-polychloroprene⁽⁴⁸⁾. The former was prepared by bulk polymerisation of 2-(tributyltin)-1,3-butadiene, followed by chlorinolysis of the resulting polymer to give essentially cis-1,4-polychloroprene. The all-trans polymer was prepared by radiation polymerisation of large crystals of chloroprene which had been formed by cooling to -130°C to -180°C .

The structures and properties of the above polymers are summarised in Table 1.1.

The crystallinity, rate of crystallisation and melt transition temperatures have been shown to be inverse functions of

polymerisation temperature (43,45). This is due to the increased introduction of structural irregularities as the polymerisation temperature rises.

The spherulitic structures which form in polychloroprene fibres lead to a considerable strengthening of the elastomer⁽⁴⁹⁾ but the degree of crystallisation has been shown to decrease on polymer ageing⁽⁵⁰⁾.

Although the kinetics of crystallisation^(51,52) and the critical size of the crystallisation nuclei are known⁽⁵³⁾ the crystal morphology of polychloroprene has not yet been completely identified^(54,55).

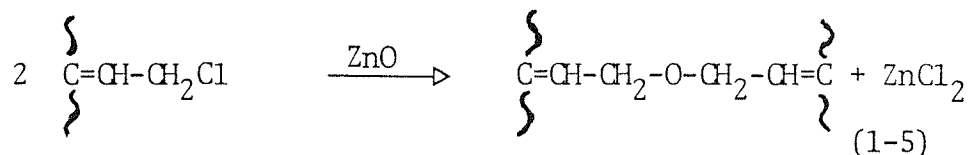
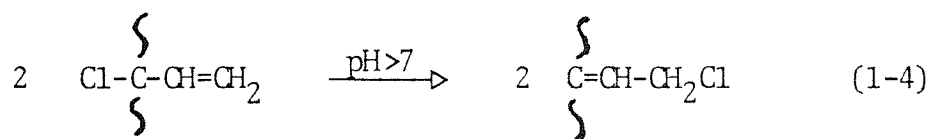
1.3 Vulcanisation of Polychloroprene

The vulcanisation of polychloroprene differs from that of other diene polymers. The allylic bonds of the chloroprene units are deactivated by the electronegative chlorine atom so that reactivity towards sulphur moieties is limited.

The tertiary allylic chloride structure produced by 1,2 addition polymerisation is the major cross-linking site. The average allylic chloride content of mercaptan modified polychloroprene is about 1.5% of the total chloride present. This corresponds to one active cure site for every 67 monomer units.

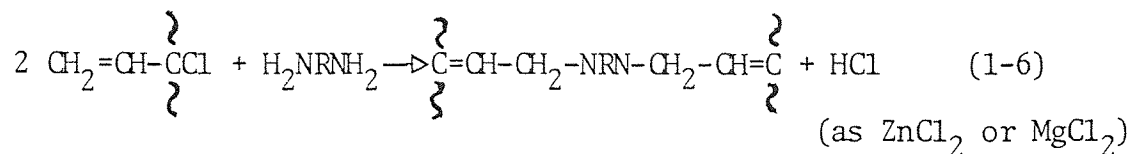
For practical vulcanisates, metal oxides must be used as part of the curing system. Combinations of zinc oxide and magnesia are most generally used. The effect of zinc oxide alone is to produce scorchy flat curing stock with low levels of cross-linking. Magnesia used alone retards the rate of cure but if sufficient time is allowed, a high state of cure is achieved.

It has been suggested that metal oxides can generate an ether cross-link between two allylic sites^(11,12) (eqn 1-4).



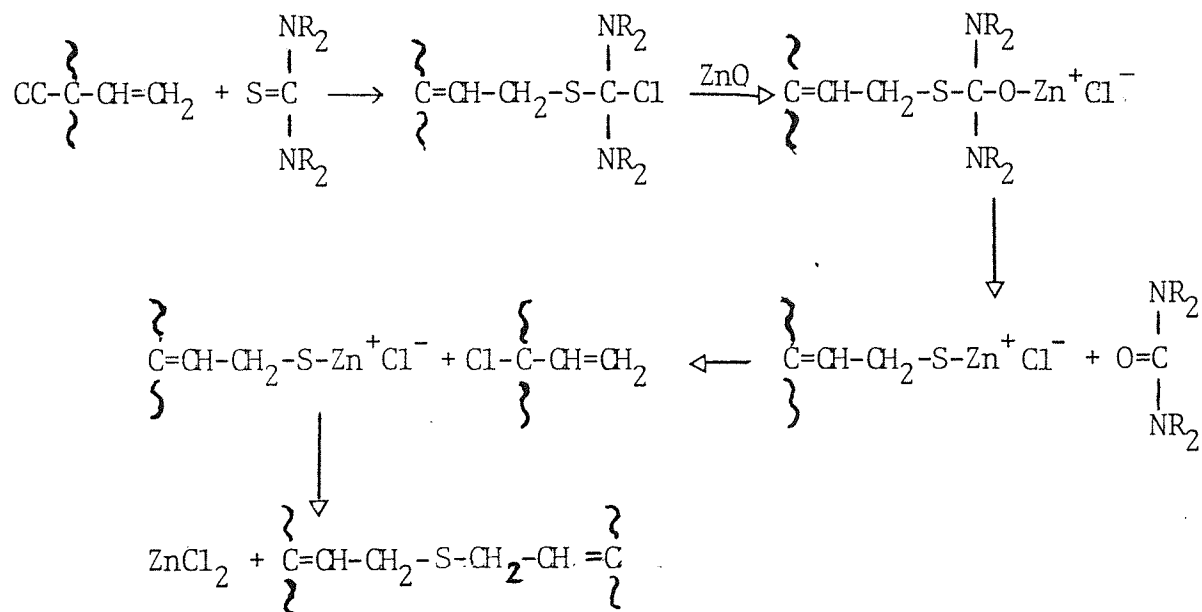
The reality of this mechanism has never been established but regardless of the cross-linking role of metal oxides, their presence is essential for control of the vulcanisation process and good ageing of the vulcanisate.

Organic accelerators used in curing polychloroprene are believed to operate by either of two mechanisms. Difunctional cross-linking agents, such as diamines and bis-phenols, can be bis-alkylated by active chlorine units in the polymer, probably by 1,3-allylic shifts, to yield stable cross-links⁽⁵⁶⁾.



The zinc chloride formed is a strong Lewis acid and can serve to accelerate the alkylation reaction. The fact that difunctional curing agents do not cross-link polychloroprene which has been previously treated with piperidine or aniline to remove allylic chlorine, supports this mechanism.

In the mechanism proposed to explain the vulcanisation of polychloroprene with substituted thioureas⁽⁵⁷⁾ (eg ethylene thiourea), the tertiary allylic chlorines participate via an isothiuronium intermediate.



The vulcanisation of chloroprene polymers containing sulphur involves rearrangement of backbone polysulphide segments as well as the above reactions of allylic chlorine structures⁽³⁷⁾.

Free radical sulphur moieties such as $RS\cdot$ and $\cdot SS\cdot$ are believed to arise from interaction of the polysulphide segments and the thiuram disulphide present in the polymer. These radicals then react with each other or with the polymer backbone to yield sulphidic cross-links.

1.4 Accelerated Sulphur Vulcanisation of Natural Rubber

Elucidation of the reactions of model compounds of natural rubber with elemental sulphur, accelerating agents and other curing agents have provided a detailed knowledge of the chemistry^(58,59) and kinetics^(60,61) of vulcanisation and of the final vulcanisate structure^(53,59).

Elemental sulphur, in the form of S_8 rings, undergoes a series of reactions with accelerators and activators to yield an active sulphurating agent. This then reacts with the rubber hydrocarbon to produce a rubber bound intermediate compound which is the immediate precursor to cross-link formation. Initial polysulphide cross-links are formed either by reactions between two rubber bound intermediates or by reaction of the intermediate with the rubber hydrocarbon. Maturing reactions then take place (Fig 1.1) to yield the final vulcanisate structure (Fig 1.2).

Cross-links are mono-, di- or polysulphidic in character (Fig 1.2, (a), (b) and (c)). The sulphur generally being attached at an allylic carbon atom. Sulphur is also combined in the

vulcanisate as cyclic monosulphide (d) and disulphide (e) groups and pendant sulphide groups terminated by accelerator fragments (f). The polymer chain may be chemically modified by the introduction of conjugated diene (g) and triene (h) unsaturation. Main chain scission (i) may take place during the vulcanisation reaction.

1.5 Fracture Mechanics

Cracks grow when the release of stored mechanical energy caused by an increase in cut length equals or exceeds the surface energy required for such an increase^(62,63). The energy available per unit area of growth is termed the tearing energy, T , and is defined by⁽⁶⁴⁾:

$$T = -\partial U / \partial A \quad (1-7)$$

where: U is the total elastic strain energy stored in the sample, and

A the undeformed area of one fracture surface of the crack.

Tearing energy may be calculated for various simply shaped test pieces⁽⁶⁴⁻⁶⁶⁾. However, when expressed in terms of T , tear or crack growth results are essentially independent of the shape of the test piece used^(62-64,66) indicating the rate-tearing energy relation to be a characteristic of the vulcanisate.

For repeated cycling through zero strain, the crack growth per cycle may be represented by:

$$dc/dn = f(T) \quad (1-8)$$

where: c is the crack length (in the unstrained state)

n the number of cycles and

T the maximum tearing energy attained during the cycle

The number of cycles required for a crack to grow from a length C_1 to C_2 would then be given by:

$$n \int_{C_1}^{C_2} dc / f(T) \quad (1-9)$$

which can be evaluated provided the reaction between T and C , which depends on the sample shape⁽⁶³⁻⁶⁵⁾ and type of deformation is known.

A test strip having an edge cut of length C , which is under simple extension, has a tearing energy given by⁽⁶⁴⁾:

$$T = 2 KWc \quad (1-10)$$

where: W is the strain energy density in the bulk of the material and

K is a slowly varying function of strain⁽⁶⁷⁾

Since T increases with C , rupture of a sample will normally occur when the tear strength T_c is attained. Hence from equations (1-9) and (1-10) the number of cycles to failure, or fatigue life, N , is given by:

$$N = \int_{T_i}^{T_c} dT / 2 K W_f(T) \quad (1-11)$$

where: T_i is the tearing energy at the start of the test,

$$\text{ie: } T_i = 2 K W c_i \quad (1-12)$$

where: c_i is the initial cut length

The predictions of equation (1-11) have been verified using test pieces containing inserted cuts of various lengths and the approach can be extended to uncut samples if it is assumed that natural flaws of a particular size are present initially^(62,63,68,69).

Taking power law approximations of the form,

$$\frac{dc}{dn} = \frac{1}{G} T^\beta \quad (1-13)$$

where: G is the cut growth constant and

β is a material constant

Lake and Lindley⁽⁶³⁾ and Gent et al⁽⁶²⁾ have shown by using

equations (1-10) and (1-13) and integrating for $C \gg C_0$ that

$$N = \left(\frac{G}{(\beta-1) C_0 (\beta-1)} \right) (2 \text{ KW})^{-\beta} \quad (1-14)$$

where: C_0 is the 'effective' size (equivalent cut length) of the naturally occurring flaws

By plotting fatigue results as a function of 2 KW , then β may be found from the slope and gradients of -2 and -4 for natural rubber⁽⁶²⁾ and SBR⁽⁶³⁾ respectively have been obtained. The flaw size, C_0 , required to give the best quantitative correlation is $2.5 \times 10^{-3} \text{ cm}$ ⁽⁶²⁾ for natural rubber and about $5 \times 10^{-3} \text{ cm}$ for SBR⁽⁶³⁾. Observable flaws of this magnitude are present in rubber due to moulding or die stamping imperfections, particulate impurities or other inhomogeneities.

The above approach may be extended to fatigue life at lower deformations⁽⁷⁰⁾ where different forms of crack growth characteristics apply^(68,71) and has been explained in terms of the effect of hysteresis on the stress concentration at a crack tip⁽⁷²⁾.

1.6 Factors Affecting Crack Growth and Fatigue

It has been reported that a finite tearing energy, T_0 , is required for the initiation of mechanical growth⁽⁶⁸⁾. This is

of the order of 5×10^4 erg/cm² for a range of elastomers⁽⁷³⁾, under relaxing conditions, including natural rubber, SBR and polychloroprene, which have widely differing strength properties. When T_0 is exceeded, the cut growth behaviour appears to be controlled by the mechanical hysteresis of the rubber at high strains⁽⁷²⁾. Crystallising rubbers, such as natural rubber, exhibit quite pronounced high strain hysteresis owing to strain induced crystallisation⁽⁷⁴⁾ which confers great resistance to crack growth. Amorphous rubbers display hysteresis resulting from viscoelastic behaviour⁽⁷⁵⁻⁷⁷⁾ and, although this is generally of a lower order than that arising from crystallisation, the extent of the hysteresis again markedly influences resistance to crack growth and fatigue.

For non-crystallising rubbers at large deformations, ^{fatigue}behaviour shows dependence on rate and temperature of test which can be directly correlated with the change of viscoelastic properties on these variables^(75,76,78-80). The effect of strain diminishes at low severities and a point is reached at which the fatigue life becomes very long for all rubbers⁽⁷³⁾. This strain limit, e_0 , which corresponds to T_0 is, therefore, not much influenced by hysteresis or the detailed composition of the rubber. The similarity of T_0 values for different elastomers prompted an attempted explanation of the occurrence of T_0 in relation to the carbon-carbon bond strength of the elastomers⁽⁷²⁾ and fairly good agreement with experimental results has been obtained.

1.6.1 Non-Relaxing Conditions

If complete relaxation of a sample through zero strain does not occur on each cycle then the crack growth and fatigue resistance of crystallising rubbers can be considerably increased^(68,81,82). This effect is due to an increase in the T_0 value and a subsequent reduction of cut growth rate⁽⁶⁸⁾. The effects of non-relaxing conditions on non-crystallising rubbers are far less pronounced because of their time-dependent cut growth characteristics⁽⁶³⁾.

The susceptibility to crack growth and fatigue indicates a qualitative difference between the behaviour of amorphous and crystallising rubbers; the former show both time dependent and cyclic growth according to frequency⁽⁶³⁾, whilst the latter undergoes only cyclic growth when not in the critical tearing energy region⁽⁷⁴⁾. Another disadvantage of non-crystallising rubbers is that the modulus : strain ratio tends to remain relatively constant, irrespective of the magnitude of the deformation so that high strength is obtained at the expense of low resilience. For moderate deformations in a crystallising rubber, however, high hysterisial behaviour occurs only in the highly strained areas around flaws^(74,83) which is ideal from both strength and resilience view points.

1.6.2 Effect of Atmosphere on Fatigue

1.6.3 Oxygen

Atmospheric oxygen is known to play a major role in the fatigue failure of rubber^(62,63,34-39). The process is distinct from oxidative ageing in that it can and normally does occur in the absence of detectable changes in bulk properties⁽⁸⁹⁾. Large increases in cut growth rate occur over a very narrow range of tearing energy immediately above a critical value T_0 . As the tearing energy exceeds T_0 , the cut growth per cycle rapidly reaches a value of a few nanometers (which indicates rupture of one or more chains during each cycle) for a wide range of vulcanisates⁽⁷³⁾.

The fatigue life of unprotected NR and SBR vulcanisates has been observed to increase by about an order of magnitude if tests are carried out in vacuo⁽⁸⁴⁾ or nitrogen⁽⁸⁵⁾ instead of air. This is due to a reduction in the rate of crack growth. The threshold tearing energy (T_0) required for the initiation of mechanical growth is lower in the presence of oxygen⁽⁸⁴⁾ and appears to decrease with increasing oxygen concentration^(85,88). This growth may, therefore, be termed mechanico-oxidative in nature.

The mechanism of this oxidative effect remains obscure. However, it has been suggested that the very high mechanical energy in the rubber at the tip of a crack acts similarly to high thermal

energy and accelerates the rate of oxidative scission⁽⁸⁹⁾. In support of this hypothesis, oxidative scission has been shown to be 'time at strain dependent'; the rate of reaction being substantially affected by the mechanical energy present in the rubber⁽⁸⁹⁾.

The fatigue limit below which no mechanico-oxidative growth takes place is determined by a critical strain energy rather than by a critical strain⁽⁹⁰⁾. For example, a gum vulcanisate may have a critical strain of say 75% whilst a vulcanisate of higher modulus containing filler may have a fatigue limit of only 25%.

1.6.4 Ozone

The attack of ozone on rubber differs from that of oxygen in that it has a very low energy requirement⁽⁹¹⁾. Ozone cracking may, therefore, occur at much lower stresses than those required to produce mechanico-oxidative growth.

Under static loading conditions, no growth occurs unless the energy available for crack propagation exceeds T_z , the critical energy for ozone crack growth⁽⁹⁰⁾. This small but finite energy (equivalent to $\sim 5\%$ strain in unprotected NR vulcanisates) is much less than that required for physical tearing and probably represents the strength of the ozone degraded rubber⁽⁹⁰⁾. Above T_z , for rubbers well above their glass transition temperature, the rate of crack growth is essentially proportional to the ozone

concentration and independent of the tearing energy⁽⁹¹⁻⁹³⁾. The rate of crack growth is most rapid immediately above the critical strain (e_z) required for cracking to occur and progressively decreases at higher strains.

The critical strain, e_z , represents the point at which the stress at the largest naturally occurring flaws^(62,63) is sufficient to rupture ozone degraded rubber. The largest flaws are fairly sparsely distributed so that, when e_z is just exceeded, the number of cracks which grow is small. However, there are many more smaller flaws in the rubber and as the strain is increased above e_z , the tearing energy at more and more of the smaller flaws will exceed T_z and the crack density will increase⁽⁸⁹⁾.

Static pre-exposure to ozone at strains above e_z have a significant effect on subsequent dynamic properties; pre-exposure to ozone at strains slightly above e_z result in poor fatigue life whilst pre-exposure to ozone at high strains results in vulcanisates having high fatigue lives⁽⁹⁰⁾.

The effect of ozone attack on crack growth under dynamic conditions depends on the tearing energy and hence on the deformations involved. Below the fatigue limit (T_0) no physical tearing occurs and ozone is the only cause of crack growth⁽⁹⁰⁾. In this region, cyclic deformation decreases the value of T_z calculated for static exposure to ozone⁽⁹⁴⁾. The rate of crack growth and hence fatigue life is also dependent

on the ozone concentration⁽⁹⁰⁾. However, as T_0 is exceeded, the dependence on ozone concentration rapidly diminishes⁽⁹⁰⁾.

For fairly rapid continuous cycling, the effect of ozone on fatigue life may be calculated by assuming that cracks will grow at the single crack rate all the time the rubber is stretched and that the ozone contribution is essentially additive to the mechanico-oxidative growth^(68,69).

In practice, many articles are subjected to intermittent cycling with periods of constant deformation in between. Ozone cracking during the latter period can of course contribute to subsequent fatigue failure⁽⁹⁰⁾. The mechanics of multiple cracking in surfaces under constant load is more complex than single crack growth and appears to be governed by a boundary layer diffusion control mechanism⁽⁹⁵⁾.

The addition of antiozonants can reduce the effects of atmosphere under both static or dynamic conditions⁽¹⁹⁷⁻²⁰¹⁾. Typically, N,N'-paraphenylene diamine derivatives or 6-alkoxy-2,2,4-trimethyl dihydroquinolines are used which decrease the rate of crack propagation and increase the tearing energy⁽⁷³⁾ of rubbers.

For static applications under constant deformation, the addition of a suitable antiozonant in combination with wax can completely prevent ozone cracking⁽⁸⁹⁾ by forming an ozone resistant film on the surface of the article. The efficiency of antiozonants

in preventing cracking appears to be determined by the ease with which they form a surface film^(58,96,97); the rate at which antiozonant reacting with ozone at the surface is replenished by material in the main body of the rubber⁽⁹⁷⁾; and their chemical make up.

Under dynamic conditions, wax gives no protection and may accelerate failure by concentrating ozone attack at flaws in the surface film created by flexing⁽⁸⁹⁾. Efficient antiozonants, however, may reduce the rate of ozone crack growth about three-fold giving a corresponding increase in fatigue life⁽⁹⁸⁾.

Improvements in fatigue life are also obtained through the addition of antioxidants which appear to reduce mechanico-oxidative growth⁽⁹⁹⁾. Bulk deterioration of physical properties through atmospheric oxidation also decreases the fatigue life of rubbers^(96,100). The increases in modulus as a result of ageing increase the tearing forces acting at the tip of a crack⁽¹⁰⁰⁾, thus accelerating failure.

Depletion of antiozonants may occur by oxidation^(96,99,100) or more commonly as a result of leaching by water^(100,101) or chemical solutions⁽¹⁰²⁾. It is important, therefore, that antiozonants and antioxidants be tested for specific applications.

1.6.5 Effect of Fillers on Fatigue

Fillers are generally classified into two groups: reinforcing and non-reinforcing. The reduction in fatigue limit (e_0) caused by fillers is due mainly to the increased modulus of the rubber. The tearing energy, however, remains similar to that of the gum base for a wide range of fillers⁽⁷³⁾. Consequently, while e_0 is reduced, the stress corresponding to it is increased by incorporation of a filler, the effect being most marked for reinforcing fillers. Although reinforcing fillers generally improve cut growth resistance^(62,68,69,73) they also increase the naturally occurring flaw size⁽⁷³⁾ so that a non-reinforcing filler (eg lamp black) gives superior fatigue properties^(73,103). It appears that better fatigue properties in a filled vulcanisate are obtained by using a stiff gum base with a minimum of filler, rather than a soft gum base with a larger amount of filler.

1.6.6 Effect of Cross-link Type

Fatigue resistance is known to be dependent on network structure⁽¹⁰⁴⁾. Higher T_0 values and correspondingly higher crack growth resistance are obtained with polysulphide cross-links^(72,91). Fatigue behaviour may, therefore, be improved by use of a poly- rather than monosulphidic or carbon-carbon cross-linked network⁽¹⁰⁵⁻¹⁰⁸⁾. This superiority appears to be limited to initial fatigue resistance however⁽¹⁰⁹⁾. Indeed, on ageing, a monosulphide network with poor initial fatigue resistance may become the

superior vulcanisate⁽¹⁰⁹⁾.

The degree of main chain modification associated with a polysulphidic network has a large effect on fatigue behaviour⁽¹¹⁰⁾. Appreciable modification is conducive to good fatigue resistance, even a monosulphidic network with extensive modification exhibits good fatigue resistance⁽¹¹⁰⁾. However, increasing the degree of modification reduces fatigue resistance on ageing⁽¹⁰⁹⁾. Lal⁽¹¹¹⁾ states that polysulphidic cross-links are not essential for good fatigue resistance and that the properties can be attributed to other factors, including the distribution of network chains.

1.7 Effect of Fatigue on Network Structures

Maturation reactions are known to occur within a vulcanisate both during vulcanisation and service^(58,59). However, uncertainty exists as to the effects of fatigue on the maturation process.

The work of Russell and Cunneen^(112,113) provides an indication of the chemical changes occurring during a service application. Structural differences were observed in the tread vulcanisate of new rig tested and service conditioned tyres. Near the breaker edge there was found to be a decrease in polysulphidic cross-link concentration, an increase in monosulphidic cross-link concentration and an increase in the sulphur bound to the rubber as main chain modifications. They attributed their findings

to anaerobic reactions induced by heat build up. The strength properties of vulcanisates are known to depend on cross-link type^(58,114-116) and the reduction in fatigue resistance through formation of monosulphidic cross-links was concluded to be the cause of tread lift and blow out.

Gregory, Rigby and Stuckey⁽¹¹⁷⁾ have shown that the deterioration of properties associated with the maturation reactions outlined above can occur in both gum and carbon black stocks by fatigue alone, without the influence of heat.

Dogadkin et al⁽¹¹⁶⁾ found a slight increase in polysulphidic cross-links with solvent extracted SBR vulcanisates flexed at non-elevated temperatures. Similarly, Cox and Parks⁽¹⁰⁵⁾ using sulphur accelerated black filled natural rubber stocks observed an increase in polysulphidic linkages.

As may be seen, there is far from complete agreement as to the precise effect of fatigue on network structures.

1.8 Elastomer Blends

1.8.1 Blend Morphology

Microheterogeneity in elastomer blends was originally studied by Walters⁽¹¹⁸⁾. For two component blends of several rubbers, no mixing on a molecular scale was observed which agrees well with

theory regarding molecular compatibility of high polymers⁽¹¹⁹⁻¹²²⁾. Generally disperse zones were observed although in certain cases interlocking networks were detected.

The change from disperse phases to interlocking networks in the region of 50/50 blend ratio (which precedes phase inversion) has been confirmed by Callan⁽¹²³⁾, Hess⁽¹²⁴⁾ and Powell⁽¹²⁵⁾ for a number of two-component blends. Marsh⁽¹²⁶⁾, however, has noted the absence of interpenetrating phases in many 50/50 blends, one component, preferring to adopt a discontinuous form. This was believed to be related to differences in milling behaviour of the elastomers, the lower viscosity component forming the continuous phase. A chloroprene rubber (CR), natural rubber (NR) blend was particularly unusual in that NR remained the continuous phase even when constituting only 25 weight percent of the blend.

The fineness of dispersion in elastomer blends appears to be controlled by differences in polymer viscosities and the amount of mixing involved^(118,123,126). At equal mixing times, Powell has shown that zone size decreases as the mill roll separation (nip) decreases to a limiting zone size of about $0.5\mu\text{m}$. Rehner⁽¹²⁷⁾ has reasoned that the physical processes involved in mill mixing prevent breakdown of the elastomer zones beyond this limiting size.

Investigations into the use of blends to gain improvements in

certain properties such as processing⁽¹²⁸⁻¹³¹⁾, flex cracking^(132,133) heat stability⁽¹³⁴⁻¹³⁶⁾ and cut growth resistance⁽¹³⁷⁾ indicate the wide variety of possible applications. Particular attention has been paid to blends in the field of tyre technology⁽¹³³⁻¹⁴²⁾ to fulfil specialised requirements. Similarly, a great deal of work has been carried out on ethylene-propylene rubber (EPR) which when blended with other rubbers, confers improved ozone resistance⁽¹⁴³⁻¹⁴⁷⁾.

Little systematic work on the relationship between scale of dispersion and physical properties has been undertaken. Walters⁽¹¹⁸⁾ found that tear strength fell as zone size decreased but the difference was small and could have been caused by increased breakdown of polymer under the extended milling conditions required to give the finer dispersions. Livingston⁽¹⁴⁸⁾ indicated that the physical properties of two rubber blends varied with degree of mixing up to 100 mill passes but no correlation with zone size was undertaken. Powell⁽¹²⁵⁾ has demonstrated that the ozone resistance of SBR-EPR blends increases as the fineness of dispersion increases. According to Andrews microcrack termination theory⁽¹⁴⁹⁾ the increase in the number of EPR zones leads to a consequent reduction in their separation. This factor restricts ozone cracks in the SBR phase to microscopic dimensions, thereby increasing the resistance of the vulcanisate to macroscopic failure.

1.8.2 Vulcanisation of Elastomer Blends

The distribution of soluble compounding ingredients, particularly curatives, can exert significant influence on the performance of the vulcanised product. Gardiner^(150,151) has demonstrated that diffusion of common vulcanising ingredients such as sulphur, mercaptobenzothiazole disulphide (MBTS) and tetramethylthiuram-disulphide (TMTD) occurs from compounded low unsaturation rubbers to uncompounded high unsaturation rubbers in a very short time (eg 3 seconds at 153°C). Since the solubility of certain common curatives is greater in high unsaturation rubbers such migration may be inevitable, even when concentrations are equal initially⁽¹⁵²⁾. Migration may, therefore, create an imbalance between component phases with associated over and under cure^(118,152,153).

Covulcanisation may improve certain physical properties such as resilience^(154,155). It has been reported⁽¹⁵⁶⁾ that co-cross-linking can be achieved if the cure rates of the polymers are virtually identical and if the cross-link structure is predominantly polysulphidic. In contrast, interfacial bonding in chlorobutyl-polydiene blends occurs only in the presence of very efficient thiuram di- and tetra- sulphide vulcanisation systems⁽¹⁵⁷⁾. Chemical probe analysis established that interfacial bonds are associated with a preponderance of mono-sulphidic cross-links, formed during the initial stages of vulcanisation rather than by maturation of polysulphidic cross-links.

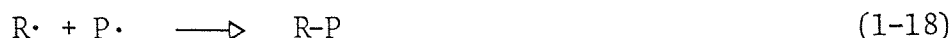
A study, which does not involve sulphur vulcanisation, is concerned with the covulcanisation of CR/NBR (nitrile rubber) rubbers⁽¹⁵⁸⁾. In the absence of metal oxides (eg zinc oxide) reasonable mechanical properties are obtained which are attributed to co-ordination 'cross-links'. In the presence of metal oxides, covulcanisation occurs. The metal chloride produced as a result of this reaction apparently increases the electrophilic nature of the chloroprene rubber, thereby improving its compatibility with the nitrile rubber domains and encouraging covulcanisation.

1.8.3 Interpolymer Formation

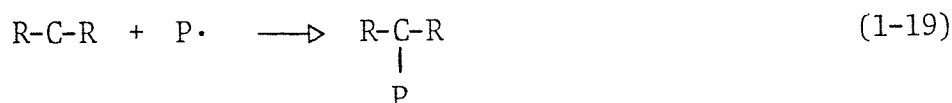
Under certain conditions, the mechanical working of a mixture of polymers can lead to interpolymerisation^(159,160). The possibility of interpolymerising two elastomers follows from the mechanism of cold mastication⁽¹⁶¹⁾. Rubber chains may be broken by shearing to yield free radicals at the ruptured ends:



These appear to be terminated by oxygen in the surrounding atmosphere to yield hydroperoxide groups⁽¹⁶²⁾ which decompose to give stable products^(163,164). However, this termination step may be reduced by decreasing the level of available oxygen. Under an inert atmosphere, therefore, mastication of two polymeric materials may lead to block copolymer formation⁽¹⁶⁵⁾ through recombination of reactive terminal radicals (eqn 1-18).



Alternatively, if sites for halogen or hydrogen abstraction are present in one of the polymeric constituents, graft copolymer formation may be favoured (eqn 1-18).



Angier^(159,160) has studied interpolymers of NR, CR, NBR, styrene-butadiene rubber (SBR) and butyl rubber (BR) produced by cold mastication under nitrogen in an internal mixer. Evidence for interpolymerisation was provided by differences in gel contents of the products after mastication compared with those of simple polymer mixtures. Slominskii⁽¹⁶⁶⁾ in an investigation of SBR and BR blends found that in the absence of oxygen, mechanochemical grafting produced materials whose property-composition relationships differed from those of simple mill mixtures.

Recombination mechanisms of the type indicated above yield a wide range of reaction products and the difficulty in isolating and identifying pure products has been emphasised in previous publications^(167,168).

CHAPTER TWO

EXPERIMENTAL THEORY

2.1 Introduction to Network Structure Analysis

As outlined earlier, one of the general aims is to observe the effect of cross-link structure and cross-link density on the fatigue behaviour of chloroprene rubber and chloroprene rubber/natural rubber blends. To achieve this aim, a knowledge of the following parameters is required:

- (a) the original cross-link density of the vulcanisates investigated,
- (b) the nature of the cross-linked network formed during vulcanisation, and
- (c) the changes in cross-link density or cross-link structure during fatigue tests.

2.2 Measurement of the Degree of Cross-linking

2.2.1 Introduction

An understanding of the elastomeric nature of rubber was made possible by the development of the theory of elasticity. This has been utilised in later years to calculate the degree of cross-linking.

Major developments by Staudinger⁽¹⁶⁹⁾ and Mayer et al⁽¹⁷⁰⁾ showed that rubber molecules were of a long polymeric nature and assumed irregular and statistically random configuration under thermal motion. On deformation they tended to straighten with a corresponding decrease in entropy. The application of these ideas to a cross-linked network⁽¹⁷¹⁻¹⁷³⁾ led to the statistical theory of rubber elasticity.

2.2.2 Dry Extension

The statistical theory of rubber elasticity^(119,170,174,175) gives the force, F , required to sustain a perfectly elastic network in a small extension, λ , by the expression:

$$F = fA_0NkT (\lambda - \lambda^{-2}) = 2C_1A_0(\lambda - \lambda^{-2}) \quad (2-1)$$

where: A_0 is the unstrained cross-sectional area

N the number of network chains per unit volume at

T the absolute temperature

k the Boltzmann's constant

f is a 'front factor'^(171,176-178) usually taken to be near unity (but which may relate to the conformational aspects of network chains⁽¹⁷⁹⁾)

C_1 is an elastic constant for a given temperature

Significant deviations from behaviour predicted by statistical theory occur at low and moderate extensions. At moderate

extensions the use of a Gaussian distribution of network chain displacement lengths no longer applies since the network approaches a limiting extension. By removing the restriction that the distance between junction points of the molecule is minute compared to the length of the molecule the error may be reduced.

This extended theory now provides a description of elastomeric behaviour in the region of moderate or large extensions in contrast to the statistical theory. Equations for vulcanised rubber have been derived by Rivlin and Saunders⁽¹⁸⁰⁾, Mooney⁽¹⁸¹⁾ and Gent and Thomas⁽¹⁸²⁾. The stress-strain behaviour of dry networks up to moderate strains complies with the Mooney-Rivlin expression^(180,181).

$$F = 2A_0 (C_1 + C_2 \lambda^{-1}) (\lambda - \lambda^{-2}) \quad (2-2)$$

where: C_1 and C_2 are constants

C_1 is identifiable with that predicted by statistical theory⁽¹⁸³⁻¹⁸⁵⁾.

If we now assume the front factor, f , to be unity, then

$$C_1 = \frac{1}{2} NkT \quad (2-3)$$

$$\text{or } C_1 = \frac{1}{2} \rho RTMc^{-1} \quad (2-4)$$

where: ρ is the density of the rubber

Mc the number average molecular weight of the chain

segments of the rubber between adjacent cross-links
R the gas constant

Hence the degree of cross-linking is $1/2 Mc$.

From equation (2-2) a graph of $F/(\lambda - \lambda^{-2})$ against $1/\lambda$ should ideally be a straight line of slope $2A_0C_2$. However, the value of stress increases more rapidly than is predicted by equation (2-2) at high extensions. This was initially associated with strain induced crystallisation^(186,187) but later work indicated the deviation to result from the finite extensibility of the network chain segments⁽¹⁸⁸⁻¹⁹²⁾.

Experimental error alone can cause significant deviation at low extensions since $(\lambda - \lambda^{-2})$ is very small if $\lambda - 1$ is small.

Taking data obtained at a variety of extensions and using the graphical procedure outlined above, both the C_1 and C_2 constants may be obtained. Using the C_1 term, the degree of cross-linking may be calculated from equation (2-4).

2.2.3 Swollen Compression

Measurements made on swollen rubbers in extension and compression show that at low and moderate extensions the departures from ideal behaviour are less than in dry rubbers; indeed, for highly swollen samples ($v_r < 0.2$ where v_r is the volume fraction

of rubber hydrocarbon in the swollen network) the deviations can be ignored⁽¹⁸⁵⁾.

With a modification to allow for the volume fraction of the network the Mooney-Rivlin equation^(180,181) becomes:

$$F = 2A_0 \nu_r^{-1/3} (C_1 + C_2 \lambda^{-1}) (\lambda - \lambda^{-2}) \quad (2-5)$$

For high degrees of swelling, C_2 becomes zero⁽¹⁸⁵⁾ and the dependence of stress on strain agrees with statistical theory⁽¹⁹³⁾.

Thus,

$$F = 2A_0 \nu_r^{-1/3} C_1 (\lambda - \lambda^{-2}) \quad (2-6)$$

Giving

$$C_1 = \frac{F \nu_r^{-1/3}}{2A_0 (\lambda - \lambda^{-2})} \quad (2-7)$$

By measuring the strain induced by a compression stress

Where: F is the compressive force

A_0 the unswollen cross-sectional area

ν_r the equilibrium volume fraction of rubber in the swollen sample

λ the actual compression ratio of the swollen sample

For a test specimen having an unstrained unswollen height, h_0 ,

an unstrained swollen height, h_s , and a height, h_d , on application of a force, F , the compression ratio then approximates to:

$$\lambda = h_d/h_s \quad (2-8)$$

and

$$(\lambda - \lambda^{-2}) = (h_d^3 - h_s^3) / h_s h_d^2 \quad (2-9)$$

Assuming isotropic swelling for the rubber, $\nu_r^{1/3}$ may be expressed in terms of h_o and h_s .

$$\nu_r^{1/3} = h_o / h_s \quad (2-10)$$

Substituting equations (2-10) and (2-9) into equation (2-7),

$$C_1 = \frac{F h_o h_d^2}{2 A_o (h_d^3 - h_s^3)} \quad (2-11)$$

Equation (2-11) derived by Kay, Moore and Thomas⁽¹⁹⁴⁾ may be used for the calculation of C_1 from a single compression measurement⁽¹⁹⁵⁾.

By defining the compressive strain, Δh , as

$$\Delta h = h_s - h_d \quad (2-12)$$

Then from equation (2-10),

$$(\lambda^{-2} - \lambda) = \left(1 - \frac{\Delta h}{h_s}\right)^{-2} - \left(1 - \frac{\Delta h}{h_s}\right) \quad (2-13)$$

Binomially expanding the first part of equation (2-13) gives

$$(\lambda^{-2} - \lambda) = 1 + \frac{2\Delta h}{hs} + \frac{3\Delta h^2}{hs^2} + \frac{4\Delta h^3}{hs^3} - \left(1 - \frac{\Delta h}{hs}\right) \quad (2-14)$$

Using the first term of the binomial expression and assuming that $hs > \Delta h$, Cluff, Glading and Pariser⁽¹⁹⁶⁾ arrived at the expression:

$$(\lambda^{-2} - \lambda) = \frac{3\Delta h}{hs} \quad (2-15)$$

which, after substitution into equation (2-7) yields:

$$C_1 = \frac{Fho}{6\Delta hAo} \quad (2-16)$$

Similarly, Khadim and Smith⁽¹⁹⁷⁾, using the second term, gave for C_1 :

$$C_1 = \frac{Fho}{6\Delta hAo} \frac{1}{1 + \nu_r^{1/3} \Delta h h o^{-1}} \quad (2-17)$$

Equation (2-11) has been rewritten⁽¹⁹⁸⁾ in more meaningful parameters suitable for the microcompression technique now in common use:

$$C_1 = \frac{F\nu_r^{1/3}}{2Ao} \left[\frac{3hs\Delta h^2 - 3hs^2\Delta h - \Delta h^3}{hs^3 - 2hs^2\Delta h + hs\Delta h^2} \right]^{-1} \quad (2-18)$$

Using equation (2-18), experimental results for values of C_1 obtained by compression of samples swollen to equilibrium and by extension of dry samples, have shown them to agree well within

the experimental error of the methods⁽¹⁹⁸⁾. In addition, variations of C_1 determined by microcompression were less than variations due to the inherent experimental error⁽¹⁹⁸⁾.

2.2.4 Equilibrium Volume Swelling

Cross-linked networks swell to equilibrium extents when immersed in liquids. The fundamental equation relating the equilibrium degree of swelling to the cross-link concentration is that due to Flory and Rehner^(173,199).

$$- [\ln(1-\nu_r) + \nu_r + \chi \nu_r^2] = e V_0 (Mc)^{-1} \nu_r^{1/3} \quad (2-19)$$

Later modified to:

$$- [\ln(1-\nu_r) + \nu_r + \chi \nu_r^2] = e V_0 Mc^{-1} (\nu_r^{1/3} - \nu_r/2) \quad (2-20)$$

where: ν_r is the volume fraction of rubber network in the swollen gel

Mc the number average molecular weight of network chains between cross-links

V_0 the molar volume of the swelling liquid

e the density and

χ the polymer/solvent interaction coefficient

The major difficulty in using this technique is that χ must first be determined by substituting Mc values obtained by an independent

method (eg swollen compression or stress strain) together with corresponding values of ν_r . For simple cross-linking systems, such as tertiary peroxides, consistent values of χ may be obtained appropriate to a wide range of M_c values^(183,201,202). However, for sulphur vulcanisation it has been shown that χ changes both with level of curative and with time of cure because of alteration in the chemical constitution of the network chains⁽²⁰³⁻²⁰⁵⁾ and the extent of cross-linking.

Erroneous values of cross-link concentration may be obtained within the context of network structure determination if the original value of χ is used after chemical treatment since χ changes significantly after the use of chemical reagents^(205,206).

Assuming that χ is known precisely, then equation (2-21) (derived from equations (2-20) and (2-4)) usefully enables the translation of ν_r values to values of C_1 .

$$-\left[\ln(1-\nu_r) + \nu_r + \chi \nu_r^2\right] = 2C_1 V_0 (\nu_r^{1/3} - \nu_r/2) / RT \quad (2-21)$$

2.2.5 Calculation of the Degree of Cross-linking

From equations (2-3) and (2-4) it can be seen that:

$$C_1 = \frac{1}{2} Nkt = \frac{1}{2} \chi RIMc^{-1}$$

and the physical degree of cross-linking equates to:

$$1/2 Mc = C_1 / RT$$

It is necessary to standardise any determination of C_1 since its value will change with conditions and with any pre-treatment. As vulcanisates in this work have all been extracted, all that remains is the super coiled rubber network plus a small percentage of filler.

The measured C_1 value is corrected to 25°C by means of the expression:

$$C_{1ERV} = C_1 \text{ (measured at } t^\circ\text{C)} \cdot 298 / (273 + t) \quad (2-22)$$

Where: C_{1ERV} is the C_1 term for the extracted vulcanisate at 25°C.

C_{1ERV} may now be corrected to allow for the stiffening effect of non-reinforcing fillers⁽²⁰⁷⁾, eg zinc oxide.

$$C_{1ERM} = C_{1ERV} (1 + 2.5 V_f + 14.1 V_f^2)^{-1} \quad (2-23)$$

Where: V_f is the total volume fraction of fillers in the vulcanisate and C_{1ERM} is the C_1 term for the extracted rubber matrix.

The magnitude of the correction for C_{1ERV} to C_{1ERM} is of the order of ~5% which is a little over the experimental error for C_1 determinations (ca 2-3%). However, it is necessary that

these corrections are applied so that values may be compared.

2.3 Network Structure Analysis

2.3.1 Chemical Probes

2.3.2 Introduction

A chemical probe may be described as a reagent which, when introduced into a vulcanised rubber network, quantitatively cleaves specific cross-links. It must be capable of being introduced homogeneously into the network and be easily extracted once reaction is complete.

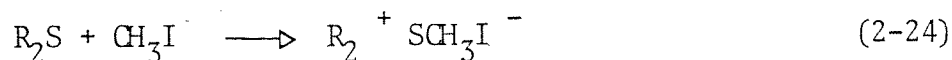
By obtaining cross-link density measurements before and after application of a chemical probe an estimation of the concentration of mono- di- and polysulphidic cross-links present in a sulphur vulcanised elastomer may be obtained.

The following chemical probes were used:

- (a) Methyl Iodide - to cleave all sulphur cross-links
- (b) Propan-2-thiol - to cleave all polysulphidic cross-links
- (c) n-Hexan-thiol - to cleave all di- and polysulphidic cross-links.

2.3.3 Methyl Iodide Probe

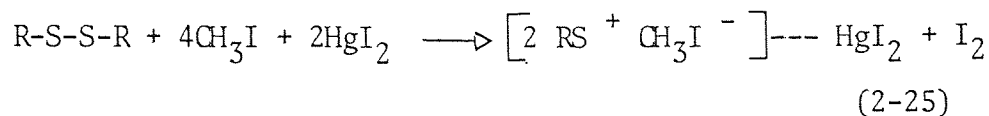
Methyl iodide was first introduced to estimate monosulphidic linkages in sulphur vulcanised natural rubber⁽²⁰⁸⁾. Subsequent work⁽²⁰⁹⁻²¹²⁾ indicated di-allyl sulphides reacted preferentially to di-alkyl sulphides at room temperature and under nitrogen in the following way:



Since only allylic sulphides appeared to breakdown easily to yield extractable trimethyl sulphonium salts⁽²¹⁵⁻²¹⁸⁾, the removable sulphur from vulcanised natural rubber and SBR networks after treatment with methyl oxide was originally assigned to di-alkenyl monosulphidic linkages. Later studies⁽²¹⁹⁻²²¹⁾, however, indicated other sources of removable sulphur after the above treatment including di-alkenyl, t-alkyl alkenyl and di-t-alkyl monosulphidic cross-links and certain monosulphidic main chain modifications.

Di- and polysulphidic cross-links react very slowly with methyl iodide at room temperature but their rate of reaction and those of monosulphides are catalysed by the addition of mercuric iodide^(213,214) (eqn 2-25). Alternatively, the work of Moore⁽²⁴³⁾ and Moore and Watson⁽²⁴⁴⁾ has shown the application of methyl iodide at eighty degrees centigrade for natural rubber vulcanisates under vacuum to cause extensive reaction of all

sulphur linkages over a period of four to fourteen days.



Although methyl iodide is a powerful tool for network analysis, some problems exist as to its specificity when applied to unsaturated elastomer networks⁽²²²⁾ and interpretation is known to be difficult in certain cases⁽²²²⁾.

2.3.4 Thiol-Amine Probes

Both the propan-2-thiol and n-hexan thiol piperidine complexes exhibit ideal properties for a probe since they are easily transported into and out of the rubber network and quantitatively cleave polysulphide and combined di and polysulphide cross-links respectively.

The application of thiol disulphide reactions to rubber analysis was developed by Moore, Saville and Trego^(223,221). It was found that a solution of propan-2-thiol (0.4 M) and piperidine (0.4 M) in n-heptane when swollen into a rubber network cleaved the polysulphidic cross-links but was unreactive towards disulphidic, monosulphidic and carbon-carbon cross-links when reacted for two hours at 20°C.

Evans and Saville⁽²²⁴⁾ indicated that the above mixture

cleaves di-(2-alkenyl) polysulphides by the formation of an ion-pair possessing enhanced nucleophilic properties so that although organic trisulphides are cleaved, the reaction with organic disulphides is many times slower⁽²²⁴⁾. The rates of reaction of di-alkenyl tri- and polysulphides with the propan-2-thiol/piperidine/n-heptane solutions were found to be 1000 times faster than with di-alkenyl disulphides⁽²²⁵⁾ and after treatment for two hours at 25°C decomposition of the trisulphides had taken place whilst the disulphides were unaffected.

By increasing the nucleophilic character of the reagent, the rate of cleavage of poly and disulphidic bonds is found to increase, although the monosulphides still remain intact.

By using a primary alkane thiol, such as n-hexan thiol, at increased concentrations with piperidine, di-(2-alkenyl) disulphides react to equilibrium in a few hours at 25°C⁽²²⁵⁾, after which time a small concentration of unreacted disulphide is present^(225,226). The equilibrium is important⁽²²⁷⁾ but it has been shown that when the thiol concentration is in ten-fold excess over the reactant disulphide concentration in a rubber network, virtually no unreacted disulphide remains⁽²²⁶⁾.

The absolute rates of sulphide cleavage in a vulcanisate are unlikely to be the same as for the model systems but the relative rates of cleavage are believed to be similar^(225,226).

2.4 Fatigue Testing

2.4.1 Introduction

A wide range of fatigue equipment is available to evaluate the cut growth and fatigue resistance of rubber vulcanisates. Most of the methods employ bending or flexing motions to impose strain in the sample. The five most widely used machines are:

2.4.2 De Mattia Flex Tester^(228,229)

In this test a sample with a moulded groove in one surface is bent repeatedly at 300 rpm and the degree of cracking in the groove is assessed at various stages. The method has a number of limitations: the strain acting on a sample is too complex to be measured directly and varies across the sample thickness; reproduction of the same strain condition in each sample is difficult, especially when comparing vulcanisates of different moduli. As a consequence of these features, reproducibility can be poor and, although it is probably the most commonly used instrument, there is a general dissatisfaction with the results of this method of assessment.

2.4.3 Flipper or Torrens

A rubber-like strip is fixed in the periphery of a rotating disc and is bent against a fixed but freely rotatable roller.

The radius of curvature and hence the maximum surface strain is not precisely controlled which leads to extensive result variability. However, this equipment is popular in the shoe industry since the deformations produced appear to simulate the bending of a shoe sole.

2.4.4 Du Pont Fatigue Tester

Test strips are attached to an endless belt which runs over a series of pulleys of specified radii. Although the overall radius of bending is controlled, the surface strain cannot be calculated accurately since each sample has a series of transverse grooves moulded into the surface.

2.4.5 The Ross Flex Tester^(230,231)

This technique involves bending a rubber strip against a rod through 90° and then imparting a small strain to the sample. The maximum surface strain is more precisely controlled than in any of the above techniques. This is also the first tester of those discussed so far which ensures zero strain is achieved during each cycle. In (a)-(c) great care must be taken in initially setting the test pieces to zero strain if this is to be achieved.

2.4.6 The Monsanto Fatigue to Failure Tester⁽²³²⁾

The equipment was originally developed by the Natural Rubber Producers Research Association (NRPRA)⁽²³²⁾. Two banks of twelve samples may be examined simultaneously at two different extensions. The dumbbell shaped samples are gripped by a moulded beading at their edges by sample clamps. The sample clamps are attached to beams which ride on cams connected to a 100 rpm motor drive. The required extension is obtained by selecting an appropriate cam and, since each is 180° out of phase with the other, the extension occurs for half a cycle. The extension set which develops in samples after a number of cyclic deformations is taken up by adjustable supports after approximately 1000 cycles. This ensures that the preselected strain is maintained throughout the test.

The number of cycles to failure is recorded automatically for each sample by individual fatigue life counters. The lower sample clamps rise approximately 4 mm when a verticle stress is applied to the sample and in so doing operate microswitches which trigger individual impulse counters. A second pair of adjustable cams are attached to a 100:1 reduction gear which actuates the circuit controlling the fatigue life counters and registers one cycle for every 100 cycles of the main drive. Insignificant digits are, therefore, not registered. Failure of the sample automatically stops the appropriate counter.

A minimum of six test pieces are fatigued and the fatigue life calculated by using a weighted average known as the JIS average⁽²³³⁾:

$$\text{JIS average} = 0.5 A + 0.3 B + 0.1 (C+D)$$

where ABCD are the fatigue lives of the samples showing maximum resistance and where $A > B > C > D$.

The reason for using samples with maximum fatigue resistance is that premature failure may be due to flaws and surface imperfections caused by the moulding or cutting processes. If these are taken into the averaging process then results would be low and would not reflect the true value.

This technique provides the best control of surface strain of all the methods discussed. Samples may be tested under iso strain conditions or, for materials having widely different moduli, at similar strain energy. The minimum strain may also be adjusted to achieve relaxing or non-relaxing conditions.

Brake hose assemblies experience a predetermined maximum elongation during operation and cycling generally passes through zero strain. The Monsanto fatigue to failure tester was, therefore, used throughout this project to evaluate fatigue and cut growth resistance as it was believed this method would most closely reflect actual service conditions.

2.5 Phase Contrast Microscopy

Phase contrast microscopy was introduced by Zernicke⁽²³⁴⁻²³⁷⁾ in 1934 and has since been extensively used to investigate the morphology of heterogeneous polymer blends^(118,124,154,238,239).

The mechanism of phase contrast has been dealt with in detail elsewhere^(234-237,240,241) but essentially it involves light transmission through say a thin polymer sample. This transmitted light consists of a central wave and an out of phase diffracted wave. By using a suitable diffraction plate the central wave may now be partly absorbed and retarded. If, after this treatment, the central and diffracted waves are now in phase, they will combine, thus increasing the intensity of the transmitted light and producing a bright image. If the central wave (c) is partially absorbed, however, and the diffracted wave (d) is partially retarded by the diffraction plate such that (c) and (d) are out of phase, a dark image will be observed.

Taking the above facts into consideration, the mechanism of the phase contrast microscope may now be explained. A specimen placed on the microscope stage deviates some of the light away from the objective. The undeviated rays pass through the specimen and enter the objective in a diverging hollow cone to form the image of the annulus at the back focal plane of the objective. The image is known as the conjugate annulus. The diffraction plate in the back focal plane of the objective is

made to fit the image of the annulus. The diffraction plate weakens and retards the undeviated background light without effecting the light deviated by the sample. Thus the regions of high refractive index in the sample appear brighter than regions of lower index. This is known as negative phase contrast. However, if the deviated rays are weakened by the retarding material, dark or positive phase contrast is produced and the regions of higher index appear darker.

By using phase contrast microscopy to observe a thin section of a heterogeneous blend of polymers having different refractive indices a clear indication of the morphology may, therefore, be obtained.

2.6 The Monsanto Rheometer⁽²⁴²⁾

The Monsanto oscillating disc rheometer⁽²⁴²⁾ measures the changes in shear modulus that occur during vulcanisation. This is achieved by surrounding an oscillating biconical disc with the rubber compound under pressure and at vulcanising temperature. The resistance offered to the constant amplitude oscillation of the disc is measured by strain gauges during the vulcanisation and this is plotted in terms of inch-lbs of torque versus time on an X-T plotter. The sample and cavity are electrically heated and maintained to within $\pm 0.5^{\circ}\text{C}$ of the set temperature. The disc is oscillated through a 1° , 3° or 5° arc by a motor driven eccentric, the drive being connected to a torque transducer and

so to the disc shaft.

The disc oscillation frequency of the Monsanto 100 model used for this work is 100 cycles per minute. The 100 cycle per minute signal is too high in frequency to be recorded directly and must, therefore, first be converted to a direct current signal by the AC to DC converter. The converter consists of magnetically actuated proximity switches and a rotating magnet. The actuating magnet is located in a wheel connected to the motor driven eccentric. The proximity switches are so positioned with respect to the synchronised magnet that the stress signal is sampled at the maximum of each strain cycle. The resulting direct current signal is then recorded to yield a continuous curve of elastic modulus versus cure time.

The recorder is equipped with a range selector which provides full scale chart spans of 25, 50, 100 and 200 inch-lbs of torque. The chart speed is set by means of an electronic time base giving full scale sweeps of three to six hundred minutes.

A typical rheograph may be seen in Fig 2.2. The data obtained may then be used in the mathematical treatment of Coran^(245,246) to calculate the induction period (t_i), rate of cure (k), maximum modulus (R_{\max}) and time to optimum modulus to give a complete vulcanisation picture.

CHAPTER THREE

GENERAL EXPERIMENTAL

The following chapter describes the experimental techniques and empirically established operating procedures used for the investigation of Neoprene GS, Neoprene W and natural rubber formulations.

All compounding ingredient sources are listed in Table 3.1.

For network analysis measurements, the molar volumes of the swelling solvents, V_0 , and the gas constant, R , are quoted from the literature without qualification.

The densities of raw Neoprene GS and natural rubber were determined using Archimedes bridge principle.

3.1 Fatigue Life Measurements

3.1.1 Sample Preparation

The Monsanto fatigue to failure tester⁽²¹⁸⁾, Section 2.4.6, was used to determine the fatigue lives of all vulcanisates. Materials were cured to their optimum level at 150°C in the double sheet Monsanto fatigue mould^(217,218). Dumbell shaped test pieces were cut at right angles to the grain direction

using a BS type E cutter. Twelve test pieces having identical thickness were cut from the central area of each sheet to avoid possible edge effects. The samples were then examined for moulding or cutting imperfections before being tested.

Cut initiated samples were prepared using a template. Dumbells were loaded in a groove in the template such that their central portion was aligned between parallel engraved marks. A needle of 0.30 mm diameter was then placed in a perpendicular hole located in the centre of the engraved marks and pushed through the rubber sample. In this way, a central cut of given dimensions was initiated in the test piece.

3.1.2 Operation of the Monsanto Fatigue to Failure Tester

To ensure fatigue samples were loaded in an unstrained state, the long axis of the chosen cams were manually adjusted, using a crank handle to operate the main drive, to align with a horizontal line engraved on the equipment (both main beams are then resting on their stops and the distance between each set of top and bottom beams is identical). The gap between the top and bottom sample holders was then adjusted to 6 cm by means of an adjustable support on each of the top sample clamps. Having thus ensured identical starting conditions, each dumbell was loaded into the sample clamps and locked in place with a spring clip. The counters were then set to zero and the equipment switched on.

After 1000 cycles, the equipment was stopped, reset to zero extension as described above and the set which had developed taken up by means of the adjustable supports to maintain the original strain. The fatigue tester was then restarted and the samples fatigued to failure.

3.1.3 Determination of Test Conditions for Fatigue Evaluations

3.1.4 Introduction

The fatigue conditions for both the original black compounds and their non-black equivalent formulations (Table 3.2) were established experimentally and subsequently used throughout each fatigue evaluation.

3.1.5 Method

Formulations A-D, Table 3.2 were prepared as detailed in sections 4.6.1 and 4.6.2. Two samples of each batch were vulcanised using a Monsanto oscillating disc rheometer at 150°C, the second trace checking the dispersion of compounding ingredients. Optimum modulus cure times were found from each batch from the rheometer. Sheets of the compounded stocks were preheated for 2 minutes at 150°C under slight pressure in the Monsanto fatigue mould placed in a steam heated press. They were then vulcanised at 150°C under full pressure for the optimum cure time observed from Monsanto rheometer traces at the same

temperature. Fatigue samples were cut from the vulcanised sheets as described in section 3.1.1. Cut initiated samples were prepared by the method detailed in section 3.1.1 using 0.85 mm and 0.30 mm diameter needles (Table 3.3). Samples of the uncut and cut black and gum vulcanisates were fatigued to failure over a range of extensions (Tables 3.3 - 3.6). Needles of 0.85 mm diameter (Table 3.3) were found to be unsuitable for preparing cut initiated samples, failure occurring over a relatively small number of cycles. 0.30 mm diameter needles, were, therefore, used to prepare cut initiated samples.

For black vulcanisates (Tables 3.3 and 3.4) the fatigue conditions were experimentally determined as:

- (a) Uncut = 78% strain \equiv 8 cam
- (b) Cut initiated (0.30 mm needle) = 61% strain \equiv 4 cam

For gum vulcanisates (Tables 3.5 and 3.6) fatigue conditions were established as:

- (a) Uncut = 89% strain \equiv 10 cam
- (b) Cut initiated (0.30 mm needle) = 68% strain \equiv 6 cam

The above conditions are the best compromise which give a relatively high fatigue life (for accuracy) and a relatively short testing time (for convenience) and were used throughout this investigation unless otherwise stated.

3.2 Scanning Electron Microscopy

3.2.1 Introduction

The function of a scanning electron microscope (SEM) is very similar in concept to that of a reflectance optical microscope. In place of the light source, however, an electron beam (or probe) is directed at the specimen. Probe electrons striking the sample do not penetrate very deeply and the majority of the secondary electron emissions caused by the electron beam are from atoms in the surface of the sample. The secondary electron emissions and primary electrons (reflected from the surface of the specimen) are then collected and used to modulate the brightness of a television display unit. In this way an accurate representation of the topography of the sample may be obtained. Since high energy electrons have a much shorter wavelength than light, however, far greater magnification (typically 100,000 X) is obtainable than for an optical microscope (typically 1000 X).

3.2.2 The Scanning Electron Microscope

A stereoscan S600 (Cambridge Instruments Ltd) scanning electron microscope (SEM) was used to observe the fracture surfaces of fatigued samples.

The electron gun produces an electron beam having a diameter

of about 50 microns. The beam is then condensed and focused onto the sample through a series of lenses and finally passes through a stigmator coil to give a circular source. The probe is scanned across the specimen in a raster. With increasing magnification, the area over which the raster is scanned decreases, thereby obtaining better resolution.

Low energy secondary electrons and high energy primary electrons then travel towards the collector system. The collector comprises a grid which can be biased either positively, such that only high energy electrons are able to pass, or negatively so that both low and high energy electrons may be detected. Behind the grid is a positively biased scintillator, optically coupled to a photomultiplier. Electrons impinging on the scintillator cause photons to be emitted which then travel along the light guide to the photocathode of the photomultiplier. The signal from the photomultiplier passes through a head amplifier to the display unit where the amplified signals control the brightness of the cathode ray tube. The tube is then scanned in synchronism with the raster scanning the electron beam.

The electron optics include a small (50 micron) aperture, producing an effective F number of 1000 - 2000. This gives a much greater depth of focus than an optical system (typically F2 - F10) and renders a marked three-dimensional appearance to the image obtained.

3.2.3 Preparation of Samples for Scanning Electron Microscopy

The fractured parts of a number of gum vulcanisates were cut from dumbbells after fatigue. Samples were mounted on small metal stubs for electron microscopy using double sided cellotape and electrical contact between the specimen and the stub ensured using a colloidal silver preparation (Acheson Colloids Ltd). A conductive fluid was then sprayed onto each sample to prevent the surface charging up under the electron beam. The stub was secured in the mounting pallet which enables X, Y (lateral) and Z (vertical) rotation and tilt movements of the specimens to be achieved in the SEM. This was positioned in the vacuum chamber of the equipment, the front plate replaced and the clamping lever turned to lock the pallet to the front plate. The chamber was then evacuated to working vacuum (indicated by the Vacuum Ready Light) before obtaining photographs⁽²³¹⁾.

3.3 Preparation of Microtome Sections for Optical Microscopy

Thin sections of gum vulcanisates for phase contrast microscopy were obtained in the following manner. Samples of approximately 3 mm x 4 mm were cut with a scalpel from the centre of approximately 1.5 mm thick sheets of gum vulcanisate prepared for fatigue testing. The 3 mm edges were tapered at both ends to enable easier cutting. Each sample was mounted on the sample stage of a Leitz sledge microtome with 'Stephens' gum and frozen using liquid nitrogen.

The sample stage had to be modified to permit the use of liquid nitrogen since it had been designed for cooling by carbon dioxide gas but this did not freeze the samples sufficiently. A glass knife was preferred to the metal knives often used on sledge microtomes and a glass knife holder was manufactured to replace the existing knife holder.

Sections of 10μ thickness were microtomed from frozen samples until the surface was smooth and flat. The thickness setting was then adjusted to 2μ and sections obtained as follows.

The blade was first wetted with methanol and the sections cut slowly to avoid blade judder. As each section was cut, it tended to curl tightly. This was then removed from the glass blade with a small soft bristled brush and immersed in a bath of methanol. Generally, 10 - 20 sections were cut from each sample. The sections were retrieved from the methanol bath using the brush and gently uncurled and laid flat on a microscope slide, (this was found to be easiest when the sample was moist with methanol). Normally six sections were mounted on each slide. The solvent was allowed to evaporate and the sections mounted using glycerol. A microslide was then placed over the sections and bubbles expelled by gently pressing on the microslide. Phase contrast micrographs were then obtained.

3.4 Phase Contrast Microscopy

A Nikon phase contrast microscope was used to examine microtome sections of gum rubber vulcanisates prepared for fatigue testing.

Before starting measurements, the phase contrast microscope was adjusted. The light source was switched on and adjusted to the required intensity. The objective was then centred and focused on the edge of a microscope slide. The slide was then removed. In phase contrast microscopy, the size of the conjugate annulus varies with the strength of the objective and the annular condenser diaphragm must vary correspondingly. It was, therefore, necessary to repeat the following sequence for each objective and its corresponding annular diaphragm. Having selected the objective, the corresponding annular diaphragm was slid into place by means of a revolving diaphragm plate. One eye piece was replaced with a centring telescope which was used to view the back of the objective during adjustment. The phase condenser was centred by manually adjusting the floating annular diaphragm to superimpose the image of the annulus (bright ring) on the dark ring of the phase plate as viewed through the centring telescope. When this had been repeated for each objective and corresponding annular diaphragm, the centring telescope was removed and the eyepiece replaced. The microscope was now ready to be used in the phase contrast mode.

A microtomed section mounted on a microscope slide was placed

on the sample stage. The required objective was centred over the sample and the correct annular diaphragm set in place. The sample was then brought into focus and the blend morphology observed.

When photographs were required, a lever was operated which directed the image from the eyepiece into the lense of a camera (Nikon). A second eyepiece permitted the image to be observed. It was necessary to have both the sample and the crossed polars in the second eyepiece in focus at the same time to bring the image to the correct focal point of the camera. The image was first brought into focus using the sample stage adjuster and the crossed polars were then brought into view using an adjuster on the eyepiece. Photographs could now be obtained in the normal manner.

3.5 Measurement of the Degree of Cross-linking

3.5.1 Swollen Compression

The stress strain characteristics of swollen rubbers were determined using the microcompression technique developed by Cluff, Gladding and Pariser⁽¹⁹⁶⁾, later modified by Smith⁽²⁴⁷⁾. For this purpose a Wallace Reticulometer with centre reading galvanometer and thermostatted sample holder was used.

Samples of edge dimensions approximately 4 mm were cut from

adjacent areas of the centre of a vulcanised sheet. These were weighed, the linear dimensions measured with a vernier microscope (Pye Ltd) and then swollen in the chosen solvent for 24 hours.

The swollen samples were weighed before testing and, after allowing a few minutes for reswelling, the samples were progressively loaded and deloaded and corresponding deformations were recorded using the procedure detailed by Smith⁽²⁴⁷⁾. The samples were deswollen in vacuo at 50°C to constant weight and this value used to calculate the equilibrium volume swelling ratio, ν_r ⁽¹⁸³⁾.

From the resultant values of stress, F , and strain, Δh , the slope of $F/\Delta h$ was determined. C_{1ERV} was then calculated using equation 2-16.

3.5.2 Equilibrium Volume Swelling

Samples of edge dimensions approximately 4 mm were cut from adjacent areas of the centre of a vulcanised sheet. These were weighed and immersed in the chosen solvent at 25°C for 24 hours. The swollen samples were then removed from the solvent, pressed onto filter paper to remove excess solvent, placed in a tared stoppered bottle and reweighed. The samples were then deswollen in vacuo at 50°C to constant weight and ν_r calculated from a knowledge of the swollen and deswollen weights. Using the

values of C_1 derived from swollen compression (section 3.5.1) and ν_r values from equilibrium volume swelling, the polymer solvent interaction coefficient, χ , was calculated using equation 2-21.

3.5.3 Time to Equilibrium Swelling

The Neoprene GS and natural rubber formulations shown in Table 3.7 were prepared as detailed in section 4.2.1. The compounded materials were vulcanised to their optimum level in the Monsanto fatigue mould and volume swelling samples prepared as detailed in section 3.5.3. The Neoprene GS samples were then immersed in toluene and dimethyl formamide (DMF) respectively at 25°C and the natural rubber samples immersed in toluene and hexane respectively at 25°C. The swollen weights were monitored over a range of times and the samples were then deswollen in vacuo at 50°C to constant weight. These values were then used to calculate ν_r for each polymer/solvent system (Tables 3.8 and 3.9).

Figs 3.1 to 3.3 show ν_r as a function of time for the two formulations in their respective solvents. The equilibrium swelling time was taken as the time to reach a constant ν_r value. This was experimentally determined to be ten hours in toluene and sixteen hours in DMF for Neoprene GS and ten hours in toluene and eleven hours in hexane for natural rubber. To ensure equilibrium swelling was achieved, a swelling time of 24 hours was subsequently used for both equilibrium volume

swelling and swollen compression modulus measurements.

3.6.1 Chemical Probes

Equilibrium volume swelling (section 3.5.2) and swollen compression modulus determinations (section 3.5.1) were used to determine the χ values and cross-link densities of the vulcanisates before and after treatment with the chemical probes. Samples approximately 4 mm square were prepared from each vulcanisate as detailed in section 3.5.1.

3.6.2 Methyl Iodide

Two methods were evaluated for the application of methyl iodide probe with Neoprene GS vulcanisates:

- (1) Methyl iodide with mercuric iodide catalyst at 25°C under nitrogen, and
- (2) Methyl iodide in vacuo at 80°C.

3.6.3 Methyl Iodide and Mercuric Iodide at 25°C

A modified form of the apparatus described by Saville and Watson⁽²⁴⁸⁾ was used which had several compartments to separate each group of samples. Free flow of the probe solution and nitrogen was ensured by making holes in the glass dividing walls of each compartment.

The reagent was prepared by mixing 100 ml of redistilled methyl iodide and 10 g mercuric iodide. The samples were placed in the apparatus and purged with nitrogen. The reagent was added under nitrogen so that the vulcanisates were covered and further purged with nitrogen for a few minutes. The stoppers were then placed in each of the compartments, beginning with that closest to the nitrogen source. The nitrogen flow was maintained throughout this procedure. Finally, the gas taps were closed to retain the nitrogen blanket and the apparatus occasionally agitated for a set period of time decided upon by a second experiment (section 3.6.6).

At the end of the time interval, the nitrogen flow was restored and the reagent run out. The samples were then extracted with petroleum ether (bpt 30-40) for one hour and dried overnight under vacuo.

3.6.4 Methyl Iodide under Vacuum at 80°C

The 'H' tube apparatus described by Saville and Watson⁽²⁴⁸⁾ was used for the application of the methyl iodide probe according to the method of Moore and Watson⁽²⁴⁴⁾. 15 ml of methyl iodide was added to one limb together with the sample. The liquid was degassed twice while cooling in liquid nitrogen. The apparatus was then sealed and the arm containing the sample and probe solution covered with aluminium foil to provide a dark environment. The tubes were then placed in an oil bath

maintained at 80°C until reaction was complete (section 3.6.6). The samples were then extracted with petroleum ether (bpt 30-40) for one hour and deswollen overnight under vacuo.

3.6.5 Determination of the Reaction Times for Methyl Iodide

For natural rubber vulcanisates having sulphur cross-links reaction with methyl iodide at 25°C is known to be very slow^(243,244). At 80°C, however, reaction appears to be complete after 120 hours⁽²⁴³⁾.

Little work had been done using methyl iodide with Neoprene GS and reaction times were, therefore, determined experimentally.

3.6.6 Method

500 g of Neoprene GS was compounded with 5 phr zinc oxide and 4 phr magnesium oxide on a 12" laboratory mill with full water cooling to a Wallace plasticity number of 15.

The material was then vulcanised at 150°C for 30 minutes in the Monsanto fatigue mould using a steam heated press. Triplicate samples approximately 3 mm square were cut from adjacent areas of the centre of the vulcanised sheet and treated at 25 and 80°C as detailed in sections 3.6.3 and 3.6.4, using a range of reaction times. Samples were also treated at 80°C in the absence of methyl iodide to act as a control. ν_r values were then calculated



by swelling the samples to equilibrium at 25°C in toluene. These values were then recorded against reaction time (Tables 3.10 and 3.11) and plotted (Figs 3.4 and 3.5).

The reaction time was to be taken as the time after which ν_r remained constant. However, methyl iodide appeared to cause further cross-linking of the Neoprene GS vulcanisate, both at 25 and 80°C and was, therefore, felt to be unsuitable for the evaluation of total sulphur cross-links present in this vulcanisate.

3.6.7 Propan-2-thiol/Piperidine

The same equipment as that used for the application of methyl iodide probe at 25°C was used. The reagent was prepared by mixing 4.07 ml propan-2-thiol, 4.82 ml piperidine (redistilled and stored under nitrogen) and 100 ml of pure n-heptane under a nitrogen atmosphere. The samples were then placed in the apparatus and purged with nitrogen. The reagent was added under nitrogen so that the samples were covered and further purged with nitrogen for a few minutes. The same procedure as that detailed for the application of methyl iodide at 25°C was then followed (section 3.6.3). Reaction times were determined by a second experiment described in section 3.6.10.

χ values and the degree of cross-linking were then determined (sections 3.5.1 and 3.5.2).

3.6.8 n-Hexan-thiol/Piperidine

The 'H' tube apparatus described by Saville and Watson⁽²⁴⁸⁾ for the application of the sodium dibutyl phosphite probe was used. 10 ml of piperidine (redistilled and stored under nitrogen) was added to one limb under a blanket of nitrogen, together with the sample. n-Hexan-thiol (2.1 ml) was added to the other limb, the liquids were degassed twice while cooling in liquid nitrogen then mixed and degassed for a final time. The tubes were then placed in a water bath and maintained at 25°C for the predetermined reaction time (section 3.6.10). The samples were then extracted with petroleum ether (bpt 30-40) for one hour and subsequently deswollen overnight under vacuo. χ values and cross-link density were then determined (sections 3.5.1 and 3.5.2).

3.6.9 Determination of Reaction Times for the Thiol/Amine Reagents

For natural rubber vulcanisates the reaction times for propan-2-thiol/piperidine and n-hexan-thiol/piperidine have been found to be 2 and 48 hours respectively^(112,113,221,248).

Little network analysis appears to have been done using thiol/amine reagents with Neoprene GS vulcanisates and reaction times were, therefore, determined experimentally.

3.6.10 Method

500 g of Neoprene GS was compounded with 5 phr zinc oxide and 4 phr magnesium oxide on a 12" laboratory mill with full water cooling to a Wallace plasticity number of 15.

The material was vulcanised for 30 minutes at 150°C in the Monsanto fatigue mould using a steam heated press. Triplicate samples, approximately 3 mm square, were cut from adjacent areas of the centre of the vulcanised sheet and treated as described in sections 3.6.7 and 3.6.8 using a range of reaction times.

ν_r values were then calculated by swelling the samples to equilibrium at 25°C in toluene and the data recorded against reaction time (Table 3.12). The information was plotted in Figs 3.6 and 3.7 and the reaction time taken as the time after which ν_r remained constant.

The reaction time for propan-2-thiol/piperidine and n-hexan-thiol/piperidine with Neoprene GS was experimentally determined to be 4 hours and 30 hours respectively.

3.7 Interpolymer Formation

3.7.1 Introduction

The effect on compatibilisation and fatigue characteristics of Neoprene GS/natural rubber blends through the addition of small

quantities of interpolymer were investigated. Fractional precipitation (250,251) was used to monitor interpolymer formation. This technique makes use of the fact that the formation of a chemical bond between two different rubbers produces a polymer chain having solubility intermediate between the two parent materials. The addition of increasing quantities of a non-solvent to a solution containing two rubbers would precipitate each rubber separately according to its solubility in the solvent used. The presence of an interpolymer in such a blend, however, would give rise to a gradual increase in the weight of the rubber precipitated at given non-solvent additions for the reasons outlined above.

3.7.2 Method

3.7.3 Preparation of Blends

Three blends were used to confirm interpolymer formation.

- (a) Neoprene GS and natural rubber were masticated separately on a 12" laboratory mill with full water cooling to Wallace plasticity numbers of 18 and 11 respectively. Approximately 5 g of each material was weighed and added to the same 250 ml of chloroform (ie total quantity of rubber was approximately 10 g) and the flask shaken vigorously to effect solution.

- (b) A 50 : 50 blend of Neoprene GS and natural rubber were masticated together on a 12" laboratory mill with full water cooling to a Wallace plasticity number of 15. 10 g of this blend was then dissolved in 250 ml of chloroform.
- (c) A 50 : 50 blend of Neoprene GS and natural rubber were masticated together on a 12" laboratory mill with full water cooling to a Wallace plasticity number of 25. 10 g of this material was then placed in the mixing chamber of a Unirotor mixer⁽²⁵²⁾ and the chamber sealed. A nitrogen blanket was obtained by passing nitrogen (bubbled through pyrogallol solution to remove trace quantities of oxygen) through the outer chamber which totally enclosed the mixing chamber. The mixing chamber was immersed in ice water to prevent heat build up during mastication and hence maintain a high level of shear. The materials were then masticated for 20 minutes using a rotor speed of 100 rpm.

Approximately 10 g of this blend was then weighed and dissolved in 250 ml of chloroform. The gel which had formed during inter-polymerisation was removed by filtering the solution. The residue was then dried under vacuo overnight and weighed so that the total quantity of rubber in solution could be calculated.

3.7.4 Determination of Interpolymer Formation

Approximately twenty x 5 ml samples of the above solutions were pipetted into pre-weighed test tubes and the test tubes stoppered to prevent loss of solvent and immersed in a thermostatted water bath at 25°C. To each of these, increasing quantities of non-solvent (methanol) were added from a 5 ml microburette to precipitate various fractions of the blend. The test tube was shaken to ensure good mixing of the solvent, restoppered and centrifuged to solidify the precipitate. The excess solvent was then decanted, the rubber fraction dried under vacuo overnight and the test tube reweighed. The weight of rubber precipitated for increasing methanol additions was then recorded (Tables 3.13 to 3.15) and the results plotted as weight percent of rubber precipitated against mls of methanol added (Figs 3.8 to 3.10).

For blends (a) and (b) (Figs 3.8 and 3.9), it may be seen that the two rubbers precipitate separately indicating no interpolymer formation as expected. For blend (c) however (Fig 3.10) a gradual increase in the weight of rubber precipitated for increasing non-solvent additions is observed which is indicative of interpolymer formation.

3.8 Differential Scanning Calorimetry (DSC)

DSC was used to investigate the morphology of Neoprene GS/Neoprene

W and Neoprene GS/natural rubber blends. Thermograms were obtained using a Perkin-Elmer Differential Scanning Calorimeter (DSC-2) fitted with a liquid nitrogen subambient accessory.

The samples were heated under a helium atmosphere from 160^oK to 295^o K at 20^o/min. The thermogram was recorded on a Servocribe IS 542-20 potentiometric recorder fitted with a temporary event marker.

A glass transition is observed as a step change in the baseline. Two glass transitions observed for a two component polymer blend are generally indicative of a heterogeneous blend whilst a single transition would indicate homogeneity. The temperature at which the glass transition occurred was conventionally taken as that temperature at which the change in heat capacity was one half of its maximum.

CHAPTER FOUR

EXPERIMENTAL

4.1 Experimental

As stated in the introduction (section 1.1), the aim of this project was to understand the reason for the differences in fatigue failure of the chloroprene rubber (CR) and CR/natural rubber (NR) blends and, if possible, to optimise the fatigue resistance of both. Experimentally, this investigation studied the following areas:

- (1) Evaluation of the original GS/W and GS/NR formulations supplied.
- (2) The effect of morphology and blend ratio on fatigue behaviour of gum vulcanisates of the above blends.
- (3) Investigation of the network structure of GS/NR blends.
- (4) The effect of additional cureatives on fatigue behaviour of a 50 : 50 GS/NR blend.

4.2.1 Preparation of Gum Formulations

A water cooled 12" laboratory mill with a friction ratio of 1.25 : 1, capable of being water cooled and steam heated, was used to prepare all rubber blends and gum formulations. Each rubber base was prepared according to sections 4.2.1(a) to 4.2.1(f) below

unless otherwise shown. For the following blends, the elastomers were masticated for sufficient time to achieve a workable consistency. As a result of the different chemical and physical characteristics of each of the rubbers, their Wallace plasticities before the addition of compounding ingredients were, therefore, slightly different.

Compounding ingredients were added to the rubber blends once good mixing was achieved. The compounding ingredients were then mixed with the rubber until a good dispersion was observed (ca. 10 minutes).

The same bale of natural rubber grade SMR5 CV20 and batches of Neoprene GS and Neoprene W were used throughout the work. All compounding ingredient sources are shown in Table 3.1.

(a) Neoprene GS Only Formulations

Neoprene GS was masticated to a Wallace plasticity of 18. The compounding ingredients were then added according to section 4.2.1.

(b) Natural Rubber Only Formulations

Natural rubber was masticated to a Wallace plasticity of 15 before the compounding ingredients were added.

(c) Neoprene W Only Formulations

Neoprene W was masticated to a Wallace plasticity of 22 before compounding; section 4.2.1.

(d) Neoprene GS/Natural Rubber Formulations

Natural rubber was masticated to a Wallace plasticity of 15. The appropriate quantity of unmasticated Neoprene GS was then added to obtain the required blend ratio. The two rubbers were blended together until good mixing was obtained and compounding ingredients were then added.

(e) Neoprene GS/Neoprene W Formulations

Neoprene GS and Neoprene W were masticated separately to Wallace plasticities of 18 and 22 respectively. Neoprene W was then banded on to the mill and the appropriate quantity of Neoprene GS added. Vulcanising ingredients were mixed into the blend as detailed in section 4.2.1.

(f) Neoprene W/Natural Rubber Formulations

Natural rubber and Neoprene W were masticated separately to Wallace plasticity numbers of 15 and 22 respectively. Natural rubber was banded on to the mill and the appropriate quantity of Neoprene W thoroughly blended with it. Compounding ingredients

were added as detailed in section 4.2.1.

4.2.2 Preparation of Black Formulations

Black formulations were prepared using a water cooled one litre capacity laboratory size Banbury mixer, capable of being water cooled and steam heated, at a set rotor speed of 3. All rubbers were prepared according to section 4.2.1 before being placed in the Banbury. Compounding ingredients were then added to the prepared polymer base in the mixer.

4.2.3 Curing of Formulations

A steam heated double daylight press equipped with a thermocouple and maintaining 50 tons on an eight inch ram was used for the vulcanisation of sheets. Formulations were preheated for two minutes under slight pressure in a hot mould and test sheets were vulcanised at 150°C in the Monsanto fatigue mould under full pressure for the cure time determined. Unless otherwise shown, optimum cure times were determined from the Monsanto rheometer at the chosen temperature. The mould was then opened and the sheets quenched in cold water to stop further vulcanisation. All vulcanisates were kept for 24 hours at room temperature before being tested to allow any maturation reactions to take place.

Formulations used for fatigue testing and network analysis were

cured in the Monsanto fatigue mould at 150°C unless otherwise shown.

4.3 Determination of Isostress Fatigue Conditions

Isostress fatigue testing was carried out on vulcanisates of the GS : NR blends shown in Table 4.8 to determine the effect of modulus on fatigue behaviour. Isostress fatigue conditions were experimentally determined in the following way.

Dumbbells of similar cross-sectional area were fatigued at a maximum strain of 68% in the Monsanto fatigue to failure tester. After 1000 cycles, the samples were removed and tensile measurements made using a jaw separation speed of 50 cm/minute. From the stress-strain curves obtained, the strain at a stress of 1 MPa was determined (this stress was chosen as being the only value which would permit the range of extensions available for the Monsanto fatigue to failure tester to be used for subsequent fatigue evaluations). Uncut and cut initiated samples were then fatigued to failure (section 3.1.1) using the strain conditions determined above.

4.4 Tear Strength Measurements

Tear strength was determined according to BS No 903:Part A3: (1972). Crescent tear test pieces were cut from sheets vulcanised at 150°C to their optimum level in a four cavity mould of dimensions 10 cm x 10 cm x 0.2 cm. The thickness of each specimen was

determined and a 0.5 mm cut then made in the sample using a Wallace-Shawbury nick cutter. The notched test pieces were placed in the grips of a type E tensometer (Tensometer Ltd) and the tear strength determined using a jaw separation speed of 500 mm/minute. Results were recorded as Tear Strength (N) per standard test piece, the average value of four samples being quoted.

4.5 Network Analysis

4.5.1 Soxhlet Extractions

Unless otherwise stated, all vulcanisates used for network analysis were continuously acetone extracted for 48 hours in the dark under a nitrogen atmosphere. The extracted vulcanisates were then deswollen to constant weight in vacuo and network analysis carried out.

4.5.2 Calculation of χ

χ was calculated for swollen vulcanisates using swollen compression (section 3.5.1) and equilibrium volume swelling measurements (section 3.5.2). C_{1ERV} values were calculated using equation 2-16 and this value then substituted into equation 2-21 to give values of χ for a given polymer/solvent system.

4.6 Evaluation of Original GS/W and GS/NR Formulations

4.6.1 Preparation of GS/W Formulations

A 75 : 25 GS/W blend was prepared according to section 4.2.1. This blend was then used to prepare black and gum stocks of the original all-chloroprene blend (Formulations A and B, Table 3.2). The following cycle times were used to compound formulation A in the Banbury.

| | |
|--------------------------------|--------------|
| Neoprene GS/Neoprene W (blend) | 30 seconds |
| Carbon black |] 90 seconds |
| Plasticiser | |
| Antioxidant | |
| Zinc oxide |] 60 seconds |
| Magnesium oxide | |
| Wax |] 60 seconds |
| Stearic acid | |

4.6.2 Preparation of GS/NR Formulations

A 50 : 50 GS/NR blend was prepared as detailed in section 4.2.1. This blend was used to prepare black and gum formulations of the original chloroprene/natural rubber blend (Formulations C and D, Table 3.2). The following cycle times were used to compound formulation C in the Banbury.

| | |
|------------------------------------|-------------|
| Neoprene GS/natural rubber (blend) | 30 seconds |
| Carbon black | 120 seconds |
| Zinc oxide | |
| Magnesium oxide | |
| White Factice | |
| Antioxidant | 60 seconds |
| Wax | |
| Stearic acid | |
| MBTS | |

4.6.3 Testing of Original Formulations

Sheets for formulations A-D, Table 3.2, were vulcanised to optimum cure at 150°C in the Monsanto fatigue mould and used to establish conditions for all subsequent isostrain fatigue testing (section 3.1.5).

The effect of antioxidant depletion on the uncut fatigue life of formulations A and C was determined. Dumbells were extracted for six weeks at room temperature in water. Other samples were heat aged in an air circulating oven for 70 hours at 100°C. Fatigue behaviour was then determined and compared with the unconditioned vulcanisates.

4.6.4 Effect of Carbon Black Content on the Fatigue Behaviour of a 75 : 25 GS : W Vulcanisate

The formulations shown in Table 4.2 were prepared as detailed in section 4.6.1. Sheets were vulcanised to optimum cure at 150°C in the Monsanto fatigue mould. Uncut and cut initiated fatigue life (section 3.1.1) was then determined for each formulation.

4.7.1 Effect of Blend Ratio on Fatigue

Formulations shown in Table 4.4 were prepared according to section 4.2.1. Sheets were vulcanised to optimum cure at 150°C. Uncut and cut initiated fatigue life were then determined (section 3.1.1) for each formulation under isostrain conditions. Photographs were taken of fatigue failures of GS : W vulcanisates (Formulations A, C, F, G and H, Table 4.4) using the scanning electron microscope (sections 3.2.2 and 3.2.3). Tear strength measurements were also made (section 4.4) on the GS/W blends shown in Table 4.4. DSC thermograms (section 3.8) were obtained for formulations A, B, C, E, G and J (Table 4.4) using a heating rate of 20°C per minute.

4.7.2 Effect of Morphology on Fatigue of GS/NR Blends

Formulation A, Table 4.8, was prepared as detailed in section 4.2.1. Formulations B-E, Table 4.8, were prepared using Neoprene GS premasticated to a Wallace plasticity of 11. The

appropriate quantity of unmasticated natural rubber was added and the two rubbers blended together. Compounding ingredients were then mixed into the above blends until a good dispersion was achieved.

Formulations F-I, Table 4.8, were prepared using natural rubber premasticated to a Wallace plasticity of 5. Unmasticated Neoprene GS was added to this material in the appropriate quantity and the two rubbers blended together. Compounding ingredients were added as described above.

Sheets were vulcanised to optimum cure at 150°C. Fatigue behaviour was determined under isostrain (sections 3.1.1 and 3.1.5) and isostress (section 4.3) conditions. Scanning electron microscope (SEM) photographs were taken of the fracture surfaces of samples which failed under isostrain conditions (sections 3.2.2 and 3.2.3). Phase contrast micrographs were obtained for each GS/NR blend as detailed in sections 3.3 and 3.4. Tear strength measurements were made according to section 4.4 on vulcanisates cured at 150°C to their optimum level.

4.7.3 Effect of Interpolymer on the Fatigue Behaviour of GS/NR Blends

The 50 : 50 GS/NR interpolymer was prepared as detailed in section 3.7.3. The GS/NR blends shown in Table 4.9 were prepared according to section 4.2.1. The appropriate quantity of interpolymer was added and the rubbers blended together.

Compounding ingredients were then mixed with the rubber matrix until a good dispersion was observed.

Sheets were vulcanised at 150°C in the Monsanto fatigue mould and fatigue behaviour determined under isostrain conditions (sections 3.1.1 and 3.1.5).

Phase contrast micrographs were obtained (sections 3.3 and 3.4) to observe the effect of interpolymer addition on morphology.

4.8.1 Network Structure Analysis

4.8.2 Determination of Cureatives for NR in Original GS/NR Blend

Formulations A and B, Table 4.10, were prepared according to section 4.2.1. All attempts made to vulcanise the above formulations at 150, 170 and 190°C in the Monsanto rheometer, however, proved unsuccessful.

4.8.3 Effect of Neoprene GS on Cure of Natural Rubber

Formulations C-F, Table 4.10, were prepared according to section 4.2.1. Sheets were vulcanised at 150°C in the Monsanto fatigue mould to optimum cure. The vulcanisates were soxhlet extracted in the dark with toluene for 24 hours under a nitrogen atmosphere and dried to constant weight under vacuo. Chlorine determinations⁽²⁴⁷⁾ before and after toluene extraction were

then carried out to determine the quantity of unvulcanised natural rubber present in each CR/NR blend.

4.8.4 Level of Sulphur in Neoprene GS and Neoprene W

Nephelometric sulphur determinations⁽²⁴⁸⁾ were carried out on raw, unextracted, Neoprene GS and Neoprene W. The levels of sulphur were found to be 2.3% and 0.2% respectively.

4.8.5 Calculations from Preferential Swelling Measurements

To a first approximation, the solvent swelling ratio, ν_r , of a 50 : 50 blend of two rubbers, A and B, may be given as:

$$\nu_{rBLEND} = \frac{V_A + V_B}{V_A + V_B + V_{SA} + V_{SB}} \quad (4-1)$$

where V_A = volume of swelling rubber in the blend

V_B = volume of non-swelling rubber in the blend

V_{SA} = volume of solvent absorbed by A

V_{SB} = volume of solvent absorbed by B

ν_{rBLEND} = solvent swelling ratio of the 50 : 50 A/B blend

Equation (4-1) may be rewritten as:

$$V_{SA} = \left(\frac{V_A + V_B}{\nu_{rBLEND}} \right) - V_A - V_B - V_{SB} \quad (4-2)$$

The volume of solvent absorbed by B will be quite low and may be

experimentally determined from equilibrium volume swelling measurements on vulcanisates of B only in the non-swelling solvent. Hence:

$$V_{SB} = \left(\frac{V_B}{\nu_{rB_{NSS}}} \right) - V_B \quad (4-3)$$

where $\nu_{rB_{NSS}}$ = solvent swelling ratio of B in the non-swelling solvent

Assuming that the two polymers form a totally heterogeneous blend and that the non-swelling rubber component has no effect on the polymer/solvent interaction coefficient, ν , of the swelling rubber, the volume of solvent, V_{SB} , absorbed by the non-swelling rubber may now be substituted into equation (4-2) to give:

$$V_{SA} = \left(\frac{V_A + V_B}{\nu_{rBLEND}} \right) - \left(\frac{V_B}{\nu_{rB_{NSS}}} \right) \quad (4-4)$$

By assuming 2 g of the A/B blend were used and 1 g of B was used to calculate V_{SB} , the volume of solvent absorbed by 1 g of A in the blend may be calculated; ie for 1 g of A in the blend,

$$V_{SA} = \left(\frac{\frac{1}{e_A} - \frac{1}{e_B}}{\nu_{rBLEND}} \right) - \left(\frac{\frac{1}{e_B}}{\nu_{rB_{NSS}}} \right) - \frac{1}{e_A} \quad (4-5)$$

Hence the solvent swelling ratio of the swollen rubber in the blend (ν_{rBLEND}) may be calculated:

$$\nu_{rA}^{\text{BLEND}} = \frac{\frac{1}{\rho_A}}{\left(\frac{1}{\rho_A} + \frac{1}{\bar{V}_{SA}}\right)}$$

From a knowledge of χ for A in the chosen solvent (experimentally determined on vulcanisates of A only) the cross-link density of A in the blend may now be determined using equation (2-20).

4.8.6 Identification of Preferential Swelling Solvents

To assess the cross-link density of Neoprene GS and natural rubber in a vulcanised 50/50 blend of the two polymers, two solvents were sought. One to swell the GS phase without swelling natural rubber and one to swell the natural rubber domain without swelling the GS. By using equilibrium volume swelling measurements in conjunction with the preferential swelling solvents, it was expected that an indication of the cure response of each phase of the blend may be obtained.

Natural rubber and Neoprene GS vulcanisates were prepared using formulations C and I (Table 4.10) according to section 4.2.1 and vulcanised to optimum cure at 150°C in a four-cavity mould of dimensions 10 cm x 10 cm x 0.2 cm. Samples of nominal dimensions 2.5 cm x 0.3 cm x 0.2 cm were cut from the centre of the sheets and immersed in a range of solvents for 36 hours at 25°C. The linear dimensions of the swollen samples were then measured and compared to the original dimensions. From the increase in length of the sample, the degree of swelling may be

approximated and the compatibility of each solvent with the given GS and NR polymer bases assessed. From the results, two solvents were identified, one of which swelled the NR vulcanisate without substantially swelling the GS vulcanisate (hexane) and one which swelled the GS vulcanisate without affecting the NR vulcanisate (dimethyl formamide, DMF).

4.8.7 Preferential Swelling Measurements

The GS, NR and 50/50 GS/NR blend (Formulations C, I and E, Table 4.10) were prepared according to section 4.2.1. All three formulations were then cured at 140°C in a four-cavity mould of dimensions 8 cm x 3 cm x 0.3 cm for 10, 20, 40, 65 and 120 minutes.

Vulcanisates of C and I were swollen to equilibrium at 25°C in their respective 'non-swelling' solvents (ie hexane for GS and DMF for NR) and V_r calculated for each cure time (section 3.5.2).

χ values were determined for vulcanisates of formulations C and I cured for 30 minutes at 140°C and swollen in DMF and hexane respectively (section 4.5.2).

Vulcanisates of formulation E were swollen to equilibrium in hexane and DMF at 25°C (section 3.5.2) and the cross-link density of the swollen rubber in the blend calculated according to section 4.8.5.

4.8.8 Effect of Cure Time on Network Structure of Neoprene GS

Formulation C, Table 4.10, was vulcanised at 140°C in the Monsanto fatigue mould for 10, 20, 30, 40 and 60 minutes. The vulcanisates were treated with propan-2-thiol (section 3.6.7) and n-hexan-thiol (section 3.6.8) as detailed. Swollen compression (section 3.5.1) measurements were carried out using toluene solvent before and after application of the thiol/amine probes. From the results, the change in network structure of Neoprene GS vulcanisates with cure time was determined.

4.8.9 Effect of Blending on GS and NR Network Structure

Formulations C, E, G, H and I, Table 4.10, were prepared according to section 4.2.1 and vulcanised for 30 minutes at 150°C in a four-cavity mould of dimensions 8 cm x 3 cm x 0.3 cm. Samples were treated with propan-2-thiol and n-hexan-thiol probes as detailed in sections 3.6.7 and 3.6.8. The specimens were then swollen to equilibrium at 25°C in toluene and swollen compression measurements (section 3.5.1) taken on each sample before and after application of the thiol/amine probes.

4.8.10 Effect of Fatigue on GS and NR Network Structure

Formulations C and I, Table 4.10, were prepared as detailed in section 4.2.1 and vulcanised to optimum cure in the Monsanto fatigue mould at 150°C.

Nine dumbbells from each vulcanisate were fatigued on the Monsanto fatigue to failure tester (sections 1.1 and 3.1.2) for 0, 100, 200, 1000, 15,000, and 100,000 cycles and to failure at a maximum strain of 68%. Specimens of about 0.3 cm square dimensions were then cut from the centre of each dumbbell. χ values were established before and after application of thiol/amine reagents (sections 3.6.7 and 3.6.8) on the unfatigued samples according to section 4.5.2 using toluene as the swelling solvent. The calculated χ values were subsequently assumed to remain unchanged by fatigue testing.

Equilibrium volume swelling measurements (section 3.5.2) were carried out in toluene for each fatigued sample before and after application of the thiol/amine probes. The cross-link density was then determined using the calculated ν_r values with the χ values determined above in equation (2-21).

4.9.1 Effect of Additional Cureatives on Fatigue Behaviour of a 50 : 50 GS/NR Blend

Before carrying out fatigue evaluations, it was necessary to ensure all vulcanisates were of a similar cross-link density. Formulations A-M shown in Table 4.31 were prepared according to section 4.2.1. Sheets were cured for three different cure times at 150°C in the Monsanto fatigue mould. The solvent swelling ratio, ν_r , was then determined (section 3.5.2) for each vulcanisate at 25°C in toluene. Appropriate cure times required

to obtain γ_r values of 0.18 ± 0.005 for all formulations were then determined. Sheets for fatigue evaluations were vulcanised to the determined cure times shown in Table 4.31. The uncut and cut initiated fatigue behaviour of each formulation was then evaluated under isostrain conditions according to section 3.1.1.

CHAPTER FIVE

DISCUSSION OF RESULTS

5.1 Effect of Compounding Ingredients on Fatigue Behaviour

The difference in fatigue life and failure mechanism of the original GS : NR and GS : W formulations supplied by the manufacturer are believed to be due to the different compounding ingredients used in each formulation. The effects of antioxidant depletion and carbon black content on the fatigue life of these compounds have, therefore, been investigated.

5.1.1 Effect of Antioxidant Depletion on the Fatigue Behaviour of Filled GS : W and GS : NR Formulations

Depletion of antioxidant either by leaching or heat ageing is known to reduce the fatigue life of vulcanisates⁽⁹⁹⁻¹⁰¹⁾. These two parameters were investigated using both the original all chloroprene rubber and the chloroprene rubber : natural rubber formulations supplied by the manufacturer. The effect of water leaching on fatigue behaviour is of particular interest in view of the application for which these compounds are used.

From Table 4.1 it may be seen that the untreated 75 : 25 GS : W formulation (formulation A, Table 3.2) gave a markedly better fatigue life than the 50 : 50 GS : NR vulcanisate (formulation C,

Table 3.2). A comparison of the fracture surfaces of the two materials, however, highlighted the differences observed by the manufacturers. The failed surface of the GS : W vulcanisate was smooth, generally indicative of rapid cut growth, whilst that of the GS : NR specimen was rough and suggested a slow cut growth mechanism (Frames 5.1 and 5.2).

Neither water leaching nor heat ageing of formulations A and C followed by fatigue testing had a significant effect on the failure mechanism described but major changes in fatigue life were observed.

Samples of the GS : NR vulcanisate conditioned in water for six weeks at room temperature gave slightly better fatigue lives than those of similarly aged GS : W specimens (Table 4.1). A decrease in life of 87% and 19% was observed for GS : W and GS : NR samples respectively when compared with the untreated vulcanisates. The poor performance of the GS : W vulcanisates after conditioning appeared to be due to the high solubility of the antioxidant (isopropyl-p-phenylene diamine, IPPD) used in this compound in water^(100,101). In comparison, the antioxidant combination present in the GS : NR formulation (Nonox B and Nonox DPPD) is relatively insoluble in water^(100,101) and would, therefore, be less prone to leaching by water. The concentration of antioxidant in the vulcanisate should hence remain at a higher level and provide greater protection for subsequent fatigue testing which appears to be the case.

After heat ageing formulations A and C for 70 hours at 100°C, the GS : NR blend (formulation C) again gave slightly better fatigue resistance than the GS : W vulcanisate (Table 4.1). The reduction in fatigue life was more marked than for water conditioned samples (97% and 72% for GS : W and GS : NR respectively) but did suggest the antioxidant system used in the GS : NR blend had a greater efficiency than that in the GS : W formulation.

5.1.2 Effect of Black Content on the Fatigue Failure of a 75 : 25 GS : W Formulation

The original 72 : 25 GS : W formulation supplied by the manufacturer (formulation A, Table 4.2) was quite highly loaded with 125 phr of a medium thermal black. The smooth fatigue failure surface of vulcanisates of this compound suggested rapid cut growth was occurring^(62-64,66). Under isostrain fatigue conditions, a reduction in the modulus of a vulcanisate effectively decreases the tearing energy acting upon it during each fatigue cycle, thus slowing down the rate of cut growth. Formulations A-D, Table 4.2, were, therefore, prepared to observe the effect of decreasing the modulus of the 75 : 25 GS : W vulcanisate (by reducing black loading) on its fatigue life and failure mechanism under isostrain conditions.

The uncut and cut initiated fatigue lives of formulations A-D, Table 4.2, are recorded in Table 4.3 and summarised in Table 4.2 and Fig 4.1. Results for uncut and cut initiated samples show

similar trends. As expected, the fatigue life of the vulcanisates increased with decreasing carbon black content from a minimum at 125 phr to an apparent maximum at 60 phr (Fig 4.1). Surprisingly, formulations loaded with only 30 phr of black showed poorer performance than vulcanisates containing twice this quantity. This may be a result of lower shear and poorer mixing in the Banbury as the level of carbon black is decreased. Under such conditions, the carbon black agglomerates would be less well broken down and hence poorly dispersed in the elastomer. The larger particles of black may then act as flaws or stress raisers during fatigue testing and lead to premature failure of the vulcanisate. The wide distribution of fatigue lives for samples loaded with 30 phr of black (Table 4.3) appears to support this argument.

Each of the compounds evaluated exhibited a smooth failure surface in the same manner as the original highly loaded formulation obtained from the manufacturer (Frames 5.3 - 5.6). This suggested the elastomer base rather than the compounding ingredients was responsible for the rapid, smooth failure mechanism. All further work was, therefore, carried out on gum vulcanisates of less complex formulae than those so far described so that the reasons for the difference in fatigue failure of all chloroprene rubber and the chloroprene rubber/natural rubber blends were more obvious.

5.2 Effect of Elastomer Blend Ratio on Fatigue Behaviour

As seen in sections 5.1.1 and 5.1.2, Neoprene GS : natural rubber and Neoprene GS : Neoprene W blends exhibited very different fatigue behaviour. Formulations A-K, Table 4.4 were, therefore, prepared to evaluate the effect of the elastomer base on the fatigue life and failure mechanism. The following section shows the significantly different effects observed when GS : W, W : NR and GS : NR combinations are used.

5.2.1 Effect of Neoprene GS : Neoprene W Blend Ratio on Fatigue Behaviour

The fatigue lives of the Neoprene GS : Neoprene W blends of weight percent ratios 100 : 0, 75 : 25, 50 : 50, 25 : 75 and 0 : 100 (formulations A, C, F, G and H, Table 4.4) are shown in Table 4.5 and summarised in Table 4.4 and Fig 4.2.

From Fig 4.2 it may be seen that the uncut and cut initiated fatigue lives of these blends fall between the respective maximum and minimum values for the Neoprene GS and Neoprene W vulcanisates. A marked decrease in the cut initiated fatigue resistance is observed over the 100 : 0 GS : W to 50 : 50 GS : W range. Increasing the level of Neoprene W beyond this point, however, had only a small effect on the now very low cut initiated fatigue life of the vulcanisates.

Similar results were observed for uncut fatigue testing. The decrease in fatigue life with increasing W content in the blend was less marked than for cut initiated samples but showed an almost linear dependence on the GS : W blend ratio.

The fracture surfaces of all the vulcanisates after fatigue testing were smooth (Frames 5-7 - 5.9) and were representative of the failure mode already described for the 75 : 25 GS : W vulcanisates evaluated earlier (sections 5.1.1 and 5.1.2).

The linear dependence of fatigue life on the GS : W ratio in each formulation and the smooth failure surface observed for all vulcanisates (Frames 5.7 - 5.9) suggested that Neoprene GS and Neoprene W may form a homogeneous blend, (perhaps not surprising in view of their chemical similarity).

This was supported by phase contrast microscopy determinations on each GS : W blend shown in Table 4.4. In no case could the presence of separate domains be detected. This is not conclusive proof of homogeneity, however, since the densities (and the refractive indices) of the two elastomers are virtually identical and separate domains may not be observed in such circumstances. An alternative reason for the absence of observable heterogeneity may also be that the two polymers form a microheterogeneous blend in which the domain size of the dispersed elastomer is lower than the wavelength of light. Such a system would not be detectable by optical microscopy.

The glass transition temperature (T_g) of polymeric components in a truly heterogeneous blend are not affected by blending. If a degree of physical or chemical bonding occurs during blending, however, the tendency will be for the two transitions to move closer together. The more compatible the blend, the closer the T_g 's move until, when a homogeneous blend is obtained, only one glass transition is observed. This T_g lies intermediate between the glass transition of the polymers present in the blend and will vary according to the ratio of one polymer to the other.

Differential scanning calorimetry (DSC) is able to detect the glass transition of a polymer (section 3.8). DSC thermograms were therefore obtained for vulcanisates of Neoprene GS, Neoprene W and a 50 : 50 GS : W blend. From Fig 4.3 it may be seen that the glass transition temperatures of the two homopolymers were very similar. The single transition observed for the 50 : 50 GS : W vulcanisate did not, therefore, provide conclusive evidence for the homogeneity of this blend.

Tear strength measurements obtained on the GS, W and GS : W vulcanisates, shown in Fig 4.4 (Table 4.4), exhibited similar characteristics to the fatigue results obtained for the same formulations. The values for the blends fell intermediate between those obtained for the two homopolymers and exhibited a linear decrease with increasing levels of Neoprene W in the formulation. This appears to be related to the poorer strain crystallisation behaviour of Neoprene W vulcanisates⁽¹¹⁾.

In view of the evidence presented here, it appears that Neoprene GS and Neoprene W form a homogeneous blend when mixed together. The physical properties of homogeneous blends are known to lay mid-way between the constituent homopolymers. The fatigue failure mechanism observed for GS : W vulcanisates is unlikely, therefore, to be significantly different from pure GS or pure W vulcanisates when changes in additives and curatives are made. Further testing of GS : W vulcanisates was therefore curtailed in view of this finding.

5.2.2 Effect of W : NR Blend Ratio on Fatigue Behaviour

Fig 4.5 (Tables 4.4 and 4.6) shows that the uncut fatigue lives of Neoprene W : natural rubber blends fell well below either of the homopolymers. Increasing additions of natural rubber to Neoprene W, however, caused the failure surface to become progressively rougher, despite the reduced fatigue life.

DSC thermograms indicated a 50 : 50 W : NR vulcanisate was heterogeneous as shown by the two glass transition temperatures (Fig 4.6). Phase contrast micrographs (Frames 5.10 and 5.11) also showed that gross phase separation occurred and suggested Neoprene W and natural rubber are very incompatible when blended together.

A 25 : 75 W : NR blend gave no indication of cure after one hour in the Monsanto rheometer at 150°C (Table 4.4). From Table 4.4 it may be seen that no additives other than those required to cure

Neoprene W were added to blends containing natural rubber. To determine the state of cure of natural rubber in the W : NR blends, chlorine determinations were carried out on W, NR and 50 : 50 W : NR vulcanisates before and after toluene extraction. An increase in the total concentration of chlorine after extraction would, therefore, be indicative of the loss of NR from the blend. From Table 5.1 it may be seen that the total concentration of chlorine increased from 18.1% for the unextracted 50 : 50 W : NR vulcanisate to 32.1% for the same vulcanisate after extraction. This suggested all the natural rubber had been removed from the vulcanisate and that the natural rubber was therefore uncured.

The morphology and cure characteristics of these vulcanisates appears to determine their fatigue behaviour. As may be seen in Frames 5.10 and 5.11 natural rubber tends to become the continuous phase at a weight percent loading of less than 50% of the blend. This appears to be related to the contrasting processing behaviour of the two elastomers. With extended milling, natural rubber becomes less viscous whilst Neoprene W showed little sign of decreasing below a Wallace plasticity of 22. The low viscosity polymer in a two component polymer blend tends to become the continuous phase at lower loadings than 50 weight percent of the blend and it appears that natural rubber is assuming this role in the W : NR vulcanisates.

Under fatigue conditions, therefore, the unvulcanised natural rubber would be the stress supporting network (ie continuous

phase), the Neoprene W phase acting more as a cross-linked particulate rubber filler. With increasing levels of natural rubber in the blend an increase in surface roughness of the failed vulcanisates would be expected (and is observed) as a result of the strain crystallisation behaviour of the natural rubber. With natural rubber as the continuous phase, however, more of the fatigue stress would be transferred to this weak, unvulcanised matrix resulting in a poorer fatigue life.

5.2.3 Effect of GS : NR Blend Ratio on Fatigue Behaviour

The GS : NR blends of weight percent ratios 100 : 0, 75 : 25, 50 : 50 and 0 : 100 (formulations A, D, E and B, Table 4.4) were prepared to monitor the effect of natural rubber on the uncut and cut initiated fatigue behaviour of Neoprene GS. The fatigue results for these formulations are shown in Table 4.7 and summarised in Table 4.4 and Fig 4.7.

Similar effects were observed for uncut and cut initiated fatigue samples. Fig 4.7 shows that the 75 : 25 GS : NR vulcanisate exhibited more than double the fatigue life of the Neoprene GS vulcanisate and almost a decade improvement over the natural rubber vulcanisate. Further additions of natural rubber to Neoprene GS, however, decreased the fatigue life.

The fracture surfaces of the vulcanisates also changed with increasing natural rubber content. Neoprene GS exhibited a smooth

failure surface, typical of earlier all chloroprene rubber formulations prepared. As the natural rubber content of the blends increased, the fractured area of the fatigue samples became progressively rougher. The apparent reduction in the rate of cut growth, however, did not result in an increased fatigue life for formulations containing more than 25 weight percent natural rubber. This suggested there may be an optimum NR concentration which gave a high fatigue life and a slow cut growth failure mechanism.

DSC thermograms of Neoprene GS, natural rubber and a 50 : 50 GS : NR vulcanisate (Fig 4.8) showed the GS : NR blend to be heterogeneous.

In contrast to the W : NR vulcanisate, however, chlorine determinations carried out on Neoprene GS, natural rubber and a 50 : 50 GS : NR vulcanisate before and after toluene extraction (Table 5.2) indicated natural rubber was completely bound to the 50 : 50 GS : NR blend after cure. The fact that natural rubber cured in blends with Neoprene GS but not with Neoprene W appeared to be related to the level of sulphur present in each chloroprene rubber. Nephelometric sulphur determinations indicated 2.3% and 0.2% sulphur was present in raw, unextracted Neoprene GS and Neoprene W respectively (section 4.8.4). The availability of sulphur in the two chloroprene rubbers also appears likely to influence the vulcanisation of natural rubber in these blends.

In Neoprene GS, the sulphur exists as polysulphidic groups in

the backbone of the elastomer. Mastication of Neoprene GS causes cleavage of these groups, releasing elemental sulphur into the polymer matrix. In addition, tetramethyl thiuramdisulphide (TMTD) which is a known sulphur donor for the vulcanisation of natural rubber, is also present in Neoprene GS, having been used as a short stop in the polymerisation process. Sulphur in Neoprene W on the other hand mostly exists as mercaptan groups on the end of the polymer chains and is less prone to cleavage and hence less available for vulcanisation.

As with the W : NR vulcanisates, the morphology and cure characteristics of GS : NR blends appeared to be the controlling factors in determining fatigue behaviour. The trends observed in fatigue life of the GS : NR vulcanisates, however, were an almost total reversal of those observed for the W : NR blends, presumably as a result of the vulcanisation of NR.

Assuming the viscosity of the elastomers to be identical, an interconnecting network would be formed in a two component elastomer blend at a volume : volume ratio of 50 : 50. As a result of the different densities of Neoprene GS and NR, this morphology would be observed at a weight percent ratio of 57 : 43 GS : NR as shown in the calculations below.

$$\text{eg volume GS in blend} = 50 \text{ cc} = \frac{\text{mass GS in blend}}{\text{density GS}} = \frac{61.5 \text{ g}}{1.23 \text{ g/cc}}$$

$$\text{volume NR in blend} = 50 \text{ cc} = \frac{\text{mass NR in blend}}{\text{density NR}} = \frac{46 \text{ g}}{0.92 \text{ g/cc}}$$

For a blend containing 50 cc GS and 50 cc NR, the mass would therefore be 107.5 g which gives:

$$\text{weight percent of GS in blend} = \frac{61.5}{107.5} \times 100 = 57.2\%$$

$$\text{weight percent of NR in blend} = \frac{46}{107.5} \times 100 = 42.8\%$$

The molecular weight (and hence viscosity) of Neoprene GS decreases to a limiting value during mastication which is determined by the number of polysulphide units along the backbone. Continued mechanical working of natural rubber, however, decreases its molecular weight (and viscosity) to a limiting value determined by the roll separation. These two factors suggest that phase inversion may occur in GS : NR blends where natural rubber constitutes less than 43 weight percent of the blend. Above a minimum value of 43 weight percent, therefore, natural rubber appears most likely to exist in the blend as the continuous phase. In support of this hypothesis, the 50 : 50 GS : NR vulcanisate exhibited more of the fatigue characteristics of natural rubber, ie low fatigue life (in comparison to Neoprene GS) and rough failure surface.

For the 75 : 25 GS : NR vulcanisate, it appeared feasible to

assume an interconnecting network may be formed. The fatigue resistance of Neoprene GS is known to be very high but is restricted by its rapid failure mechanism. The presence of natural rubber as the interconnecting phase in this blend would prevent rapid failure since the rate of cut growth would be decreased as the cut attempted to penetrate the NR domain. Such a blend would also rely less on the softer natural rubber matrix as the stress supporting network so that the fatigue resistance would be at least of the same order as that of Neoprene GS. This hypothesis was evaluated in more detail in section 5.3.1.

5.3.1 Effect of the Morphology of GS : NR Vulcanisates on Fatigue Behaviour

In section 5.2.3, it was observed that NR had a significant effect on the fatigue behaviour of GS : NR vulcanisates. The formulations shown in Table 4.8 were, therefore, prepared to monitor the effect of the presence of NR in the blend, both as the continuous and discontinuous phase, on the fatigue behaviour of the vulcanisates.

By premasticating one of the elastomers to a low viscosity and then blending with the unmasticated form of the second part of the blend, the tendency will be for the premasticated rubber to become the continuous phase at weight percent loadings lower than 50%. For the same GS : NR ratio, therefore, it was expected that significantly different morphologies (and hence

fatigue behaviour) would be observed according to which elastomer had been premasticated.

Figs 4.9 and 4.10 indicate the premasticated GS (PGS) : NR and GS : premasticated NR (PNR) vulcanisates followed similar trends in fatigue life according to the GS : NR ratio, but exhibited important differences within the general scheme which appeared to be attributable to differences in morphology.

Maxima were observed in both series of blends at the 75 : 25 GS : NR ratio. Further additions of NR, however, decreased fatigue life (Fig 4.9). The uncut fatigue lives of the PGS : NR blends were greater (except for the 90 : 10 GS : NR combinations) than those of the GS : PNR vulcanisates.

Cut initiated samples exhibited slightly different behaviour. Both groups of vulcanisates gave maximum cut initiated fatigue resistance at the 60 : 40 GS : NR ratio. The GS : PNR vulcanisates, however, exhibited higher fatigue lives than their equivalent PGS : NR blends.

Increasing additions of NR to GS caused a gradual increase in the roughness of the failure surface. In all cases, however, the PGS : NR vulcanisates appeared somewhat smoother than their GS : PNR counterparts (Tables 5.3 and 5.4).

A comparison of the phase contrast micrographs (Tables 5.3 and 5.4) and fatigue

results for the two series of blends suggested that Neoprene GS was the controlling factor in producing a high fatigue life but that natural rubber had the greatest effect on cut initiated fatigue resistance.

When either of the two rubbers became the continuous phase (eg 90 : 10 and 50 : 50 GS : NR ratios) the blend appeared to exhibit more of the characteristics of that elastomer. On the formation of an interconnecting network (eg 75 : 25 and 60 : 40 GS : NR ratios), however, both the uncut and cut initiated fatigue resistance of the blends appeared to be enhanced. This seemed to be a function of the 'crack stopping' properties of the natural rubber.

With neoprene GS as the continuous phase, crack propagation would occur along the least line of resistance, ie through the GS continuous phase, resulting in rapid failure of the test piece. When NR is well dispersed as the discontinuous phase (eg 90 : 10 GS : PNR) in the GS matrix, a crack would have a greater probability of encountering the NR domain and being stopped (or slowed down) than where NR was less well dispersed in the blend (eg 90 : 10 PGS : NR). This appears to be the reason for the improved cut initiated fatigue resistance of the 90 : 10 GS : PNR vulcanisate.

The presence of natural rubber as part of an interconnecting network (eg 75 : 25 and 60 : 40 GS : NR ratios) appears to

prevent rapid failure of the vulcanisate for both uncut and cut initiated fatigue. The morphology of such a blend ensures that a propagating cut would have to penetrate alternate Neoprene GS and natural rubber domains to cause failure of the vulcanisate. By preventing rapid failure of the vulcanisate, therefore, the long term fatigue properties of the Neoprene GS appear to be improved.

When NR constituted the continuous phase of the blend (eg 50 : 50 GS : PNR ratio) its poorer fatigue properties appear to cause a reduction in the fatigue life of the vulcanisate.

The main load bearing matrix in each blend appeared to be responsible for the differences observed in fatigue behaviour at equivalent PGS : NR and GS : PNR ratios. When Neoprene GS appeared to be the main load bearing network (from phase contrast micrographs) uncut fatigue lives were high whilst cut initiated fatigue resistance was low. As more of the cyclic stresses appeared to be transferred to the NR phase (ie at higher NR loadings or where changes in morphology permitted this to occur) the uncut fatigue life was poorer (as with NR) but the cut initiated fatigue resistance increased (presumably because the softer vulcanisate exerted fewer stresses on the initiated cut).

Tear strength measurements (Table 4.4 and Fig 4.11) carried out on these vulcanisates appeared to substantiate the above suggestion. As may be seen, the tear strengths of the PGS : NR

blends are higher than those of the equivalent GS : PNR vulcanisates to a weight percent loading of 40% NR in the blend. This raised the question of the behaviour of these blends when subjected to fatigue under isostress conditions, ie such that the NR phase would be subjected to similar cyclic stresses as the GS domain.

Under isostress fatigue conditions (Figs 4.12 and 4.13) a very different picture emerged to that observed for isostrain fatigue tests. In comparison to Neoprene GS, the poorer uncut and cut initiated fatigue resistance of natural rubber became self-evident. A gradual reduction in fatigue life was observed for both series of blends with increasing NR content. Where Neoprene GS constituted the main load bearing matrix (ie for PGS : NR vulcanisates) a higher fatigue resistance was observed than from the corresponding GS : PNR blends. For high NR content blends, (ie 60 : 40 and 50 : 50 GS : NR ratios), however, the fatigue resistance of all vulcanisates approached a common value. The failed surfaces of the vulcanisates (particularly for high NR content blends) were significantly smoother than those observed after isostrain fatigue tests and suggested rapid failure of the specimen had occurred.

It would appear, therefore, that the crack-stopping ability of NR is most effective at low strains (and hence low stresses). This seems to be due to the lower stresses acting on a growing crack tip in the vulcanisate when a natural rubber domain is

encountered.

At high strains, however, the ability of NR to prevent cracks growing is less evident, the natural rubber phase in the blend exerting similar stresses on the growing crack as the GS phase. In such cases, the generally better fatigue properties of the chloroprene rubber appear to determine the fatigue resistance of the blend.

The surface roughness of failed vulcanisates also appears to be explicable on these grounds. Rapid failure (and hence smooth failure surfaces) occur where NR is unable to exert its crack stopping behaviour (eg at high strains or where GS constitutes the continuous phase of the blend). When NR is able to stop or slow down the rate of growth of the crack (ie at low strains), however, rough failure surfaces are observed.

5.3.2 Effect of Interpolymer on the Fatigue Behaviour of a 50 : 50 GS : NR Vulcanisate

The fatigue behaviour of GS : NR vulcanisates under isostrain fatigue conditions appeared to be closely related to their morphology. The following work was carried out to observe the effect of improving the compatibility of Neoprene GS and natural rubber (through the introduction of a 50 : 50 GS : NR interpolymer) on the fatigue behaviour.

From Fig 4.14 it may be seen that the uncut fatigue life of the vulcanisates decreased with increasing interpolymer additions whilst the cut initiated fatigue life remained relatively unaffected. Phase contrast micrographs obtained from vulcanisates containing 0 and 6% interpolymer gave no indication of the reason for this behaviour. Phase contrast micrographs obtained from solutions of the same two blends (Frames 5.12 and 5.13), however, suggested that the interpolymer may form a third discrete phase within the GS : NR matrix. It may be possible that this phase would act as a stress raiser, initiating flaws in the original GS : NR vulcanisate and hence causing premature failure of the vulcanisate. Such behaviour would probably not be apparent in the cut initiated fatigue samples since the introduced notch is substantially larger than the size of the interpolymer phase.

In retrospect, a better approach for the use of the GS : NR interpolymer may have been to use it as an additive in Neoprene GS. If sufficient compatibility were achieved, an interconnecting network may have been formed at NR levels as low as 10-15% of the blend giving possibly novel fatigue characteristics.

5.4.1 Determination of the Cross-link Density of Natural Rubber and Neoprene GS in a 50 : 50 GS : NR Vulcanisate

As noted in section 5.2.3 (Table 5.2), the natural rubber component in a 50 : 50 GS : NR vulcanisate appeared to be cured, despite the fact that no additives, other than those required

to cure Neoprene GS had been added to the formulation. The reason for this appeared to be a result of the high (2.3%) level of sulphur present in Neoprene GS.

Formulations A and B, Table 4.10, were prepared to ensure no other additives were present in the original GS : NR formulation supplied by the manufacturer which alone would cure natural rubber. As may be seen (Table 4.10) no cure response was observed for either of the formulations after one hour at 150°C on the Monsanto rheometer.

This suggested that the necessary vulcanisation ingredients required to cure the NR in the GS : NR blend were provided by Neoprene GS. Since curatives would need to be transported from one elastomer to the other to enable both to cure this raised the question of whether both components of the blend were cured to the same level or if one cured in preference to the other.

Using the preferential swelling technique described in sections 4.8.5 to 4.8.7, the cross-link densities (CLDs) of Neoprene GS and natural rubber in a 50 : 50 GS : NR vulcanisate (formulation E, Table 4.10) were determined as a function of cure time at 140°C (Tables 4.13 and 4.14 respectively).

Fig 4.15 shows the two elastomers in the blend exhibited very different cure characteristics. Neoprene GS continued to increase in cross-link density (CLD) with increasing cure time.

The natural rubber phase of the blend, however, appeared to decrease in CLD from a maximum after only 10 minutes vulcanisation. The behaviour of the natural rubber phase appears to be explicable in terms of the reversion characteristics exhibited by many conventionally cured natural rubber vulcanisates. This also suggested that a primarily polysulphidic network was formed in natural rubber (these being more susceptible to breakdown during extended vulcanisation).

The level of cure occurring in the two phases of the blend was also very different. As may be seen, the natural rubber phase exhibited a relatively low cross-link density in comparison to the Neoprene GS phase. It must be stated, however, that the apparently high CLDs observed for the GS phase may be partly due to the high ν_r values obtained using the preferential swelling method. It has been shown⁽¹⁸⁵⁾ that the value of C_2 (equation 2-5, section 2.2.3) used in the calculation of CLD from compression modulus is very small when the ν_r value of the swollen vulcanisate is less than 0.3. Above this value of ν_r , however, deviations occur from statistical theory. Under such conditions, the C_2 parameter becomes increasingly larger and hence exerts a greater influence on the calculated cross-link density of the material. As may be seen in Table 4.13, ν_r values of 0.34 to 0.39 were observed for the GS phase in the blend. Some slight adjustment would, therefore, ideally have to be made to obtain accurate values of CLD. For a vulcanisate comprising one rubber, this could have been achieved using swollen compression to

calculate the C_2 parameter, however, similar measurements on vulcanisates of a blend of two elastomers render meaningless results in view of the physical interactions of the two phases.

The uncertainty as to the precise CLD of the GS phase should not detract from the more general observation that Neoprene GS exhibited a significantly higher level of cure than natural rubber in the vulcanisate. This is particularly valid in view of the fact that the recorded ν_r values for the GS domains are quite close to 0.3 and any adjustment is likely to be relatively small.

The existence of a highly cross-linked GS phase and a lightly cross-linked NR phase in GS : NR vulcanisates appeared to substantiate many of the suggestions outlined in section 5.3.1 to explain the uncut and cut initiated fatigue behaviour of these materials.

5.4.2 Effect of Cure Time on the Network Structure of a Neoprene GS Vulcanisate

As described in section 1.6.6, the network structure of a vulcanisate exerts an appreciable effect on its fatigue performance. In section 5.3.1 it was suggested that the Neoprene GS in GS : NR blends, when present either as a continuous phase or interconnecting phase, determined the uncut fatigue resistance of the vulcanisates. The following work was therefore carried out to identify the network structure of

Neoprene GS with cure time and to eventually relate this structure to its fatigue behaviour.

From Table 4.18 (Fig 4.16) it appears that a predominantly polysulphidic network is formed in the early stages of the vulcanisation of Neoprene GS. At longer vulcanisation times a decrease in the number of polysulphidic cross-links is observed which corresponds with an increase in the number of di-sulphidic linkages. Unfortunately, no distinction could be made between S_1 and C-O-C cross-links (believed to be formed from ZnO, MgO vulcanisation) and the two are therefore grouped together. As may be seen, however, there is a gradual increase in S_1 and ether linkages with increasing cure time.

In determining the number of polysulphidic cross-links it is necessary to remember that S_x units are present along the backbone of the Neoprene GS. This may well be responsible for the apparently high number of polysulphidic linkages present during the early stages of vulcanisation.

The presence of sulphidic cross-links in Neoprene GS is likely to confer good fatigue properties to the vulcanisate. This appears particularly true in view of the poor fatigue resistance of Neoprene W vulcanisates. The ether linkages believed to be present in W vulcanisates are likely to behave in a similar manner to C-C cross-links in that once they are broken, they are incapable of reforming. This would lead to a gradual

deterioration of the elastomer network resulting in early failure. Polysulphidic cross-links, however, when broken, are believed to reform when the elastomer network is in a less strained state. In this way, the cyclic stresses acting on the vulcanisate during fatigue are reduced and better fatigue characteristics observed than with a predominantly C-C network.

5.4.3 Effect of Blending on the Network Structure of Neoprene GS and Natural Rubber in a 50 : 50 GS : NR Vulcanisate

This work was carried out to determine the effect of blending on the network structure formed in GS : NR vulcanisates and to relate this information to the fatigue behaviour of the blends.

From Table 4.20 it appears that Neoprene GS vulcanised with zinc oxide and magnesium oxide (formulation C) contained 54.5% S_2 cross-links with lower percentages of S_x , S_1 and C-O-C linkages. Natural rubber, vulcanised with a conventional vulcanisation system (formulation I) exhibited almost equal levels of S_1 , S_2 and S_x cross-links. A 50 : 50 GS : NR vulcanisate cured only with zinc oxide and magnesium oxide (formulation E), however, formed an extremely lightly cross-linked gel after treatment with the propan-2-thiol/piperidine probe. Chlorine determinations carried out on the dried gel indicated it contained 73% Neoprene GS : 27% natural rubber. Approximately half of the natural rubber in the blend, therefore, appeared to be entirely bound into the network with polysulphidic cross-links. When swollen in toluene

to determine the cross-link density of the gel, it disintegrated on handling suggesting that predominantly polysulphidic cross-links were also formed in the GS phase of the vulcanisate.

To allow a more accurate determination of the network structure to be carried out, formulation H (Neoprene GS) and formulation G (50 : 50 GS : NR blend) were prepared containing a conventional sulphur vulcanisation system. From Table 4.20 it may be seen that the Neoprene GS vulcanisate (formulation H) showed little change in network structure when compared with a vulcanisate cured only with zinc oxide and magnesium oxide. For the 50 : 50 GS : NR vulcanisate (formulation G), however, a very high level (78%) of polysulphidic cross-links were observed. Comparing these values with vulcanisates of the two homopolymers in the blend (formulations C, H and I) it appears that the blending of Neoprene GS and natural rubber leads to the formation of a predominantly polysulphidic network, particularly when a standard chloroprene rubber vulcanisation system is used.

In view of this discovery, which appears to agree with earlier observations⁽¹⁵⁶⁾, it appears feasible that a degree of the improvement in the fatigue behaviour of certain GS : NR vulcanisates may be associated with a marked change in the network structure of the component elastomers. Additionally, the low degree of cross-linking (section 5.4.1) and the predominantly polysulphidic nature of the NR phase of these blends may allow a degree of set to occur in the vulcanisate

during fatigue. This would reduce cyclic stresses acting on the sample and enhance both the uncut and cut initiated fatigue behaviour of these vulcanisates.

5.4.4 Effect of Fatigue on the Network Structure of Neoprene GS and Natural Rubber Vulcanisates

Fatigue behaviour is known to be affected by the network structure of a vulcanisate^(72,91,104-108). The changes in network structure occurring during fatigue also appear to influence the lifetime of the material^(112,113). The following work was, therefore, carried out to determine if the changes in network structure occurring in GS and NR vulcanisates may be related to their very different fatigue characteristics.

From Table 4.25 the natural rubber vulcanisate (formulation I, Table 4.10) exhibited a slight decrease in CLD during fatigue testing. From Fig 4.17, a gradual decrease in the number of polysulphidic cross-links was also observed. This corresponded to an increased level of disulphidic linkages being formed during fatigue. The level of monosulphidic cross-links present in the vulcanisate at each stage of testing, however, appeared to remain relatively constant.

In comparison (Fig 4.18, Table 4.30), the network structure of the Neoprene GS vulcanisate (formulation C, Table 4.10) showed only minor changes during fatigue testing. These were manifested

as a gradual increase in the level of S_1 and C-O-C linkages in the material and appeared to correspond to the increasing CLD of the vulcanisate during fatigue.

The observed cross-link shortening occurring in the NR vulcanisate appears to agree with the findings of other investigators^(112,113,117) and may be partly responsible for the poorer uncut fatigue resistance of the natural rubber specimens. The gradual decrease in cross-link density observed may be associated with the mechano-oxidative degradation occurring in the elastomer which would give rise to low fatigue resistance.

The structure and relative stability of the Neoprene GS network appears to correlate with its high fatigue resistance. Not only is there a reasonable proportion of S_x cross-links present but an appreciable level of main-chain modification is inherent in the elastomer as a result of the polymerisation route employed.

The gradual increase in CLD of Neoprene GS during fatigue testing may relate to the rapid failure of these vulcanisates. This increase appears not to be a result of maturation reactions occurring in the elastomer and, therefore, appears likely to be the result of oxidation. During fatigue, greater cyclic stresses would be exerted in the vulcanisate if the modulus increased. This may push the vulcanisate closer to its critical tear strength and give rise to the smooth failure surfaces observed for these samples.

Assuming the fatigue behaviour of the homopolymers is unaffected by blending, the increasing CLD of the GS phase may be partly counter-balanced by the decrease in CLD of the NR phase giving rise to a vulcanisate with a relatively constant modulus. Such behaviour may again be partly responsible for the good fatigue characteristics of certain GS : NR vulcanisates.

5.5 Effect of Additional Curatives on the Fatigue Behaviour of a 50 : 50 GS : NR Vulcanisate

The predominantly polysulphidic network formed in a 50 : 50 GS : NR vulcanisate cured only with zinc oxide and magnesium oxide (section 5.4.3) and the disproportionate level of cross-linking occurring in the two phases of this blend (section 5.4.1) were believed to exert some influence on its fatigue behaviour. The following work was, therefore carried out to observe the effect of the addition of curatives, capable of affecting both the above parameters on the fatigue characteristics of a 50 : 50 GS : NR vulcanisate. All the formulations shown in Table 4.31 were cured to similar solvent swelling ratios which, to a first approximation, gave vulcanisates of similar modulus.

5.5.1 Effect of Increasing Additions of Sulphur on the Fatigue Behaviour of a 50 : 50 GS : NR Vulcanisate

This approach was designed to retain the predominantly

polysulphidic nature of the GS : NR network but to observe the effect of a more evenly distributed CLD between the two phases of the blend. Using sulphur added directly to the formulations the NR phase of the blend should not have to rely on curatives diffusing from Neoprene GS to cause vulcanisation, hence, the difference in CLD of the two phases should be reduced.

From Fig 4.19 a trend of increasing uncut and cut initiated fatigue life with increasing sulphur content was exhibited for these vulcanisates (formulations A-F, Table 4.31). It appears, therefore, that a more evenly distributed CLD in GS : NR vulcanisates is conducive to good fatigue resistance. This observation seems to correlate with the excellent fatigue resistance of the 75 : 25 GS : NR vulcanisates investigated in section 5.3.1. At higher GS : NR ratios, more sulphur would be available to the NR phase for vulcanisation. Under such circumstances, the NR phase of the blend is probably more highly cross-linked than in a 50 : 50 GS : NR vulcanisate and from the trends seen here this is likely to improve the fatigue resistance of the blend. Unfortunately, however, insufficient time was available to carry out the necessary probe work to confirm the above suggestions.

5.5.2 Effect of the Addition of CBS on the Fatigue Behaviour of a 50 : 50 GS : NR Vulcanisate

This evaluation was used to determine if sulphur from Neoprene GS could be used more efficiently to vulcanise the NR phase of the

blend. In addition to the increased CLD of the NR matrix, larger additions of accelerator should gradually change the natural rubber phase from a predominantly polysulphidic network to one containing higher levels of di and monosulphidic cross-links. By comparing the fatigue results for this group of vulcanisates (formulations A, G-J, Table 4.31) with those obtained in the previous section it was expected that the effect on fatigue of increasing di- and monosulphidic linkages in the blend may be monitored.

Fig 4.20 (Table 4.31) shows that increasing additions of CBS cause a marked reduction in both the uncut and cut initiated fatigue life of the vulcanisates. A comparison of Figs 4.19 and 4.20 would suggest, therefore, that, as with the homopolymers, the presence of a polysulphidic network structure is conducive to the good fatigue resistance of GS : NR blends whilst higher levels of S_1 and S_2 cross-links give rise to vulcanisates having poorer fatigue lives.

5.5.3 Effect of the Addition of TMTD on the Fatigue Behaviour of a 50 : 50 GS : NR Vulcanisate

To ensure the level of mono- and disulphidic cross-linking was increased in the 50 : 50 GS : NR blend, a second group of vulcanisates (formulations K - M, Table 4.31) were prepared containing increasing levels of a sulphur donor (tetramethylthiuram-disulphide, TMTD) and the uncut and cut initiated

fatigue lives of the vulcanisates determined. From Fig 4.21 comparable behaviour to that observed for increasing additions of CBS (Fig 4.22) were exhibited. This appeared to confirm the poorer fatigue behaviour associated with a predominantly di- and monosulphidic network outlined in section 5.5.2.

CHAPTER SIX

CONCLUSIONS AND SUGGESTIONS FOR FURTHER WORK

6.1 Summary

The presence of NR in GS : NR blends appears to exert three beneficial effects on fatigue behaviour. Firstly, the softer NR elastomer decreases the modulus of the blend thereby decreasing the cyclic stresses acting on the vulcanisate during the fatigue process. Secondly, the high strain crystallisation behaviour of the natural rubber phase prevents rapid growth of small flaws which lead to early failure of Neoprene GS vulcanisates. Finally, the addition of NR to Neoprene GS causes a marked change in the network structure of the vulcanisate from one containing a fairly even distribution of S_x , S_2 , S_1 and C-O-C cross-links to one containing almost totally polysulphidic linkages. The heterogeneous nature of these blends also influences their fatigue characteristics. The formation of an interconnecting network enhances both the uncut and cut initiated fatigue resistance of the vulcanisate. This effect appears likely to be a function of the smaller flaw size occurring in the GS phase of the vulcanisate before being stopped by the NR phase and by the fact that with an interconnecting network, no easy failure path is available. By preventing rapid failure, therefore, the excellent fatigue characteristics of the Neoprene GS exerts its influence on the vulcanisate for a longer time.

In comparison, the GS : W vulcanisates are homogeneous and exhibit physical properties intermediate between the two homopolymers. The lower strain crystallisation behaviour of the chloroprene rubbers in comparison to natural rubber appears to give rise to the smooth failure of the vulcanisates. The network structure also appears likely to influence the fatigue behaviour of these blends. The higher levels of ether cross-links, likely to be formed with increasing additions of Neoprene W, appear to exhibit none of the beneficial effects of the polysulphidic network found in GS : NR vulcanisates, giving rise instead to the poorer fatigue properties associated with, for example, peroxide cured NR formulations.

6.2 Conclusions

- (1) A filled 75 : 25 GS : W vulcanisate supplied by the manufacturer exhibited greater uncut and cut initiated fatigue resistance than a filled 50 : 50 GS : NR blend.
- (2) The same vulcanisates displayed very different fatigue failure surfaces, the all-chloroprene blend being smooth, whilst the GS : NR formulation was rough.
- (3) Immersion of the above vulcanisates in water for extended periods caused a marked decrease in the fatigue resistance of the GS : W blend whilst only minor changes were observed for the GS : NR vulcanisate. This appeared to

- be due to differences in the water solubility of the two antioxidant systems used in each blend.
- (4) Heat ageing of the above vulcanisates followed by fatigue testing caused marked decreases in the fatigue resistance of both.
 - (5) Reducing the carbon black loading in GS : W vulcanisates improves their fatigue resistance but has little effect on their smooth fatigue failure mechanism.
 - (6) GS : W vulcanisates appear to form homogeneous blends exhibiting physical properties intermediate between those of the homopolymers.
 - (7) Increasing the level of Neoprene W in GS : W blends decreases the fatigue resistance and tear strength of the vulcanisates.
 - (8) The smooth fatigue failure surfaces of Neoprene GS, Neoprene W and their blends appear to be a function of their low strain crystallisation behaviour.
 - (9) Neoprene GS : NR and Neoprene W : NR blends are heterogeneous.
 - (10) The NR phase in a 50 : 50 GS : NR vulcanisate containing only zinc oxide and magnesium oxide is apparently cured by

sulphur from the Neoprene GS. The cross-link network formed in this vulcanisate appears to be predominantly polysulphidic.

- (11) The GS phase in a 50 : 50 GS : NR vulcanisate cured only with zinc oxide and magnesium oxide is significantly more highly cross-linked than the natural rubber phase.
- (12) Increasing the CLD of NR in relation to the GS phase in the above 50 : 50 blend increases the fatigue life of the vulcanisate only when a monosulphidic network is formed. Similar changes occurring as a result of the formation of a predominantly di- or polysulphidic network decrease the fatigue resistance of the vulcanisate.
- (13) Little or no change in network structure is observed in GS vulcanisates during fatigue testing.
- (14) A decrease in the level of polysulphidic and an increase in the level of di- and monosulphidic cross-links appears to occur in a NR vulcanisate during fatigue.
- (15) A decrease in the level of polysulphidic cross-links is observed in Neoprene GS cured with zinc oxide and magnesium oxide with increasing cure time which appears to coincide with increasing levels of di- and monosulphidic linkages.

- (16) Increasing the level of natural rubber in GS : NR blends increases the roughness of the fatigue failure surface of the vulcanisates.
- (17) An optimum in the uncut and cut initiated fatigue resistance of GS : NR vulcanisates is observed with the formation of an interconnecting network morphology.
- (18) When Neoprene GS exists as the continuous phase in GS : NR blends, high fatigue lives with smooth failure surfaces are obtained.
- (19) When an interconnecting network is formed in GS : NR vulcanisates, high uncut and cut initiated fatigue lives and rough failure surfaces are observed.
- (20) When natural rubber is present as the continuous phase in GS : NR blends, poor fatigue resistance and rough failure surfaces are obtained.
- (21) Under isostress fatigue conditions, increasing the level of NR in GS : NR blends decreases the fatigue resistance of the vulcanisates.
- (22) The addition of a GS : NR interpolymer to a 50 : 50 GS : NR blend decreases the uncut fatigue resistance of the blend and appears to exist as a third phase in the formulation

which may act as a stress raiser during fatigue.

- (23) The poor fatigue resistance of W : NR vulcanisates appeared to be related to the fact that NR, although constituting the continuous network in the two W : NR blends investigated, is not cross-linked. The weaker NR network, therefore, gave rise to blends exhibiting poorer fatigue lives than either of the constituent elastomers.

6.3 Suggestions for Future Work

- (1) The cross-link network at a number of GS : NR ratios should be investigated to determine whether the polysulphidic nature of the vulcanisate is prevelant at lower NR loadings. These results should then be related to the fatigue behaviour of the blends.
- (2) It appears that the formation of an interconnecting network at high GS : low NR ratios gives rise to a material with unusually high fatigue resistance. Further work in the GS : NR range 90 : 10 to 60 : 40 would be advisable to determine exactly where the optimum fatigue properties lay and how these properties are affected by the dispersion of the network formed.

- (3) The effect on fatigue of the addition of carbon black to the 75 : 25 GS : NR blend indentified here as having good fatigue resistance should be investigated.

- (4) The stain crystallisation behaviour of Neoprene GS, Neoprene W, natural rubber and their blends should be assessed and compared to the uncut and cut initiated fatigue resistance of the vulcanisates.

APPENDIX ONE

TABLES

Table 1.1 Physical properties of all cis and all-trans
1,4-polychloroprenes

| Structure | All cis ⁽⁴⁷⁾ | All trans ⁽⁴⁸⁾ |
|---------------------------------|-------------------------|---------------------------|
| % 1,4 | 95+ | 98+ |
| % head to tail | 50-60 | 98 |
| % head to head | 25-20 | - |
| % tail to tail | 25-20 | - |
| Properties: T _g (°C) | 20 | -45 |
| T _m (°C) | 70 | 105 |
| Density (at 25°C) | 1.283 | 1.30 |

Table 3.1 Materials Suppliers Index

| <u>MATERIAL</u> | <u>SUPPLIER</u> |
|---|------------------------|
| Neoprene GS | Du Pont Ltd |
| Neoprene W | Du Pont Ltd |
| Natural rubber (SMR5-CV20) | Dunlop Ltd |
| Sevacarb MI black | Sevalco Ltd |
| Sevacarb FEF black | Sevalco Ltd |
| Zinc oxide (gold label) | Amalgamated Oxide Ltd |
| Magnesium oxide (Scorch guard O) | Hubron Sales Ltd |
| Nonox ZA (isopropyl para phenylene diamine) | ICI Ltd |
| Nonox B (aniline/acetone condensate) | ICI Ltd |
| Nonox DPPD (di-phenyl-para-phenylene diamine) | ICI Ltd |
| Stearic acid | Anchor Chemicals Ltd |
| Microcrystalline wax | Allied Chemicals Ltd |
| A C polyethylene wax | Allied Chemicals Ltd |
| White factice | Anchor Chemicals Ltd |
| Mercaptobenzthiazole disulphide (MBTS) | Monsanto Chemicals Ltd |
| Cyclohexylbenzthiazole sulphenamide (CBS) | Monsanto Chemicals Ltd |
| Tetramethyl thiuram disulphide (TMTD) | Monsanto Chemicals Ltd |
| Sulphur | Anchor Chemicals Ltd |
| Thiokol TP90B | Thiokol Products Ltd |
| NA-22 (ethylene-thio-urea) | Du Pont Ltd |

Table 3.2 Formulations used to establish operating conditions for fatigue testing

| | A | B | C | D |
|--------------------------|-----|-----|------|-----|
| Neoprene GS | 75 | 75 | 50 | 50 |
| Neoprene W | 25 | 25 | - | - |
| Natural rubber | - | - | 50 | 50 |
| Sevacarb MT | 125 | - | 35 | - |
| Sevacarb FEF | - | - | 22.5 | - |
| Zinc oxide | 5 | 5 | 5 | 5 |
| Magnesium oxide | 4 | 4 | 4 | 4 |
| MC wax | 4.5 | 4.5 | 4 | 4 |
| AC polyethylene wax | 5 | 5 | - | - |
| Stearic acid | 2 | 2 | 1 | 1 |
| Thiokol TP90B | 20 | - | - | - |
| Nonox ZA | 1.5 | 1.5 | - | - |
| Nonox B | - | - | 1 | 1 |
| Nonox DPPD | - | - | 0.3 | 0.3 |
| White factice | - | - | 5 | 5 |
| MBTS | - | - | 0.5 | 0.5 |
| Cure time @ 150°C (mins) | 25 | 28 | 16 | 18 |

Table 3.3 Effect of strain on the fatigue behaviour of a filled 75 : 25 GS : W vulcanisation (formulation A, Table 3.2)

| Fatigue Conditions | Sample Number | Fatigue life (k cycles) | | | |
|----------------------|---------------|-------------------------|--------------------|--------------------|--------------------|
| | | Maximum strain 61% | Maximum strain 68% | Maximum strain 78% | Maximum strain 89% |
| Uncut | 1 | 2500 | 2500 | 336 | 61 |
| | 2 | 2500 | 2500 | 302 | 39 |
| | 3 | 2500 | 2500 | 254 | 28 |
| | 4 | 2500 | 2500 | 229 | 24 |
| | JIS average | 2500 | 2500 | 307 | 47 |
| 0.85 mm diameter cut | 1 | 11.5 | 0.9 | 0 | - |
| | 2 | 9.5 | 0.6 | 0 | - |
| | 3 | 6.2 | 0.4 | 0 | - |
| | 4 | 5.8 | 0.3 | 0 | - |
| | JIS average | 9.7 | 0.7 | 0 | - |
| 0.30 mm diameter cut | 1 | 129 | 14.3 | 2.5 | 0.6 |
| | 2 | 116 | 11.8 | 1.6 | 0.5 |
| | 3 | 108 | 10.8 | 1.5 | 0.4 |
| | 4 | 107 | 8.1 | 1.6 | 0.4 |
| | JIS average | 121 | 12.6 | 2.0 | 0.5 |

Table 3.4 Effect of strain on the fatigue behaviour of a filled 50 : 50 GS : NR vulcanisate (formulation

C, Table 3.2)

| Fatigue Conditions | Sample Number | Fatigue life (k cycles) | | | |
|----------------------|---------------|-------------------------|--------------------|--------------------|--------------------|
| | | Maximum strain 61% | Maximum strain 68% | Maximum strain 78% | Maximum strain 89% |
| Uncut | 1 | 2500 | 844 | 67.3 | 15.8 |
| | 2 | 2500 | 824 | 61.0 | 15.7 |
| | 3 | 2500 | 808 | 48.7 | 15.2 |
| | 4 | 2500 | 761 | 41.9 | 15.0 |
| | JIS average | 2500 | 826 | 61.0 | 15.6 |
| 0.30 mm diameter cut | 1 | 35.9 | 10.7 | 2.3 | 0.7 |
| | 2 | 35.7 | 8.4 | 1.9 | 0.5 |
| | 3 | 34.1 | 8.0 | 1.6 | 0.5 |
| | 4 | 30.2 | 8.0 | 0.7 | 0.4 |
| | JIS average | 35.1 | 9.5 | 2.0 | 0.6 |

Table 3.5 Effect of strain on the fatigue behaviour of an unfilled 75 : 25 GS : W vulcanisate

(formulation B, Table 3.2)

| Fatigue Conditions | Sample Number | Fatigue life (k cycles) | | | |
|--------------------|---------------|-------------------------|--------------------|--------------------|--------------------|
| | | Maximum strain 61% | Maximum strain 68% | Maximum strain 78% | Maximum strain 89% |
| Uncut | 1 | 2500 | 2500 | 2500 | 482 |
| | 2 | 2500 | 2500 | 2500 | 415 |
| | 3 | 2500 | 2500 | 2392 | 312 |
| | 4 | 2500 | 2500 | 2185 | 291 |
| | JIS average | 2500 | 2500 | 2500 | 426 |
| 0.30 diameter cut | 1 | 2084 | 112 | 4.7 | 0.4 |
| | 2 | 1637 | 112 | 3.1 | 0.4 |
| | 3 | 1418 | 109 | 3.0 | 0.3 |
| | 4 | 1401 | 95 | 2.0 | 0.1 |
| | JIS average | 1815 | 110 | 3.8 | 0.4 |

Table 3.6 Effect of strain on the fatigue behaviour of an unfilled 50 : 50 GS : NR vulcanisate
(formulation D, Table 3.2)

| Fatigue Conditions | Sample Number | Fatigue life (k cycles) | | | |
|----------------------|---------------|-------------------------|--------------------|--------------------|--------------------|
| | | Maximum strain 61% | Maximum strain 68% | Maximum strain 78% | Maximum strain 89% |
| Uncut | 1 | 2500 | 2399 | 1408 | 260 |
| | 2 | 2500 | 2047 | 1357 | 241 |
| | 3 | 2500 | 2009 | 1198 | 239 |
| | 4 | 2500 | 1898 | 1107 | 218 |
| | JIS average | 2500 | 2204 | 1342 | 248 |
| 0.30 mm diameter cut | 1 | 931 | 346 | 38.6 | 1.7 |
| | 2 | 927 | 316 | 23.0 | 1.7 |
| | 3 | 926 | 309 | 15.9 | 1.2 |
| | 4 | 904 | 275 | 13.1 | 1.1 |
| | JIS average | 927 | 326 | 29.1 | 1.6 |

Table 3.7 Formulations used to determine equilibrium swelling time

| | A | B |
|---|-----|-----|
| Neoprene GS | 100 | - |
| Natural rubber | - | 100 |
| Zinc oxide | 5 | 5 |
| Magnesium oxide | 4 | 4 |
| Sulphur | - | 2.5 |
| CBS | - | 0.5 |
| Cure time @ 150°C (mins) | 30 | 20 |
| Time to equilibrium swelling @ 25°C (hrs) | | |
| Toluene | 10 | 10 |
| Hexane | - | 11 |
| DMF | 16 | - |

Table 3.8 Determination of swelling time for Neoprene GS vulcanisates in toluene and DMF

| Swelling time at 25°C (h) | v_r | | | | | |
|---------------------------------|---------------|--------|--------|---------------|--------|--------|
| | Toluene | | | DMF | | |
| | Sample Number | | | Sample Number | | |
| | 1 | 2 | 3 | 1 | 2 | 3 |
| 2 | 0.2217 | 0.2240 | 0.2258 | 0.3852 | 0.3799 | 0.3845 |
| 4 | 0.1995 | 0.1976 | 0.1956 | 0.3748 | 0.3700 | 0.3695 |
| 6 | 0.1910 | 0.1942 | 0.1945 | 0.3501 | 0.3476 | 0.3486 |
| 10 | 0.1826 | 0.1839 | 0.1814 | 0.3308 | 0.3362 | 0.3324 |
| 24 | 0.1816 | 0.1803 | 0.1806 | 0.3184 | 0.3171 | 0.3204 |
| 30 | 0.1804 | 0.1794 | 0.1794 | 0.3206 | 0.3215 | 0.3189 |

Table 3.9 Determination of swelling time for a natural rubber vulcanisate in toluene and hexane

| Swelling time at 25°C (h) | v r | | | | | |
|---------------------------------|---------------|--------|--------|---------------|--------|--------|
| | Toluene | | | Hexane | | |
| | Sample Number | | | Sample Number | | |
| | 1 | 2 | 3 | 1 | 2 | 3 |
| 2 | 0.1822 | 0.1829 | 0.1859 | 0.2476 | 0.2493 | 0.2480 |
| 4 | 0.1500 | 0.1526 | 0.1548 | 0.2327 | 0.2296 | 0.2285 |
| 6 | 0.1482 | 0.1439 | 0.1445 | 0.2223 | 0.2243 | 0.2220 |
| 10 | 0.1348 | 0.1390 | 0.1356 | 0.2148 | 0.2165 | 0.2155 |
| 24 | 0.1344 | 0.1341 | 0.1348 | 0.2163 | 0.2166 | 0.2191 |
| 30 | 0.1342 | 0.1344 | 0.1351 | 0.2130 | 0.2143 | 0.2131 |

Table 3.10 Determination of reaction time for Neoprene GS
vulcanisates with methyl iodide

Methyl iodide/mercuric iodide @ 25°C

| Time (h) | ν_r values | | | | | |
|----------|----------------|--------|--------|--------|--------|--------|
| | 0 | 2 | 4 | 8 | 22 | 46 |
| Sample 1 | 0.1804 | 0.1724 | 0.1729 | 0.1855 | 0.1861 | 0.1919 |
| Number 2 | 0.1823 | 0.1709 | 0.1705 | 0.1855 | 0.1850 | 0.1909 |
| 3 | 0.1809 | 0.1726 | 0.1724 | 0.1741 | 0.1852 | 0.1919 |
| Average | 0.1812 | 0.1720 | 0.1719 | 0.1750 | 0.1854 | 0.1916 |

Table 3.11 Determination of reaction time of Neoprene GS vulcanisates with methyl iodide under vacuum

(a) Methyl iodide/vacuum @ 80°C

| Time (h) | ν_r values | | | | | |
|----------|----------------|--------|--------|--------|--------|--------|
| | 0 | 4 | 8 | 22 | 40 | 76 |
| Sample 1 | 0.1804 | 0.1775 | 0.1815 | 0.1938 | 0.2044 | 0.2057 |
| Number 2 | 0.1823 | 0.1762 | 0.1809 | 0.1922 | 0.2034 | 0.2043 |
| 3 | 0.1809 | 0.1764 | 0.1818 | 0.1936 | 0.2036 | 0.2059 |
| Average | 0.1812 | 0.1767 | 0.1814 | 0.1932 | 0.2038 | 0.2153 |

(b) Neoprene GS/vacuum @ 80°C

| Time (h) | ν_r values | | | | | |
|----------|----------------|--------|--------|--------|--------|--------|
| | 0 | 4 | 8 | 22 | 40 | 76 |
| Sample 1 | 0.1804 | 0.1815 | 0.1813 | 0.1804 | 0.1815 | 0.1835 |
| Number 2 | 0.1813 | 0.1813 | 0.1819 | 0.1817 | 0.1827 | 0.1843 |
| 3 | 0.1809 | 0.1811 | 0.1809 | 0.1821 | 0.1821 | 0.1842 |
| Average | 0.1812 | 0.1813 | 0.1814 | 0.1814 | 0.1821 | 0.1840 |

Table 3.12 Determination of reaction times for Neoprene GS vulcanisates with thiol/amine probes

(a) Propan-2-thiol/piperidine

| Time (h) | ν_r values | | | | | | |
|----------|----------------|--------|--------|--------|--------|--------|--------|
| | 0 | 1 | 2 | 4 | 8 | 16 | 22 |
| Sample 1 | 0.1804 | 0.1748 | 0.1693 | 0.1632 | 0.1594 | 0.1598 | 0.1585 |
| Number 2 | 0.1823 | 0.1754 | 0.1708 | 0.1640 | 0.1587 | 0.1591 | 0.1592 |
| 3 | 0.1809 | 0.1774 | 0.1702 | 0.1619 | 0.1580 | 0.1589 | 0.1586 |
| Average | 0.1812 | 0.1758 | 0.1701 | 0.1630 | 0.1590 | 0.1593 | 0.1588 |

(b) n-Hexan-thiol/piperidine

| Time (h) | ν_r values | | | | | | | |
|----------|----------------|--------|--------|--------|--------|--------|--------|--------|
| | 0 | 4 | 8 | 15 | 24 | 30 | 42 | 76 |
| Sample 1 | 0.1804 | 0.1318 | 0.1247 | 0.1184 | 0.1055 | 0.1031 | 0.1023 | 0.1057 |
| Number 2 | 0.1823 | 0.1332 | 0.1235 | 0.1194 | 0.1047 | 0.1027 | 0.1033 | 0.1042 |
| 3 | 0.1809 | 0.1331 | 0.1235 | 0.1099 | 0.1049 | 0.1029 | 0.1019 | 0.1049 |
| Average | 0.1812 | 0.1327 | 0.1239 | 0.1159 | 0.1050 | 0.1029 | 0.1025 | 0.1049 |

Table 3.13 Determination of GS : NR interpolymer formation

Formulation (a), section 3.7.4

Weight of rubber 250 ml chloroform = 4.4671 g GS + 4.4656 g NR = 8.9327 g

| Methanol added (mls) | Weight precipitated (g) | Weight percent precipitated |
|-------------------------|----------------------------|--------------------------------|
| 1.0 | 0.0141 | 7.89 |
| 1.02 | 0.0168 | 9.40 |
| 1.03 | 0.0193 | 10.80 |
| 1.05 | 0.0140 | 7.84 |
| 1.07 | 0.0181 | 10.13 |
| 1.09 | 0.0570 | 31.91 |
| 1.1 | 0.0799 | 44.72 |
| 1.12 | 0.0815 | 45.62 |
| 1.17 | 0.0793 | 44.39 |
| 1.20 | 0.0836 | 46.79 |
| 1.23 | 0.0867 | 48.53 |
| 1.26 | 0.0842 | 47.13 |
| 1.30 | 0.0862 | 48.25 |
| 1.31 | 0.0969 | 54.24 |
| 1.33 | 0.1216 | 68.06 |
| 1.34 | 0.1463 | 81.89 |
| 1.35 | 0.1677 | 93.87 |
| 1.4 | 0.1710 | 95.72 |
| 1.42 | 0.1735 | 97.12 |
| 1.45 | 0.1752 | 98.07 |
| 1.48 | 0.1749 | 97.90 |
| 1.50 | 0.1755 | 98.23 |

Table 3.14 Determination of GS : NR interpolymer formation

Formulation (b), section 3.7.4

Weight of rubber in 250 ml of chloroform = 9.4165 g

| Methanol added (mls) | Weight precipitated (g) | Weight percent precipitated |
|----------------------|-------------------------|-----------------------------|
| 1.0 | 0.0172 | 9.13 |
| 1.03 | 0.0160 | 8.50 |
| 1.05 | 0.0205 | 10.89 |
| 1.08 | 0.0319 | 16.94 |
| 1.10 | 0.0256 | 13.59 |
| 1.11 | 0.0726 | 38.55 |
| 1.13 | 0.0788 | 41.84 |
| 1.15 | 0.0804 | 42.69 |
| 1.18 | 0.0793 | 42.11 |
| 1.20 | 0.0780 | 41.42 |
| 1.23 | 0.0785 | 41.68 |
| 1.26 | 0.0837 | 44.44 |
| 1.28 | 0.0871 | 46.25 |
| 1.29 | 0.1742 | 92.50 |
| 1.30 | 0.1591 | 84.48 |
| 1.34 | 0.1839 | 97.65 |
| 1.36 | 0.1809 | 96.05 |
| 1.39 | 0.1860 | 98.76 |
| 1.43 | 0.1853 | 98.36 |
| 1.45 | 0.1874 | 99.51 |
| 1.50 | 0.1850 | 98.23 |

Table 3.15 Determination of GS : NR interpolymer formation

Formulation (c), section 3.7.4

Weight of rubber in 250 ml chloroform = 8.8830 g

| Methanol added (mls) | Weight precipitated (g) | Weight percent precipitated |
|-------------------------|----------------------------|--------------------------------|
| 1.0 | 0.0124 | 6.98 |
| 1.02 | 0.0143 | 8.05 |
| 1.03 | 0.0143 | 8.05 |
| 1.05 | 0.0127 | 7.15 |
| 1.07 | 0.0231 | 13.00 |
| 1.08 | 0.0380 | 21.39 |
| 1.1 | 0.0405 | 22.80 |
| 1.12 | 0.0439 | 24.71 |
| 1.13 | 0.0421 | 23.70 |
| 1.14 | 0.0473 | 26.62 |
| 1.15 | 0.0658 | 37.04 |
| 1.17 | 0.0674 | 37.94 |
| 1.19 | 0.0644 | 36.25 |
| 1.20 | 0.0659 | 37.09 |
| 1.21 | 0.0877 | 49.36 |
| 1.24 | 0.0961 | 54.09 |
| 1.27 | 0.0988 | 55.61 |
| 1.29 | 0.1034 | 58.20 |
| 1.31 | 0.1002 | 56.40 |
| 1.33 | 0.1317 | 74.13 |
| 1.36 | 0.1665 | 93.72 |
| 1.40 | 0.1720 | 96.81 |
| 1.43 | 0.1748 | 98.39 |
| 1.46 | 0.1686 | 94.90 |
| 1.50 | 0.1723 | 96.98 |

Table 4.1 Effect of antioxidant depletion on the fatigue behaviour

of 75 : 25 GS : W and 50 : 50 GS : NR vulcanisates

Formulations A and C, Table 3.2

| Conditioning before fatigue | Sample number | Uncut fatigue life (k cycles) | |
|---|---------------|-------------------------------|----------------------------|
| | | Formulation A Table 3.2 | Formulation B Table 3.2 |
| Unaged | 1 | 321 | 72.4 |
| | 2 | 316 | 65.0 |
| | 3 | 269 | 41.3 |
| | 4 | 239 | 40.2 |
| | JIS average | 317 | 63.8 |
| Six weeks aged at room temperature in water | 1 | 41.7 | 55.3 |
| | 2 | 39.0 | 49.5 |
| | 3 | 36.5 | 39.7 |
| | 4 | 31.6 | 34.4 |
| | JIS average | 40.7 | 51.6 |
| Oven aged 70 hrs at 100°C | 1 | 10.9 | 21.5 |
| | 2 | 5.6 | 14.4 |
| | 3 | 3.6 | 13.1 |
| | 4 | 4.1 | 12.4 |
| | JIS average | 8.1 | 18.1 |

Table 4.2 Effect of carbon black content on the fatigue behaviour
of a 75 : 25 GS : W vulcanisate

| | A | B | C | D |
|-------------------------------------|-----|-----|-----|-----|
| Neoprene GS | 75 | 75 | 75 | 75 |
| Neoprene W | 25 | 25 | 25 | 25 |
| Sevacarb MT | 125 | 100 | 60 | 30 |
| Zinc oxide | 5 | 5 | 5 | 5 |
| Magnesium oxide | 4 | 4 | 4 | 4 |
| MC wax | 4.5 | 4.5 | 4.5 | 4.5 |
| AC polyethylene wax | 5 | 5 | 5 | 5 |
| Stearic acid | 2 | 2 | 2 | 2 |
| Thiokol TP 90B | 20 | 20 | 20 | 20 |
| Nonox ZA | 1.5 | 1.5 | 1.5 | 1.5 |
| Cure time @ 150°C (mins) | 25 | 25 | 27 | 27 |
| JIS average fatigue life (k cycles) | | | | |
| (a) uncut | 310 | 350 | 569 | 314 |
| (b) cut initiated | 142 | 293 | 447 | 387 |

Table 4.3 Effect of carbon black content on the fatigue behaviour
of a 75 : 25 GS : W vulcanisate

Formulations A-D, Table 4.2

| Carbon black content (phr) | Sample number | Fatigue life (k cycles) | |
|-------------------------------|---------------|-------------------------|---------------|
| | | Uncut | Cut initiated |
| 125 | 1 | 321 | 147 |
| | 2 | 321 | 132 |
| | 3 | 239 | 124 |
| | 4 | 189 | 119 |
| | JIS average | 310 | 142 |
| 100 | 1 | 356 | 309 |
| | 2 | 334 | 281 |
| | 3 | 308 | 280 |
| | 4 | 301 | 264 |
| | JIS average | 350 | 293 |
| 60 | 1 | 613 | 443 |
| | 2 | 548 | 428 |
| | 3 | 402 | 417 |
| | 4 | 400 | 410 |
| | JIS average | 569 | 447 |
| 30 | 1 | 391 | 381 |
| | 2 | 289 | 371 |
| | 3 | 129 | 367 |
| | 4 | 97.6 | 362 |
| | JIS average | 314 | 387 |

Table 4.4 Effect of GS : NR, GS : W and W : NR blend ratio on fatigue behaviour

| | A | B | C | D | E | F | G | H | I | J | K |
|-------------------------------------|-----|-----|------|------|-----|------|------|------|---------|------|------|
| Neoprene GS | 100 | - | - | 75 | 50 | 75 | 50 | 25 | - | - | - |
| Natural Rubber | - | 100 | - | 25 | 50 | - | - | - | 75 | 50 | 25 |
| Neoprene W | - | - | 100 | - | - | 25 | 50 | 75 | 25 | 50 | 75 |
| Zinc oxide | 5 | 5 | 5 | 5 | 5 | 5 | 5 | 5 | 5 | 5 | 5 |
| Magnesium oxide | 4 | 4 | 4 | 4 | 4 | 4 | 4 | 4 | 4 | 4 | 4 |
| NA-22 | - | - | - | - | - | - | - | - | 0.5 | 0.5 | 0.5 |
| Sulphur | - | 2.5 | - | - | - | - | - | - | - | - | - |
| CBS | - | 0.5 | - | - | - | - | - | - | - | - | - |
| Optimum cure time (mins) @ 150°C | 29 | 18 | 25 | 24 | 28 | 25 | 27 | 27 | No cure | 30 | 33 |
| Tear strength (N/test piece) | - | - | 89.5 | - | - | 94.8 | 93.1 | 91.5 | - | - | - |
| JIS average fatigue life (k cycles) | | | | | | | | | | | |
| (a) uncut | 947 | 232 | 194 | 2097 | 405 | 653 | 496 | 384 | - | 102 | 135 |
| (b) cut initiated | 211 | 140 | 28.6 | 482 | 461 | 139 | 56.8 | 43.3 | - | 49.7 | 32.7 |

Table 4.5 Effect of GS/W blend ratio on uncut and cut initiated fatigue behaviour

Formulations A, C, F, G, H, Table 4.4

| Blend ratio (wt %) | | Sample number | Fatigue life (k cycles) | |
|--------------------|------------|---------------|-------------------------|---------------|
| Neoprene GS | Neoprene W | | Uncut | Cut Initiated |
| 100 | 0 | 1 | 1005 | 232 |
| | | 2 | 879 | 205 |
| | | 3 | 795 | 138 |
| | | 4 | 724 | 130 |
| | | JIS average | 947 | 211 |
| 75 | 25 | 1 | 641 | 146 |
| | | 2 | 628 | 136 |
| | | 3 | 619 | 108 |
| | | 4 | 615 | 101 |
| | | JIS average | 653 | 139 |
| 50 | 50 | 1 | 504 | 68.1 |
| | | 2 | 492 | 49.4 |
| | | 3 | 406 | 35.2 |
| | | 4 | 395 | 27.9 |
| | | JIS average | 496 | 56.8 |
| 25 | 75 | 1 | 387 | 47.1 |
| | | 2 | 379 | 42.5 |
| | | 3 | 332 | 30.8 |
| | | 4 | 309 | 25.1 |
| | | JIS average | 384 | 43.3 |
| 0 | 100 | 1 | 220 | 32.0 |
| | | 2 | 162 | 28.4 |
| | | 3 | 159 | 17.4 |
| | | 4 | 138 | 14.0 |
| | | JIS average | 194 | 28.6 |

Table 4.6 Effect of W/NR blend ratio on uncut and cut initiated fatigue behaviour

Formulations B, C, J, K, Table 4.4

| Blend ratio (wt %) | | Sample number | Fatigue life (k cycles) | |
|--------------------|------------|---------------|-------------------------|---------------|
| Natural Rubber | Neoprene W | | Uncut | Cut Initiated |
| 100 | 0 | 1 | 294 | 147 |
| | | 2 | 280 | 128 |
| | | 3 | 221 | 125 |
| | | 4 | 198 | 116 |
| | | JIS average | 282 | 140 |
| 50 | 50 | 1 | 162 | 51.1 |
| | | 2 | 101 | 49.6 |
| | | 3 | 91.3 | 44.3 |
| | | 4 | 84.0 | 31.4 |
| | | JIS average | 102 | 49.7 |
| 25 | 75 | 1 | 139 | 33.2 |
| | | 2 | 128 | 30.9 |
| | | 3 | 116 | 30.4 |
| | | 4 | 115 | 28.0 |
| | | JIS average | 135 | 32.7 |
| 0 | 100 | 1 | 220 | 32.0 |
| | | 2 | 162 | 28.4 |
| | | 3 | 159 | 17.4 |
| | | 4 | 138 | 14.0 |
| | | JIS average | 194 | 28.6 |

Table 4.7 Effect of GS/NR blend ratio on uncut and cut initiated fatigue behaviour

Formulations A, B, D, E, Table 4.4

| Blend ratio (wt %) | | Sample number | Fatigue life (k cycles) | |
|--------------------|----------------|---------------|-------------------------|---------------|
| Neoprene GS | Natural Rubber | | Uncut | Cut Initiated |
| 100 | 0 | 1 | 1005 | 232 |
| | | 2 | 879 | 205 |
| | | 3 | 795 | 138 |
| | | 4 | 724 | 130 |
| | | JIS average | 947 | 211 |
| 75 | 25 | 1 | 2316 | 481 |
| | | 2 | 1897 | 462 |
| | | 3 | 1580 | 447 |
| | | 4 | 1490 | 428 |
| | | JIS average | 2097 | 482 |
| 50 | 50 | 1 | 421 | 455 |
| | | 2 | 380 | 449 |
| | | 3 | 352 | 421 |
| | | 4 | 327 | 419 |
| | | JIS average | 405 | 461 |
| 0 | 100 | 1 | 294 | 147 |
| | | 2 | 190 | 128 |
| | | 3 | 121 | 125 |
| | | 4 | 98.1 | 116 |
| | | JIS average | 232 | 140 |

Table 4.8 Effect of morphology on the fatigue behaviour of GS : NR vulcanisates

| | A | B | C | D | E | F | G | H | I |
|---|-------|------|------|------|------|------|------|------|------|
| Neoprene GS | 100 | | | | | 90 | 75 | 60 | 50 |
| Premasticated Neoprene GS | - | 90 | 75 | 60 | 50 | - | - | - | - |
| Natural rubber | - | 10 | 25 | 40 | 50 | - | - | - | - |
| Premasticated natural rubber | - | - | - | - | - | 10 | 25 | 40 | 50 |
| Zinc oxide | 5 | 5 | 5 | 5 | 5 | 5 | 5 | 5 | 5 |
| Magnesium oxide | 4 | 4 | 4 | 4 | 4 | 4 | 4 | 4 | 4 |
| Optimum cure time @ 150°C (mins) | 30 | 28 | 26 | 26 | 28 | 28 | 27 | 26 | 27 |
| Tear strength (N/test piece) | 100.1 | 92.0 | 86.9 | 68.2 | 64.9 | 83.5 | 62.4 | 60.1 | 59.8 |
| JIS average isostrain fatigue life (k cycles) | | | | | | | | | |
| (a) Uncut | 962 | 990 | 2508 | 1063 | 542 | 1049 | 1561 | 796 | 435 |
| (b) Cut initiated | 217 | 275 | 409 | 648 | 316 | 508 | 753 | 829 | 426 |
| Isostress fatigue conditions maximum strain (%) | 44 | 60 | 85 | 103 | 116 | 76 | 98 | 112 | 120 |
| JIS average isostress fatigue life (k cycles) | | | | | | | | | |
| (a) Uncut | 5506 | 2013 | 956 | 650 | 287 | 867 | 662 | 370 | 196 |
| (b) Cut initiated | 501 | 295 | 251 | 141 | 48.0 | 119 | 61.0 | 42.1 | 26.7 |

LIBRARY

Table 4.9 Effect of increasing interpolymer additions on the fatigue behaviour of a 50 : 50 GS : NR vulcanisate

| | A | B | C | D |
|-------------------------------------|-----|------|------|-----|
| Neoprene GS | 50 | 49.5 | 48.5 | 47 |
| Natural rubber | 50 | 49.5 | 48.5 | 47 |
| 50 : 50 GS/NR interpolymer | 0 | 1 | 3 | 6 |
| Zinc oxide | 5 | 5 | 5 | 5 |
| Magnesium oxide | 4 | 4 | 4 | 4 |
| Cure time @ 150°C (mins) | 28 | 28 | 26 | 26 |
| JIS average fatigue life (k cycles) | | | | |
| (a) Uncut | 466 | 403 | 221 | 120 |
| (b) Cut initiated | 439 | 439 | 444 | 448 |

Table 4.10 Formulations used for network analysis

| | A | B | C | D | E | F | G | H | I |
|----------------------------------|---------|---------|------|------|------|------|-----|-----|-----|
| Neoprene GS | - | - | 100 | - | 50 | - | 50 | 100 | - |
| Natural rubber | 100 | 100 | - | - | 50 | 50 | 50 | - | 100 |
| Neoprene W | - | - | - | 100 | - | 50 | - | - | - |
| Zinc oxide | 5 | 5 | 5 | 5 | 5 | 5 | 5 | 5 | 5 |
| Magnesium oxide | 4 | - | 4 | 4 | 4 | 4 | 4 | 4 | 4 |
| Sulphur | - | - | - | - | - | - | 2.5 | 2.5 | 2.5 |
| CBS | - | - | - | - | - | - | 0.5 | 0.5 | 0.5 |
| MC wax | 4 | - | - | - | - | 0.5 | - | - | - |
| NA-22 | - | - | - | 0.5 | - | - | - | - | - |
| Stearic acid | 1 | 1 | - | - | - | - | - | - | - |
| White factice | 5 | 5 | - | - | - | - | - | - | - |
| MBTS | 0.5 | 0.5 | - | - | - | - | - | - | - |
| Optimum cure time @ 150°C (mins) | No cure | No cure | 30 | 26 | 26 | 25 | 16 | 22 | 20 |
| Chlorine content (%) | | | | | | | | | |
| (a) before toluene extraction | - | - | 33.3 | 29.8 | 14.5 | 14.7 | - | - | 0 |
| (b) after toluene extraction | - | - | 31.6 | 32.4 | 13.4 | 30.6 | - | - | 0 |

L. J. ...

Table 4.11 Preferential swelling - calculation of χ constant for Neoprene GS in DMF

Formulation C, Table 4.10. Cure time, 30 mins @ 140°C

| Sample Number | h ₀ (cm) | A ₀ (cm ²) | F/Δh x 10 ⁻³ (g/cm) | C ₁ ERV x 10 ⁻⁴ (N/m ²) | M _c ERV PHYS x 10 ⁻³ (kg/kg mol) | v _r | χ |
|---------------|---------------------|-----------------------------------|-----------------------------------|--|---|----------------|--------|
| 1 | 0.3162 | 0.1441 | 4.587 | 16.46 | 9.26 | 0.3100 | 0.5796 |
| 2 | 0.3191 | 0.1475 | 4.464 | 15.79 | 9.65 | 0.2939 | 0.5671 |
| 3 | 0.3260 | 0.1564 | 4.546 | 15.49 | 9.84 | 0.3002 | 0.5740 |
| Average | - | - | - | 15.91 | 9.58 | 0.3014 | 0.5736 |

1. EDWARDS

Table 4.12 Preferential swelling - calculation of constant for NR in hexane

Formulation I, Table 4.10. Cured, 30 mins @ 140°C

| Sample Number | h_0 (cm) | A_0 (cm ²) | $F/\Delta h \times 10^{-3}$ (g/cm) | $C_{1ERV} \times 10^{-4}$ (N/m ²) | $M_{CERV} \text{ PHYS} \times 10^{-3}$ (kg/kg mol) | ν_r | χ |
|---------------|------------|--------------------------|---------------------------------------|--|---|---------|--------|
| 1 | 0.3310 | 0.1484 | 2.426 | 8.85 | 12.88 | 0.2153 | 0.4857 |
| 2 | 0.3321 | 0.1563 | 2.571 | 8.93 | 12.76 | 0.2140 | 0.4840 |
| 3 | 0.3319 | 0.1565 | 2.576 | 8.93 | 12.76 | 0.2147 | 0.4850 |
| Average | - | - | - | 8.90 | 12.80 | 0.2147 | 0.4849 |

Table 4.13 Preferential swelling - effect of cure time on the cross-link density of GS in a 50 : 50

GS : NR vulcanisate

Formulation E, Table 4.10. $\chi_{GS/DMF} = 0.5736$

| Cure time (mins) | ν_r Natural rubber/DMF | V_s Natural rubber/DMF (for 1 g) | ν_r Blend/DMF | ν_r Neoprene GS in blend | M_{cpHYS} Neoprene GS in blend ($\times 10^{-3}$ kg/mol) | $1/2M_{cpHYS}$ Neoprene GS in blend ($\text{kg mol}^{-1}/\text{kg}) \times 10^5$ |
|------------------|----------------------------|------------------------------------|-------------------|------------------------------|---|---|
| 10 | 0.8458 | 0.1982 | 0.5184 | 0.3416 | 5.35 | 9.35 |
| 20 | 0.8716 | 0.1601 | 0.5440 | 0.3725 | 3.65 | 13.70 |
| 40 | 0.8738 | 0.1570 | 0.5580 | 0.3762 | 3.50 | 14.30 |
| 65 | 0.8682 | 0.1650 | 0.5647 | 0.3848 | 3.17 | 15.77 |
| 120 | 0.8619 | 0.1742 | 0.5692 | 0.3915 | 2.94 | 16.99 |

Average of three readings quoted

Table 4.14 Preferential swelling - effect of cure time on the cross-link density of NR in a 50 : 50

GS : NR vulcanisate

Formulation E, Table 4.10. χ NR/hexane = 0.4849

| Cure time (mins) | ν_r Neoprene GS/Hexane | V_s Neoprene GS/Hexane | ν_r Blend/Hexane | ν_r Natural rubber in blend | $M_{c,PHYS}$ Natural rubber in blend x 10^{-3} kg/mol | $1/2M_{c,PHYS}$ Natural rubber in blend x 10^5 kg/mol/kg |
|------------------|----------------------------|--------------------------|----------------------|---------------------------------|---|--|
| 10 | 0.8071 | 0.1943 | 0.3280 | 0.2272 | 10.86 | 4.61 |
| 20 | 0.8134 | 0.1865 | 0.3237 | 0.2232 | 11.42 | 4.38 |
| 40 | 0.8155 | 0.1839 | 0.3130 | 0.2143 | 12.82 | 3.90 |
| 65 | 0.8159 | 0.1834 | 0.2998 | 0.2035 | 14.83 | 3.37 |
| 120 | 0.8176 | 0.1814 | 0.2932 | 0.1981 | 15.99 | 3.13 |

Average of three readings quoted

LWINTI

Table 4.15 Effect of cure time on the network structure of Neoprene GS - original network

Formulation C, Table 4.10

| Cure time (mins) | Sample number | ho (cm) | Ao (cm ²) | F/Ah x 10 ⁻³ (g/cm) | C ₁ ERV x 10 ⁻⁴ (N/m ²) | C ₁ ERM x 10 ⁻⁴ (N/m ²) | M _C ERMPHYS x 10 ⁻⁴ (kg/kg mol) | $\frac{1}{2}$ M _C ERMPHYS x 10 ⁵ (kg mol/kg) |
|------------------|---------------|---------|-----------------------|--------------------------------|---|---|---|--|
| 10 | 1 | 0.165 | 0.1613 | 5.657 | 9.46 | 10.20 | 14.94 | 3.35 |
| | 2 | 0.165 | 0.1631 | 5.754 | 9.53 | 10.27 | 14.84 | 3.37 |
| | Average | - | - | - | 9.49 | 10.24 | 14.89 | 3.36 |
| 20 | 1 | 0.165 | 0.1591 | 7.902 | 13.38 | 14.43 | 10.56 | 4.73 |
| | 2 | 0.165 | 0.1594 | 7.956 | 13.45 | 14.50 | 10.51 | 3.76 |
| | 3 | 0.165 | 0.1508 | 8.014 | 13.45 | 14.49 | 10.51 | 3.76 |
| | Average | - | - | - | 13.43 | 14.47 | 10.53 | 4.08 |
| 30 | 1 | 0.164 | 0.1637 | 8.614 | 14.11 | 15.21 | 10.02 | 4.99 |
| | 2 | 0.165 | 0.1652 | 8.735 | 14.27 | 15.39 | 9.90 | 5.05 |
| | 3 | 0.165 | 0.1654 | 8.595 | 14.01 | 15.10 | 10.09 | 4.96 |
| | Average | - | - | - | 14.13 | 15.23 | 10.00 | 5.00 |
| 40 | 1 | 0.165 | 0.1649 | 9.014 | 14.77 | 15.92 | 9.57 | 5.22 |
| | 2 | 0.160 | 0.1639 | 9.101 | 14.50 | 15.63 | 9.75 | 5.13 |
| | Average | - | - | - | 14.64 | 15.78 | 9.66 | 5.18 |
| 60 | 1 | 0.165 | 0.1591 | 9.372 | 15.89 | 17.13 | 8.90 | 5.62 |
| | 2 | 0.159 | 0.1564 | 9.442 | 15.68 | 16.91 | 9.01 | 5.55 |
| | Average | - | - | - | 15.79 | 17.02 | 8.96 | 5.59 |

Table 4.16 Effect of cure time on the network structure of Neoprene GS - after propan-2-thiol/piperidine probe Formation C, Table 4.10. Cure temperature, 140°C; solvent, toluene.

| Cure time (mins) | Average $C_{1ERY} \times 10^{-4}$ (N/m ²) | Average $C_{1ERM} \times 10^{-4}$ (N/m ²) | Average $M_{CERM} PHYS \times 10^{-3}$ (kg/kg mol) | Average $\frac{1}{2}M_{CERM} PHYS \times 10^5$ (kg mol/kg) |
|------------------|---|---|--|--|
| 10 | 3.61 | 3.89 | 39.24 | 1.28 |
| 20 | 6.85 | 7.38 | 20.64 | 2.42 |
| 30 | 9.80 | 10.56 | 14.43 | 3.47 |
| 40 | 10.40 | 11.21 | 13.59 | 3.68 |
| 60 | 13.23 | 14.27 | 10.68 | 4.68 |

Average of three readings quoted

Table 4.17 Effect of cure time on the network structure of Neoprene GS - after n-hexan-thiol/piperidine probe
 Formulation C, Table 4.10. Cure temperature, 140°C; solvent, toluene

| Cure time (mins) | Average $C_{1ERV} \times 10^{-4}$ (N/m ²) | Average $C_{1ERM} \times 10^{-4}$ (N/m ²) | Average $M_{CERM} \text{ PHYS} \times 10^{-3}$ (kg/kg mol) | Average $\frac{1}{2}M_{CERM} \text{ PHYS}$ $\times 10^5$ (kg mol/kg) |
|---------------------|--|--|---|---|
| 10 | 2.00 | 2.15 | 70.90 | 0.71 |
| 20 | 2.62 | 2.82 | 53.99 | 0.93 |
| 30 | 3.38 | 3.64 | 41.94 | 1.19 |
| 40 | 4.75 | 5.12 | 29.80 | 1.68 |
| 60 | 4.49 | 7.00 | 21.77 | 2.30 |

Average of three readings quoted

Table 4.18 Effect of cure time on the network structure of Neoprene GS Formulation C, Table 4.10. Cure temperature, 140°C; solvent, toluene

| Cure time (mins) | Cross-link density (λ_{McERM} PHYS $\times 10^5$) (kgmol/kg) | | | Network structure | | |
|------------------|--|----------------------------|---------------------------|--------------------|--------------------|------------------------------|
| | Original formulation | After propan-2-thiol probe | After n-hexan-thiol probe | Sx Cross-links (%) | S2 Cross-links (%) | S1 and C-O-C Cross-links (%) |
| 10 | 3.36 | 1.28 | 0.71 | 61.9 | 17.0 | 21.1 |
| 20 | 4.08 | 2.42 | 0.93 | 40.7 | 36.5 | 22.8 |
| 30 | 5.00 | 3.47 | 1.19 | 30.6 | 45.6 | 23.8 |
| 40 | 5.18 | 3.68 | 1.68 | 29.0 | 38.6 | 32.4 |
| 60 | 5.59 | 4.68 | 2.30 | 16.3 | 42.6 | 41.1 |

Table 4.19 Effect of blending on the network structure of GS and NR vulcanisates
 Formulations C, H, I, E, G, Table 4.10. Cured 30 mins @ 150°C; solvent, toluene; average of 3 readings quoted.

| Designation | Formulation (phr) | Chemical Treatment | Network Measurements | | | |
|-------------|---------------------------|----------------------|---|---|--|--|
| | | | Average $C_{1ERV} \times 10^{-4}$ (N/m ²) | Average $C_{1ERM} \times 10^{-4}$ (N/m ²) | Average $M_{CERM} \text{ PHYS} \times 10^{-3}$ (kg/kg mol) | Average $\frac{1}{2}M_{CERM} \text{ PHYS} \times 10^5$ (kg mol/kg) |
| C | GS 100 | Original network | 23.07 | 24.87 | 6.13 | 8.16 |
| | ZnO 5 | After propan-2-thiol | 19.08 | 20.57 | 7.41 | 6.75 |
| | MgO 4 | After n-hexan-thiol | 6.50 | 7.00 | 21.76 | 2.30 |
| H | GS 100 | Original network | 28.17 | 30.36 | 5.02 | 9.96 |
| | ZnO 5 | After propan-2-thiol | 20.31 | 21.89 | 6.96 | 7.18 |
| | MgO 4 S 2.5 CBS 0.5 | After n-hexan-thiol | 7.32 | 7.89 | 19.33 | 2.59 |
| I | NR 100 | Original network | 14.51 | 15.24 | 7.48 | 6.69 |
| | ZnO 5 | After propan-2-thiol | 9.52 | 10.00 | 11.40 | 4.39 |
| | MgO 4 S 2.5 CBS 0.5 | After n-hexan-thiol | 4.95 | 5.21 | 21.11 | 2.37 |

CONTINUED . . .

Table 4.19 CONTINUATION

| E | GS NR ZnO MgO | Original network After propan- 2-thiol After n-hexan- thiol | 16.32 | 17.28 | 18.30 | 7.28 |
|---|------------------------------------|--|-------|-------|-------|------|
| | | DESTROYED BY PROBE - RESIDUE 78% GS : 27% NR | - | - | - | - |
| G | 50 50 5 4 | Original network After propan- 2-thiol After n-hexan- thiol | 20.13 | 21.32 | 6.45 | 7.76 |
| | GS NR ZnO MgO S CBS | | 4.35 | 4.60 | 28.93 | 1.73 |
| | | | 2.26 | 2.40 | 56.04 | 0.89 |

Table 4.20 Effect of blending on the network structure of GS and NR Vulcanisates Formulations C, E, G, H and I, Table 4.10. Cured 30 mins @ 150°C

| Designation | Formulation | $\frac{1}{2}M_{CERM} PHYS \times 10^5$ (kg mol/kg) | | | Network structure | | | |
|-------------|-----------------|--|----------------------------|---------------------------|-------------------|----------------|----------------|------------------------|
| | | Original network | After propan-2-thiol probe | After n-hexan-thiol probe | Sx Cross-links | S2 Cross-links | S1 Cross-links | S1 + C-O-C Cross-links |
| C | GS | 8.16 | 6.75 | 2.30 | 17.3 | 54.5 | - | 28.2 |
| | ZnO MgO | 5 4 | | | | | | |
| H | GS | 9.96 | 7.18 | 2.59 | 27.9 | 46.1 | - | 26.0 |
| | ZnO | 100 | | | | | | |
| | MgO | 5 | | | | | | |
| | S CBS | 4 2.5 0.5 | | | | | | |
| I | GS | 6.69 | 4.39 | 2.37 | 34.4 | 30.2 | 35.4 | - |
| | ZnO | 100 | | | | | | |
| | MgO | 5 | | | | | | |
| | S CBS | 4 2.5 0.5 | | | | | | |
| E | GS | 7.28 | Destroyed | Destroyed | Probably 90-100% | - | - | - |
| | NR | 50 | | | | | | |
| | ZnO | 50 | | | | | | |
| | MgO | 5 4 | | | | | | |
| G | GS | 7.76 | 1.73 | 0.89 | 77.7 | 10.8 | - | 11.5 |
| | NR | 50 | | | | | | |
| | ZnO | 50 | | | | | | |
| | MgO S CBS | 5 4 2:5 0:5 | | | | | | |

Table 4.21 Calculation of the χ constant for natural rubber fatigue samples before and after treatment with thiol/amine probes

Formulation I, Table 4.10

| Chemical treatment | Average $C_{1ERV} \times 10^{-4}$ (N/m ²) | Average ν_r | Average χ |
|----------------------------|---|-----------------|----------------|
| Original Network | 19.90 | 0.3108 | 0.5221 |
| After propan-2-thiol probe | 12.47 | 0.2607 | 0.5099 |
| After n-hexan-thiol probe | 4.64 | 0.1970 | 0.5162 |

Average of three readings quoted

Table 4.22 Effect of fatigue on the network structure of natural rubber - original network
 Formulation I, Table 4.10. Solvent toluene; $\chi = 0.5221$. Average of three readings quoted

| Fatigue life (cycles) | Average ν_r | Average $C_{1\text{ERV}} \times 10^{-4}$ (N/m ²) | Average $M_{\text{CERV PHYS}} \times 10^{-3}$ (kg/kg mol) | Average $\frac{1}{2}M_{\text{CERV PHYS}} \times 10^5$ (kg mol/kg) |
|--------------------------------|-----------------|--|---|---|
| 0 | 0.3106 | 19.97 | 5.73 | 8.76 |
| 200 | 0.3104 | 19.80 | 5.74 | 8.68 |
| 15000 | 0.3097 | 19.70 | 5.79 | 8.64 |
| 100000 | 0.3094 | 19.74 | 5.78 | 8.66 |
| Failure (JIS average = 196000) | 0.3083 | 19.40 | 5.87 | 8.51 |

Table 4.23 Effect of fatigue on the network structure of natural rubber - after propan-2-thiol/piperidine probe
 Formulation I, Table 4.10. Solvent, toluene; $\mathcal{R} = 0.5099$. Average of three readings quoted

| Fatigue life (cycles) | Average ν_r | Average $C_{1ERV} \times 10^{-4}$ (N/m ²) | Average $M_{CERV} \text{ PHYS} \times 10^{-3}$ (kg/kg mol) | Average $\frac{1}{2} M_{CERV} \text{ PHYS} \times 10^5$ (kg mol/kg) |
|-------------------------------------|-----------------|--|---|--|
| 0 | 0.2583 | 12.11 | 9.41 | 5.31 |
| 200 | 0.2586 | 12.16 | 9.38 | 5.33 |
| 15000 | 0.2616 | 12.61 | 9.04 | 5.53 |
| 100000 | 0.2654 | 13.25 | 8.63 | 5.79 |
| Failure (JIS average = 196000 | 0.2687 | 13.75 | 8.29 | 6.03 |

Table 4.24 Effect of fatigue on the network structure of natural rubber - after n-hexan-thiol/piperidine probe

Formulation I, Table 4.10. Solvent, toluene; $\gamma = 0.5162$. Average of three readings quoted.

| Fatigue life (cycles) | Average ν_r | Average $C_{1ERV} \times 10^{-4}$ (N/m ²) | Average $M_{CERV} \text{ PHYS} \times 10^{-3}$ (kg/kg mol) | Average $\frac{1}{2}M_{CERV} \text{ PHYS} \times 10^5$ (kg mol/kg) |
|--------------------------------|-----------------|---|--|--|
| 0 | 0.1965 | 4.60 | 24.76 | 2.02 |
| 200 | 0.1963 | 4.58 | 24.87 | 2.01 |
| 15000 | 0.1967 | 4.62 | 24.69 | 2.03 |
| 100000 | 0.1977 | 4.6 | 24.50 | 2.06 |
| Failure (JIS average = 196000) | 0.1983 | 4.74 | 24.04 | 2.08 |

Table 4.25 Effect of fatigue on network structure of NR vulcanisates

Formulation I, Table 4.10

| Number of cycles | $\frac{1}{2}M_{CERV} PHYS \times 10^5$ (kg mol/kg) | | | Network structure | | |
|--------------------------------|--|----------------------------|---------------------------|--------------------------------|--------------------------------|--------------------------------|
| | Original network | After propan-2-thiol probe | After n-hexan-thiol probe | S _x Cross-links (%) | S ₂ Cross-links (%) | S ₁ Cross-links (%) |
| 0 | 8.76 | 5.31 | 2.02 | 39.4 | 37.6 | 23.1 |
| 200 | 8.68 | 5.33 | 2.01 | 38.6 | 38.2 | 23.2 |
| 15000 | 8.64 | 5.53 | 2.03 | 36.0 | 40.5 | 23.5 |
| 100000 | 8.66 | 5.79 | 2.06 | 33.1 | 43.1 | 23.8 |
| Failure (JIS average = 196000) | 8.51 | 6.03 | 2.08 | 29.1 | 46.4 | 24.5 |

Table 4.26 Calculation of \mathcal{K} constant for Neoprene GS fatigue samples before and after treatment with thiol/amine probes

Formulation C, Table 4.10

| Chemical Treatment | C_{1ERV} | Average $\times 10^{-4}$ (N/m ²) | Average \mathcal{V}_r | Average \mathcal{K} |
|----------------------------|------------|--|-------------------------|-----------------------|
| Original network | | 15.16 | 0.1802 | 0.3790 |
| After propan-2-thiol probe | | 13.52 | 0.1576 | 0.3435 |
| After n-hexan-thiol probe | | 3.792 | 0.1011 | 0.4039 |

Average of three readings quoted

Table 4.27 Effect of fatigue on the network structure of Neoprene GS - original network Formulation C, Table 4.10. Solvent, toluene; $\chi = 0.3790$. Average of three readings quoted

| Fatigue life cycles) | Average ν_r | $C_{1ERV} \times 10^{-4}$ (N/m ²) | $M_{CERV} \text{ PHYS} \times 10^{-3}$ (kg/kg mol) | Average $\frac{1}{2} M_{CERV} \text{ PHYS} \times 10^5$ (kg mol/kg) |
|--------------------------------|-----------------|---|--|---|
| 0 | 0.1913 | 17.31 | 8.80 | 5.68 |
| 100 | 0.1911 | 17.27 | 8.82 | 5.67 |
| 200 | 0.1910 | 17.24 | 8.84 | 5.66 |
| 15000 | 0.1914 | 17.33 | 8.79 | 5.69 |
| 100000 | 0.1917 | 17.38 | 8.77 | 5.70 |
| Failure (JIS average = 894000) | 0.1926 | 17.57 | 8.67 | 5.77 |

Table 4.28 Effect of fatigue on the network structure of Neoprene GS - after propan-2-thiol/piperidine

probe

Formulation C, Table 4.10. Solvent, toluene; $\chi = 0.3435$. Average of three readings quoted

| Fatigue life (cycles) | Average γ_r | $C_{1ERV} \times 10^{-4}$ (N/m ²) | $M_{CERV} PHS \times 10^{-3}$ (kg/kg mol) | $\frac{1}{2} M_{CERV} PHYS \times 10^5$ (kg mol/kg) |
|--------------------------------|--------------------|---|---|---|
| 0 | 0.1576 | 13.52 | 11.27 | 4.44 |
| 100 | 0.1580 | 13.60 | 11.21 | 4.46 |
| 200 | 0.1582 | 13.63 | 11.18 | 4.47 |
| 15000 | 0.1588 | 13.74 | 11.09 | 4.51 |
| 100000 | 0.1594 | 13.84 | 11.01 | 4.54 |
| Failure (JIS average = 894000) | 0.1600 | 13.95 | 10.92 | 4.58 |

Table 4.29 Effect of fatigue on the network structure of Neoprene GS - after n-hexan-thiol/piperidine probe

Formulation C, Table 4.10. Solvent, toluene; $\chi = 0.4039$. Average of three readings quoted

| Fatigue life (cycles) | Average ν_r | $C_{1ERV} \times 10^{-4}$ (N/m ²) | $M_{CERV} \text{ PHYS} \times 10^{-3}$ (kg/kg mol) | Average $\frac{1}{2} M_{CERV} \text{ PHYS} \times 10^5$ (kg mol/kg) |
|--------------------------------|-----------------|---|--|---|
| 0 | 0.1014 | 3.82 | 39.91 | 1.25 |
| 100 | 0.1023 | 3.88 | 39.24 | 1.27 |
| 200 | 0.1056 | 4.15 | 36.74 | 1.36 |
| 15000 | 0.1062 | 4.20 | 36.32 | 1.38 |
| 100000 | 0.1051 | 4.11 | 37.09 | 1.35 |
| Failure (JIS average = 894000) | 0.1112 | 4.62 | 33.03 | 1.52 |

Table 4.30 Effect of fatigue on the network structure of Neoprene GS

Formulation C, Table 4.10

| Fatigue life (cycles) | $\frac{1}{2}M_{CERV} PHYS \times 10^5$ (kg mol/kg) | | | Network structure (%) | | |
|--------------------------------------|--|-------------------------|------------------------|-----------------------|-------------------|---------------------------|
| | Untreated Materials | After propan-2-thiol | After n-hexan-thiol | Sx Cross-links | S2 Cross-links | S1 + C-O-C Cross-links |
| 0 | 5.68 | 4.44 | 1.25 | 21.8 | 56.2 | 22.0 |
| 100 | 5.67 | 4.46 | 1.27 | 21.3 | 56.3 | 22.4 |
| 200 | 5.66 | 4.47 | 1.36 | 21.0 | 54.9 | 24.0 |
| 15000 | 5.69 | 4.51 | 1.38 | 20.7 | 55.0 | 24.3 |
| 100000 | 5.70 | 4.54 | 1.35 | 20.4 | 56.0 | 23.6 |
| Failure (JIS average = 894000) | 5.77 | 4.58 | 1.52 | 20.6 | 53.0 | 26.4 |

Table 4.31 Effect of additional cureatives on the fatigue behaviour of 50 : 50 GS : NR vulcanisates

| | A | B | C | D | E | F | G | H | I | J | K | L | M |
|--|-----|-------|------|-----|-----|-----|------|------|------|------|-----|------|------|
| Neoprene GS | 50 | 50 | 50 | 50 | 50 | 50 | 50 | 50 | 50 | 50 | 50 | 50 | 50 |
| Natural rubber | 50 | 50 | 50 | 50 | 50 | 50 | 50 | 50 | 50 | 50 | 50 | 50 | 50 |
| Zinc oxide | 5 | 5 | 5 | 5 | 5 | 5 | 5 | 5 | 5 | 5 | 5 | 5 | 5 |
| Magnesium oxide | 4 | 4 | 4 | 4 | 4 | 4 | 4 | 4 | 4 | 4 | 4 | 4 | 4 |
| Sulphur | - | 0.125 | 0.25 | 0.5 | 1.0 | 2.0 | - | - | - | - | - | - | - |
| CBS | - | - | - | - | - | - | 0.25 | 0.5 | 1.0 | 2.0 | - | - | - |
| TMTD | - | - | - | - | - | - | - | - | - | - | 1 | 2 | 4 |
| Cure time @ 150°C (mins) to $\gamma_r = 0.18 + 0.005$ (toluene) | 26 | 22 | 20 | 18 | 14 | 11 | 20 | 15 | 12 | 9 | 21 | 14 | 10 |
| JIS average fatigue life (k cycles) | | | | | | | | | | | | | |
| (a) uncut | 400 | 416 | 462 | 469 | 538 | 571 | 363 | 431 | 240 | 94.3 | 217 | 276 | 111 |
| (b) cut initiated | 322 | 321 | 346 | 348 | 373 | 419 | 101 | 98.8 | 91.0 | 63.6 | 106 | 81.0 | 44.4 |

Table 5.1 Determination of the state of cure of NR in a 50 : 50 W : NR vulcanisate

| Designation (Table 4.4) | Elastomer Base | Chlorine Content % | |
|----------------------------|----------------|------------------------------|-----------------------------|
| | | Before Toluene Extraction | After Toluene Extraction |
| B | Natural rubber | 0 | 0 |
| C | Neoprene W | 29.8 | 32.4 |
| J | 50 : 50 W : NR | 14.7 | 30.6 |

Table 5.2 Determination of the state of cure of NR in a 50 : 50 GS : NR vulcanisate

| Designation (Table 4.4) | Elastomer Base | Chlorine Content % | |
|----------------------------|-----------------|------------------------------|-----------------------------|
| | | Before Toluene Extraction | After Toluene Extraction |
| A | Neoprene GS | 33.3 | 31.6 |
| B | Natural rubber | 0 | 0 |
| E | 50 : 50 GS : NR | 14.5 | 13.4 |

Table 5.3 Comparison of the morphology and failure surfaces of
PGS : NR vulcanisates

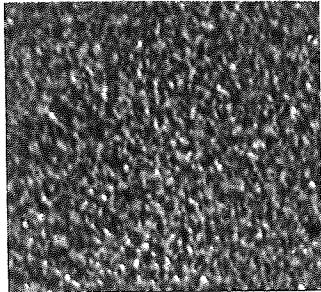
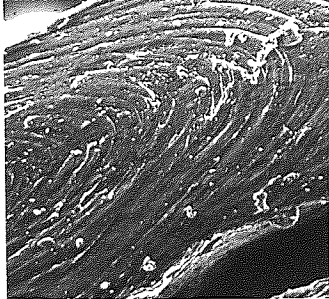
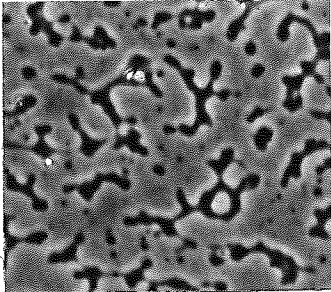
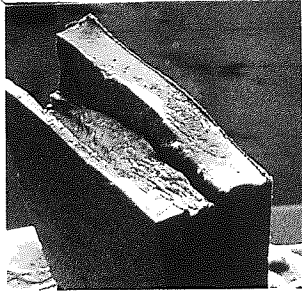
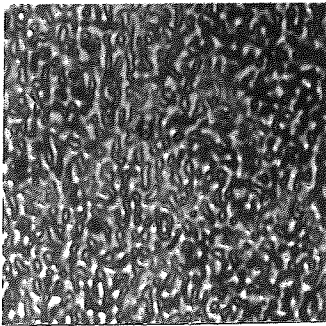
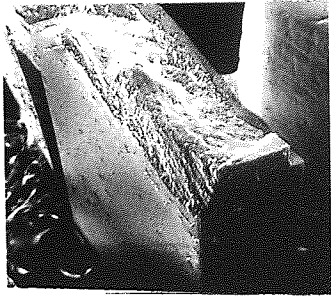
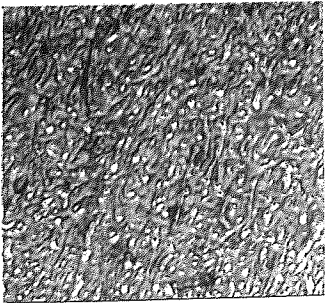
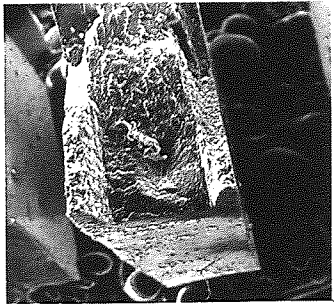
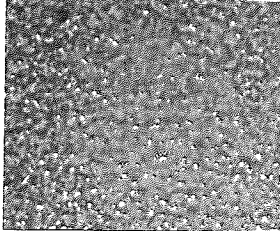
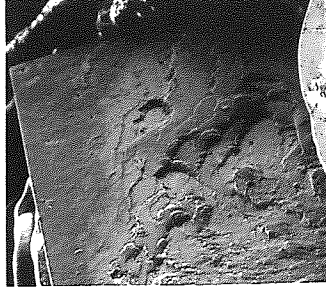
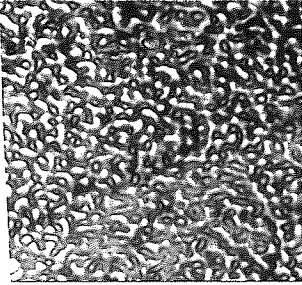
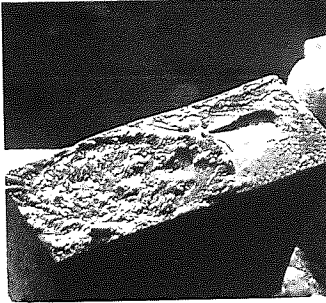
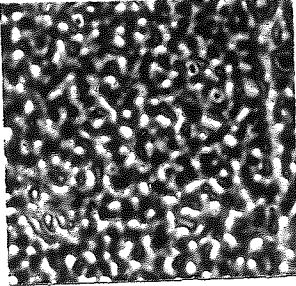
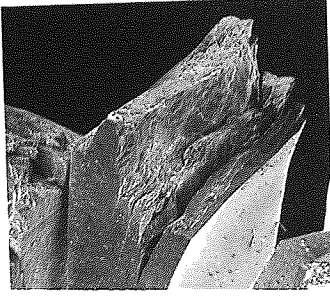
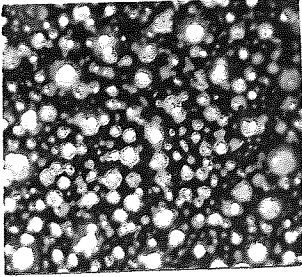
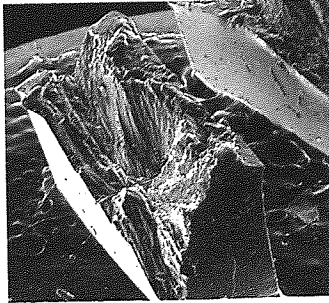
| Premasticated GS:NR Ratio (wt %) | Phase Contrast Micrographs (mag 600X) | Fatigue Failure Surfaces (mag 10X) |
|-------------------------------------|---|---|
| 90 : 10 |  | (mag 20X)  |
| 75 : 25 |  |  |
| 60 : 40 |  |  |
| 50 : 50 |  |  |

Table 5.4 Comparison of the morphology and failure surfaces of
GS : PNR vulcanisates

| GS : Premasticated NR Ratio (wt %) | Phase Contrast Micrographs (mag 600X) | Fatigue Failure Surfaces (mag 10X) |
|---|---|---|
| 90 : 10 |  | (mag 20X)  |
| 75 : 25 |  |  |
| 60 : 40 |  |  |
| 50 : 50 |  |  |

APPENDIX TWO

FIGURES

Fig 1.1 Maturation reactions of sulphur vulcanised natural rubber

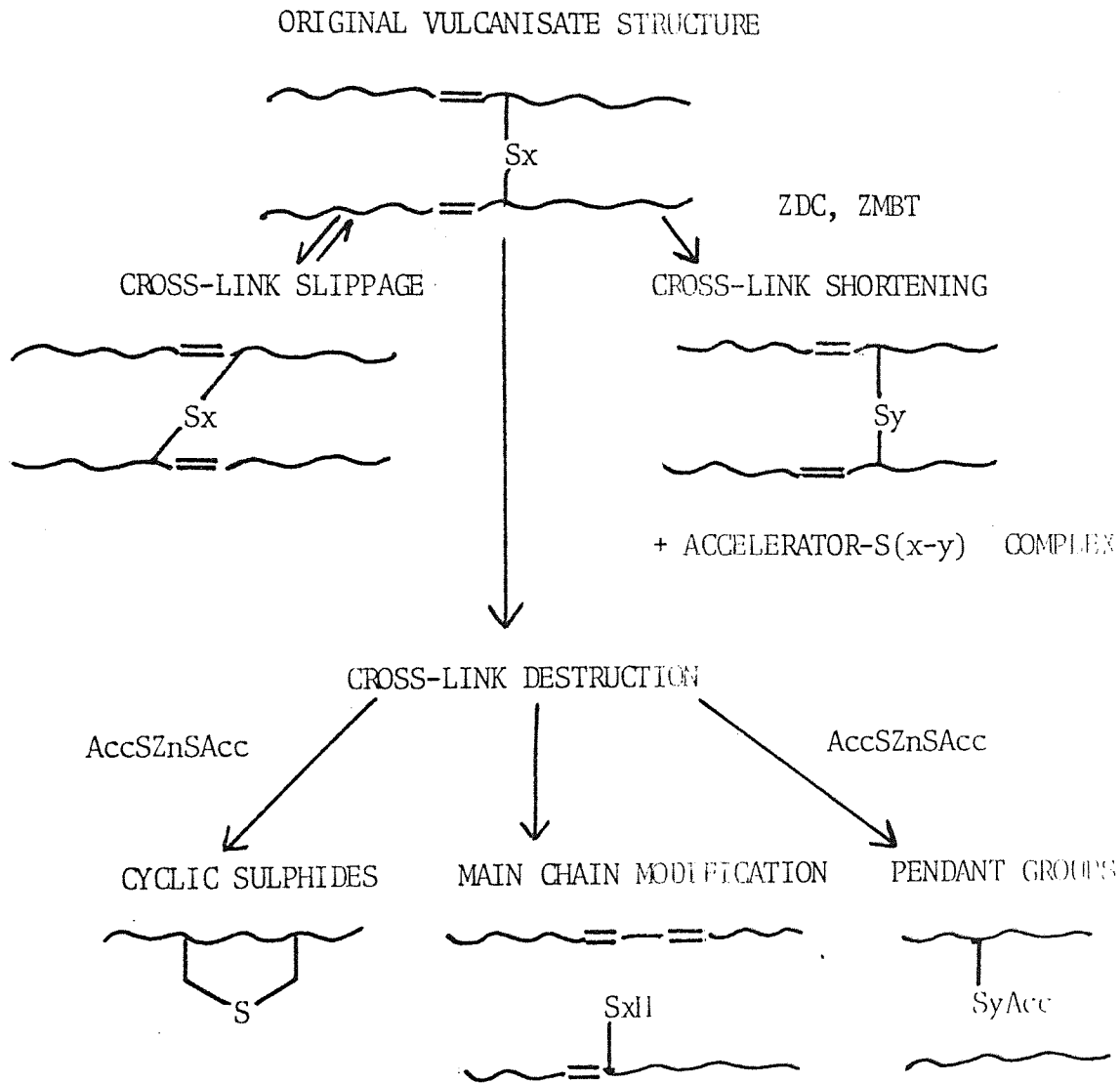


Fig 1.2 Final Vulcanisate Structure

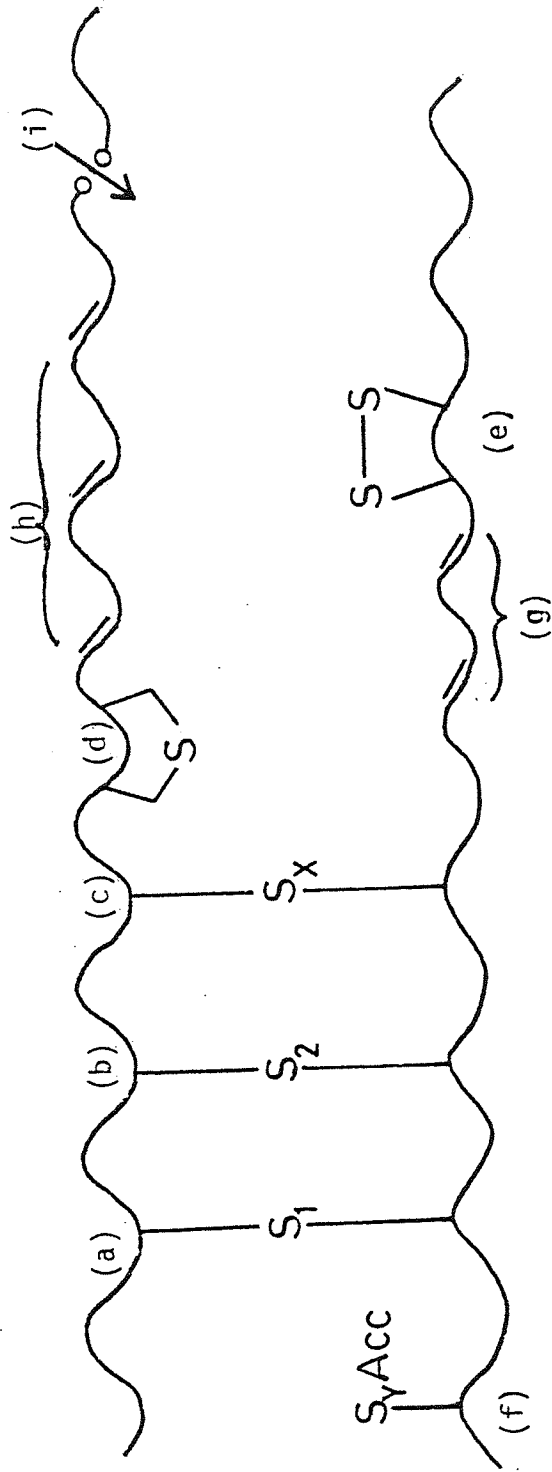
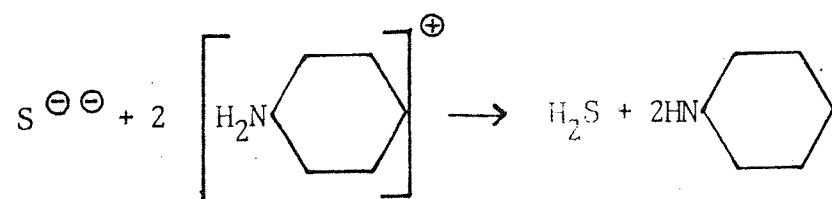
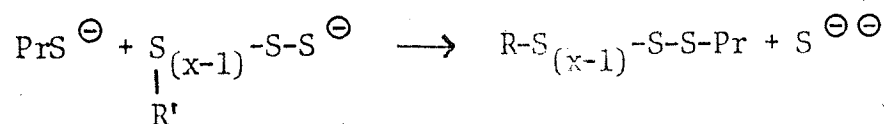
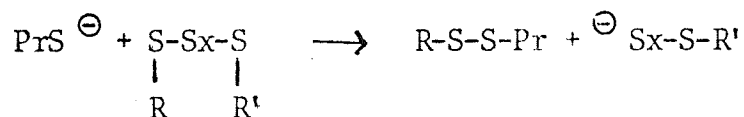
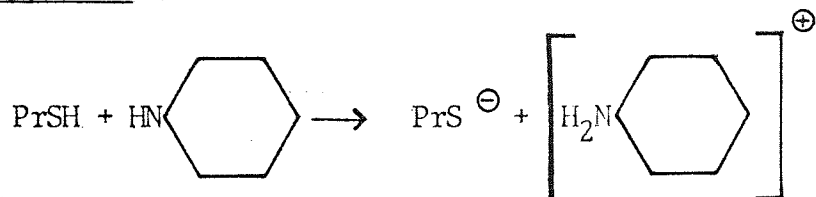


Fig 2.1 Reaction mechanisms for thiol/amine probes

Propan-2-thiol (PrSH)



Hexan-thiol (nHSH)

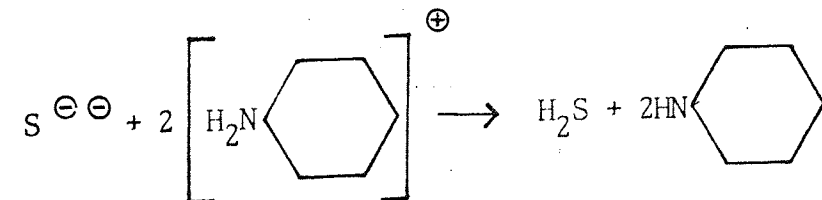
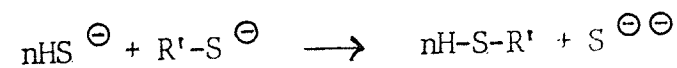
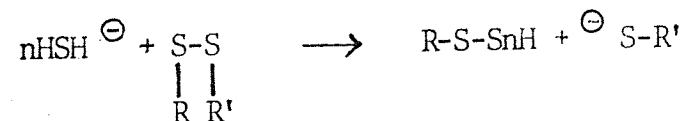
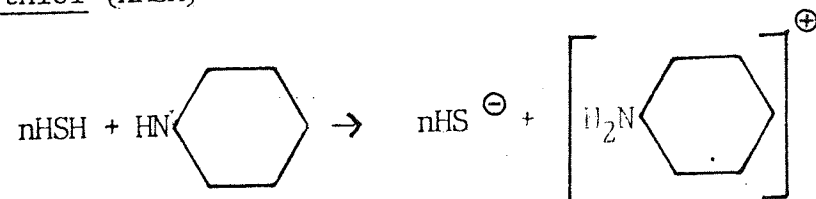


Fig 2.2 Typical Monsanto Rheograph

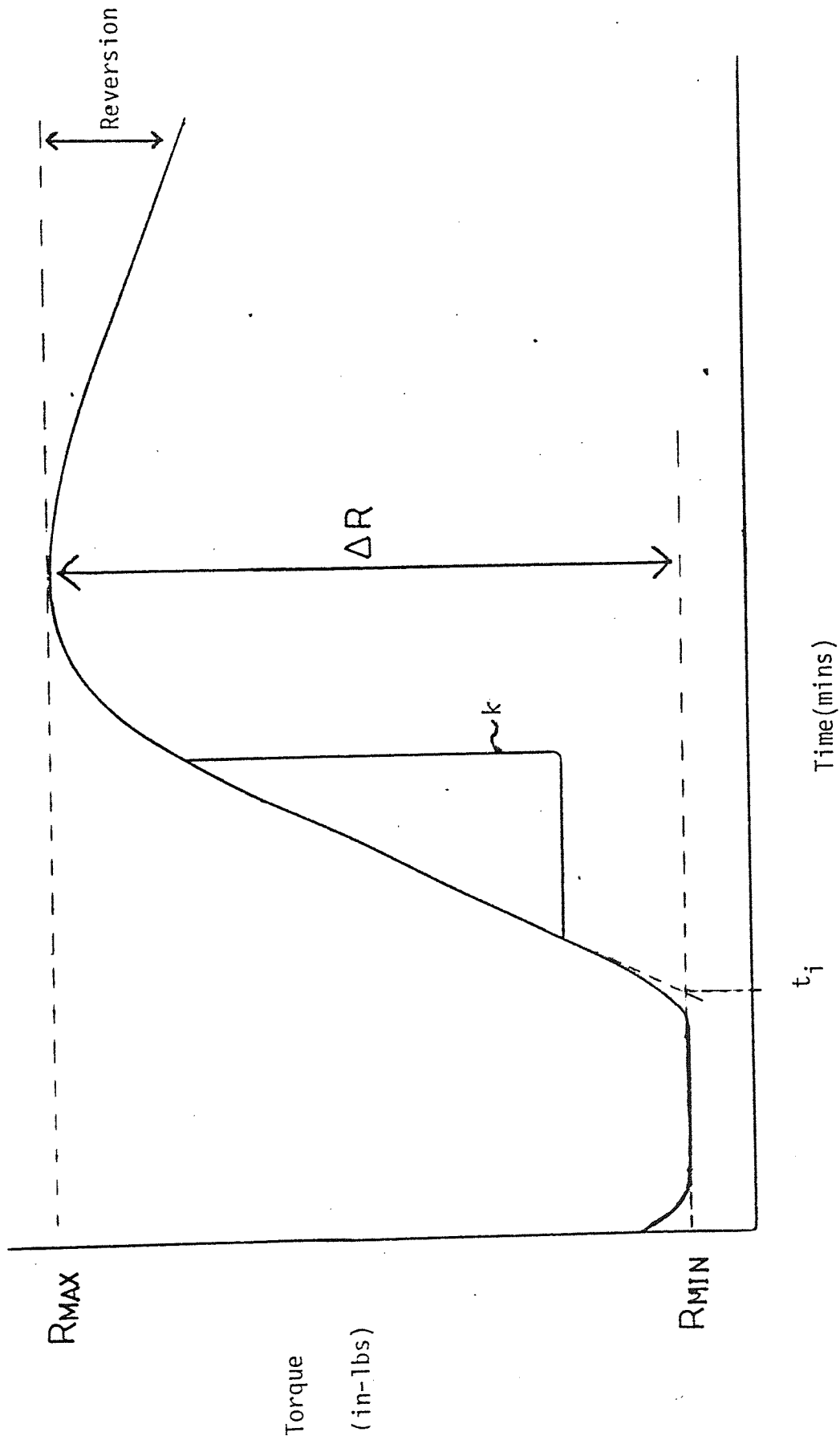


Fig 3.1 Determination of the solvent swelling times for Neoprene GS and natural rubber vulcanisates in toluene

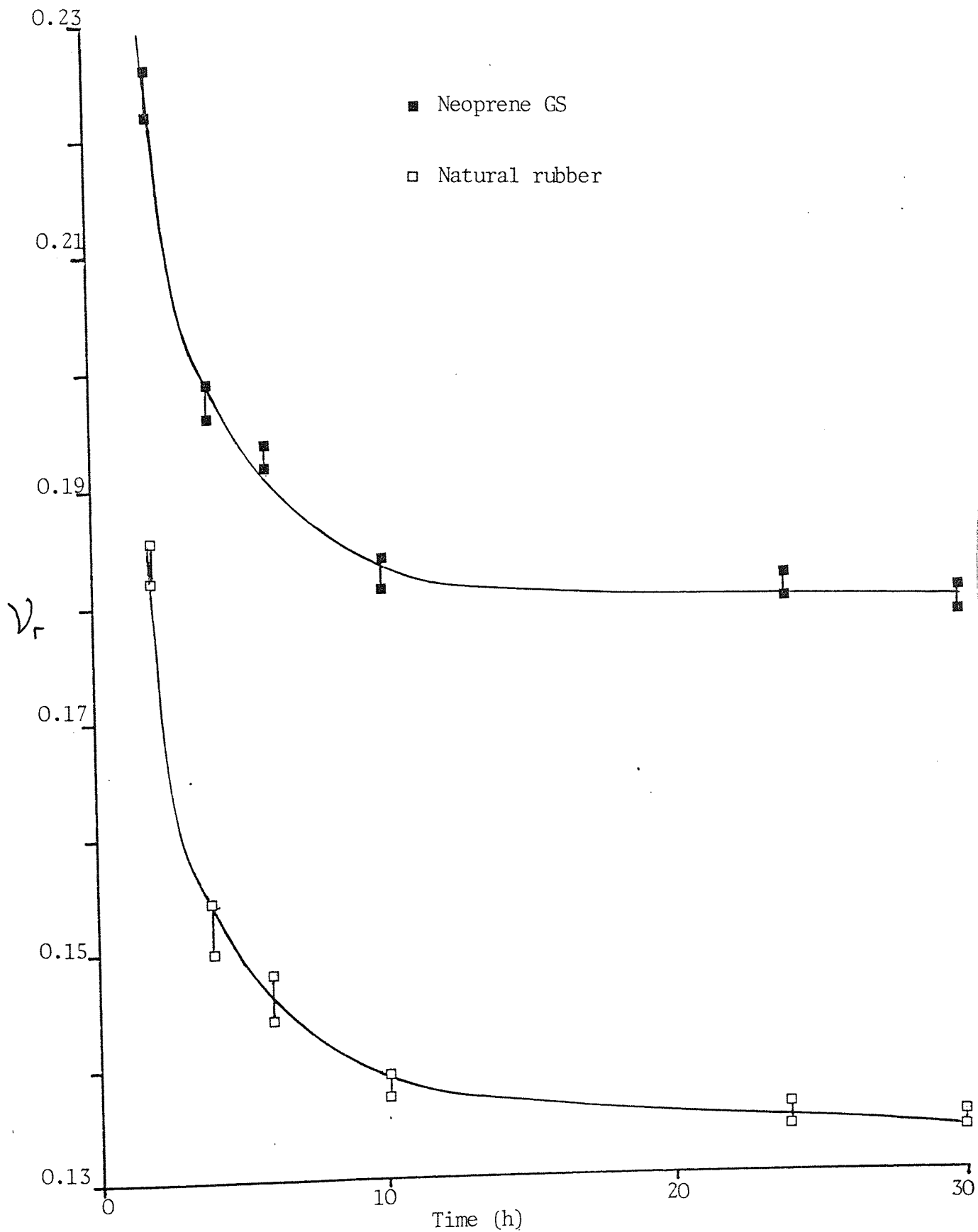


Fig 3.2 Determination of the swelling time for a Neoprene GS vulcanisate in DMF

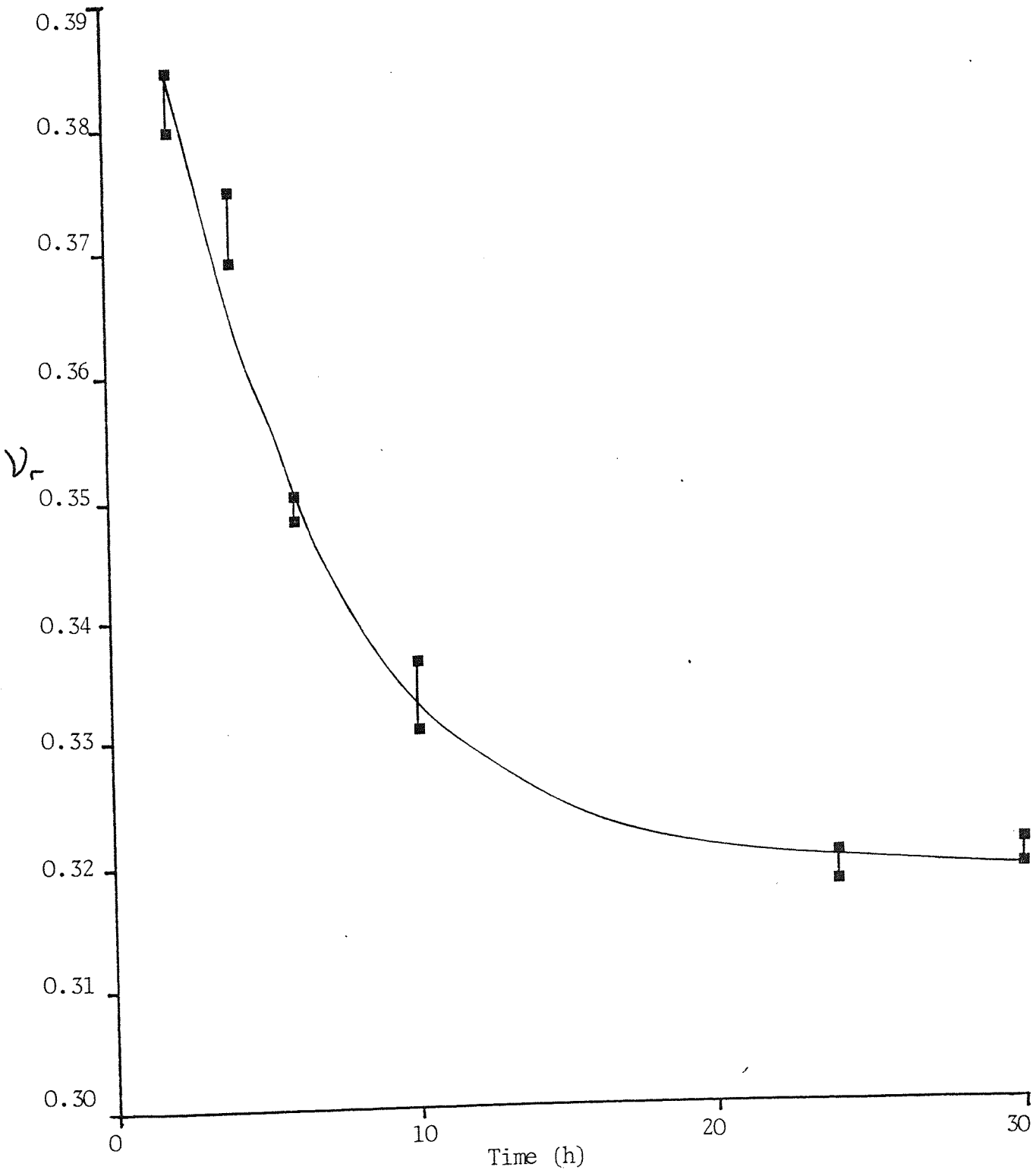


Fig 3.3 Determination of the swelling time for a natural rubber vulcanisate in hexane

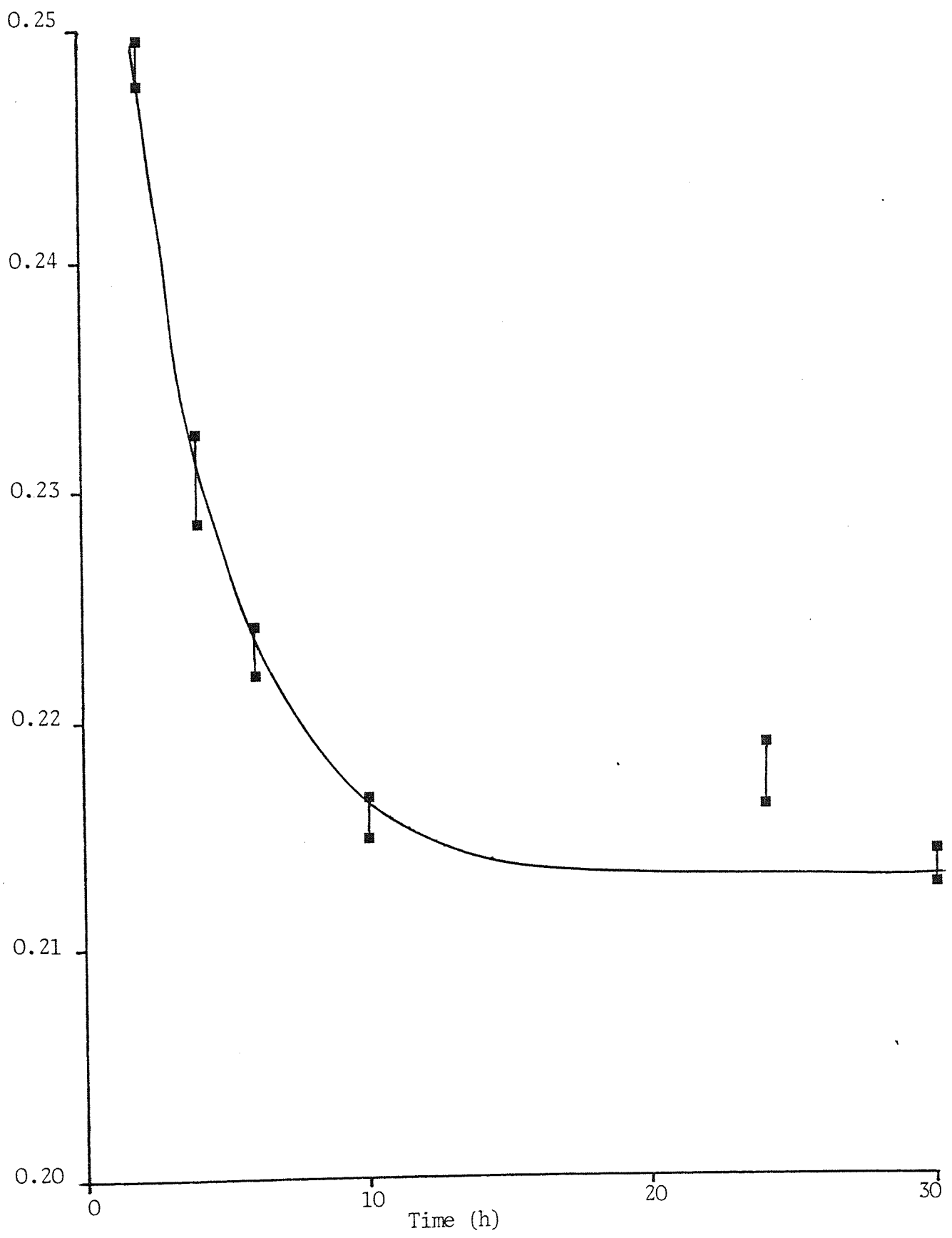


Fig 3.4 Determination of the reaction time of a Neoprene GS vulcanisate with methyl iodide/mercuric iodide probe at 250C

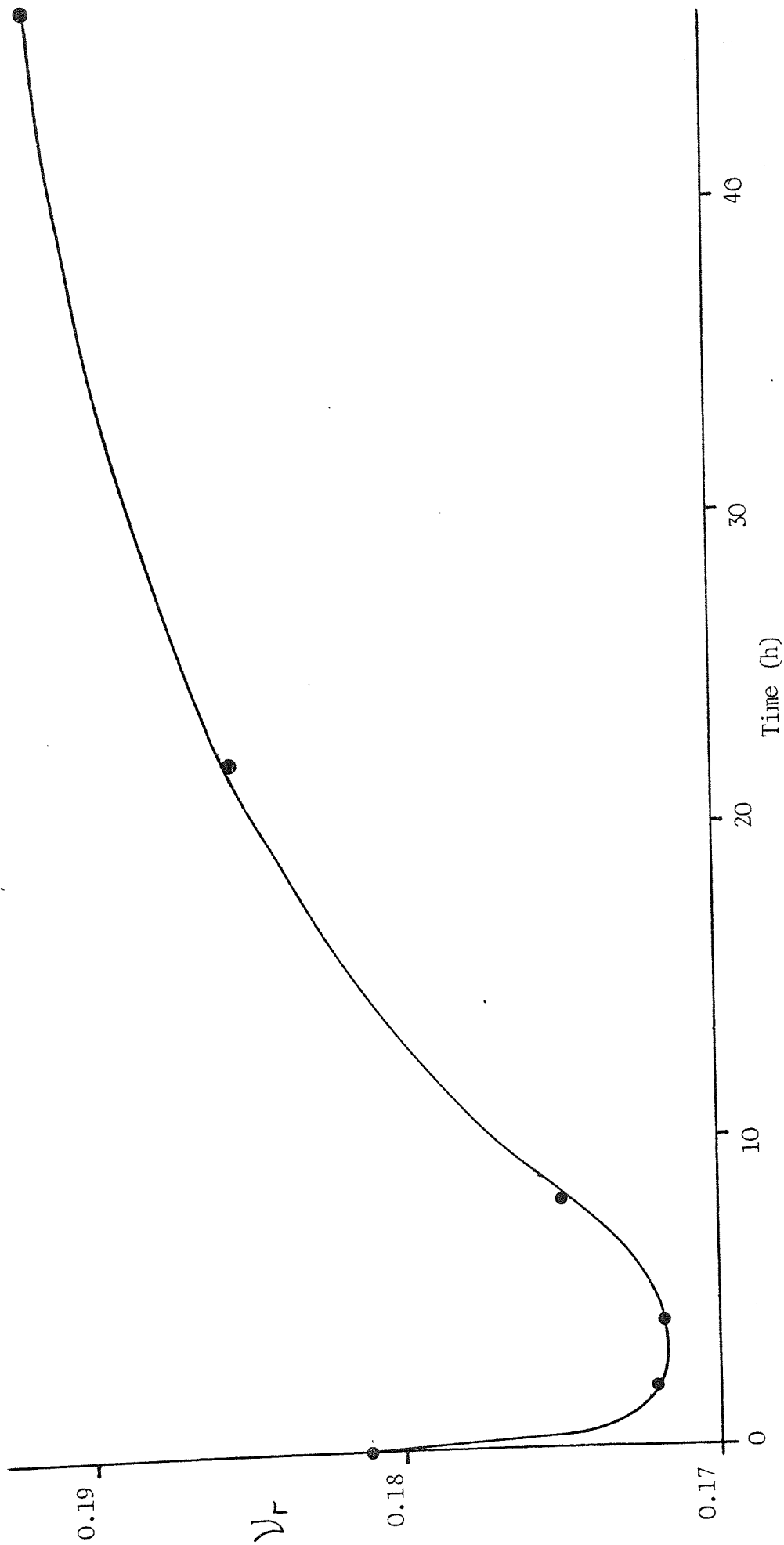
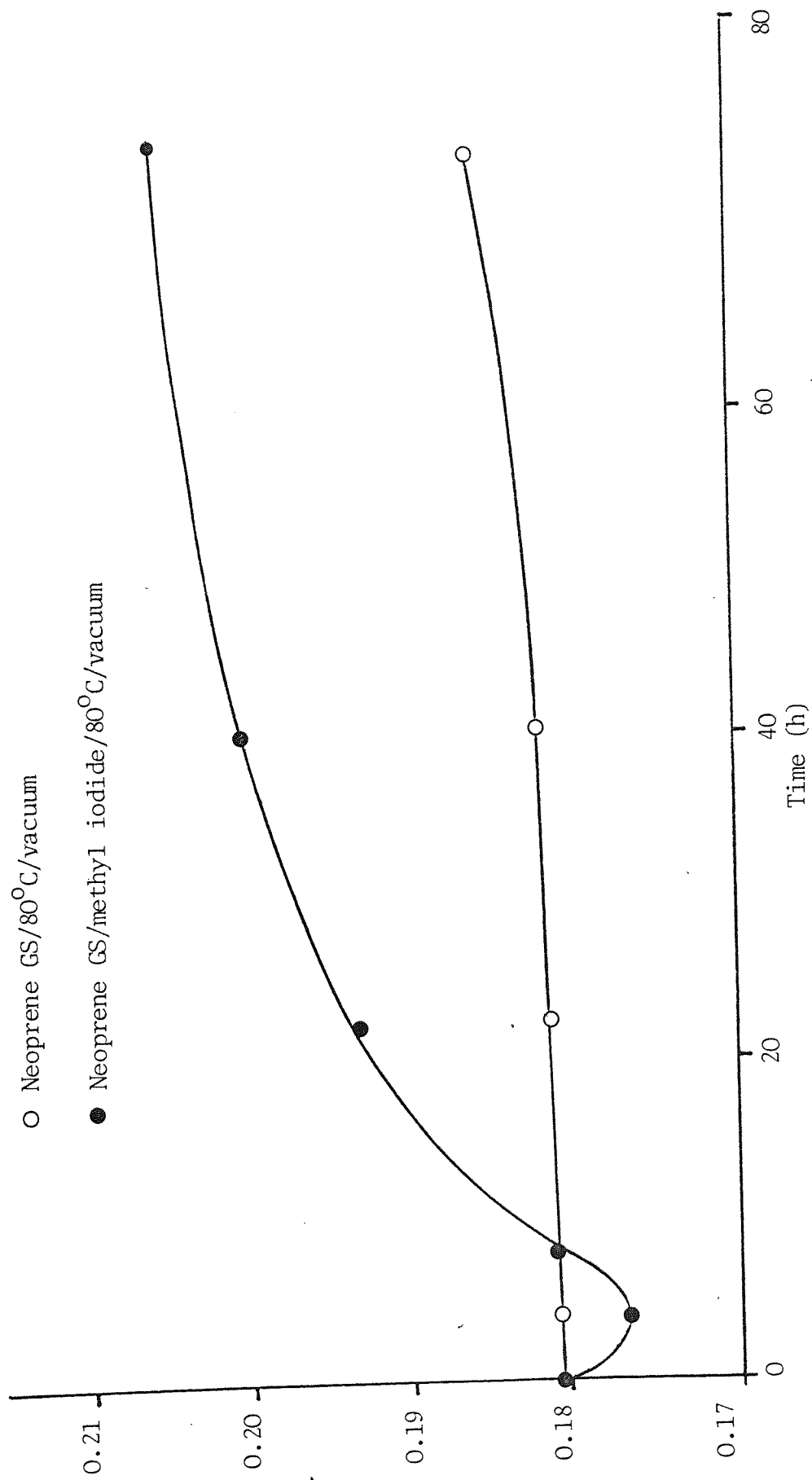


Fig 3.5 Determination of the reaction time of a Neoprene GS vulcanisate with methyl iodide at 80°C



V_r

Fig 3.6 Determination of the reaction time of a Neoprene GS vulcanisate with propan-2-thiol

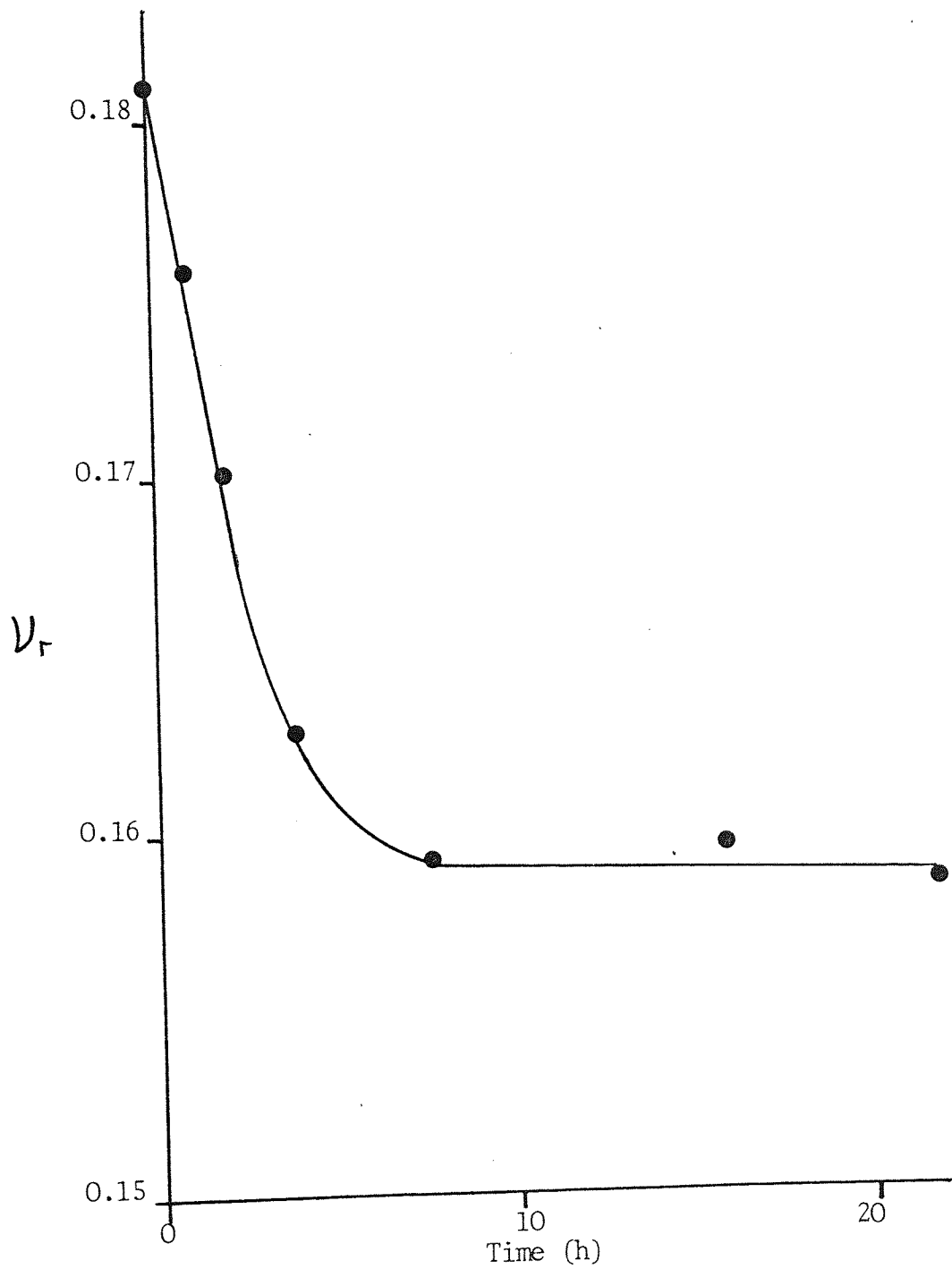


Fig 3.7 Determination of the reaction time of a Neoprene GS vulcanisate with n-hexan-thiol

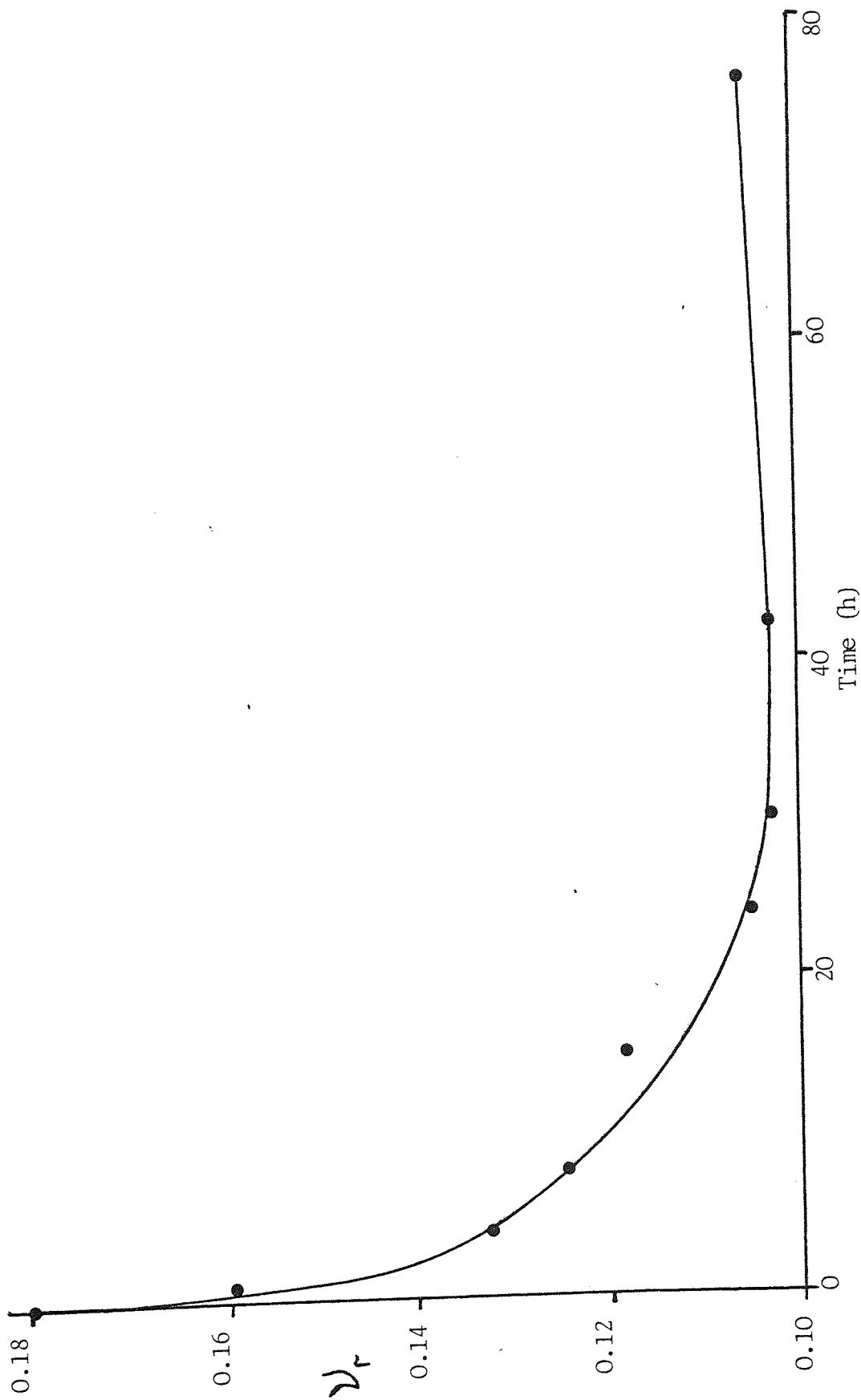


Fig 3.8 Determination of GS : NR interpolymer formation (formulation A, section 3.7.4)

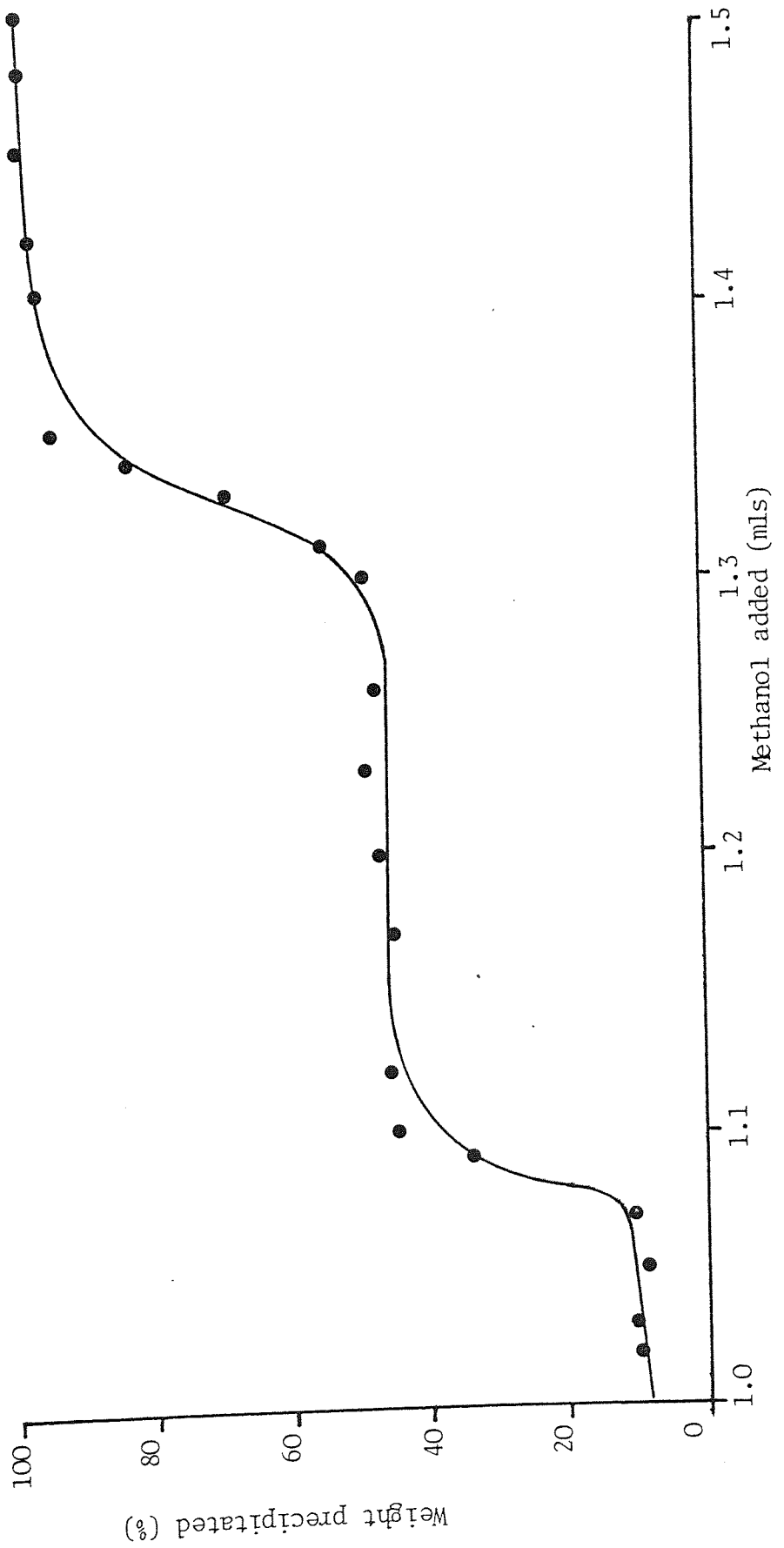


Fig 3.9 Determination of GS : NR interpolpolymer formation (formulation B, section 3.7.4)

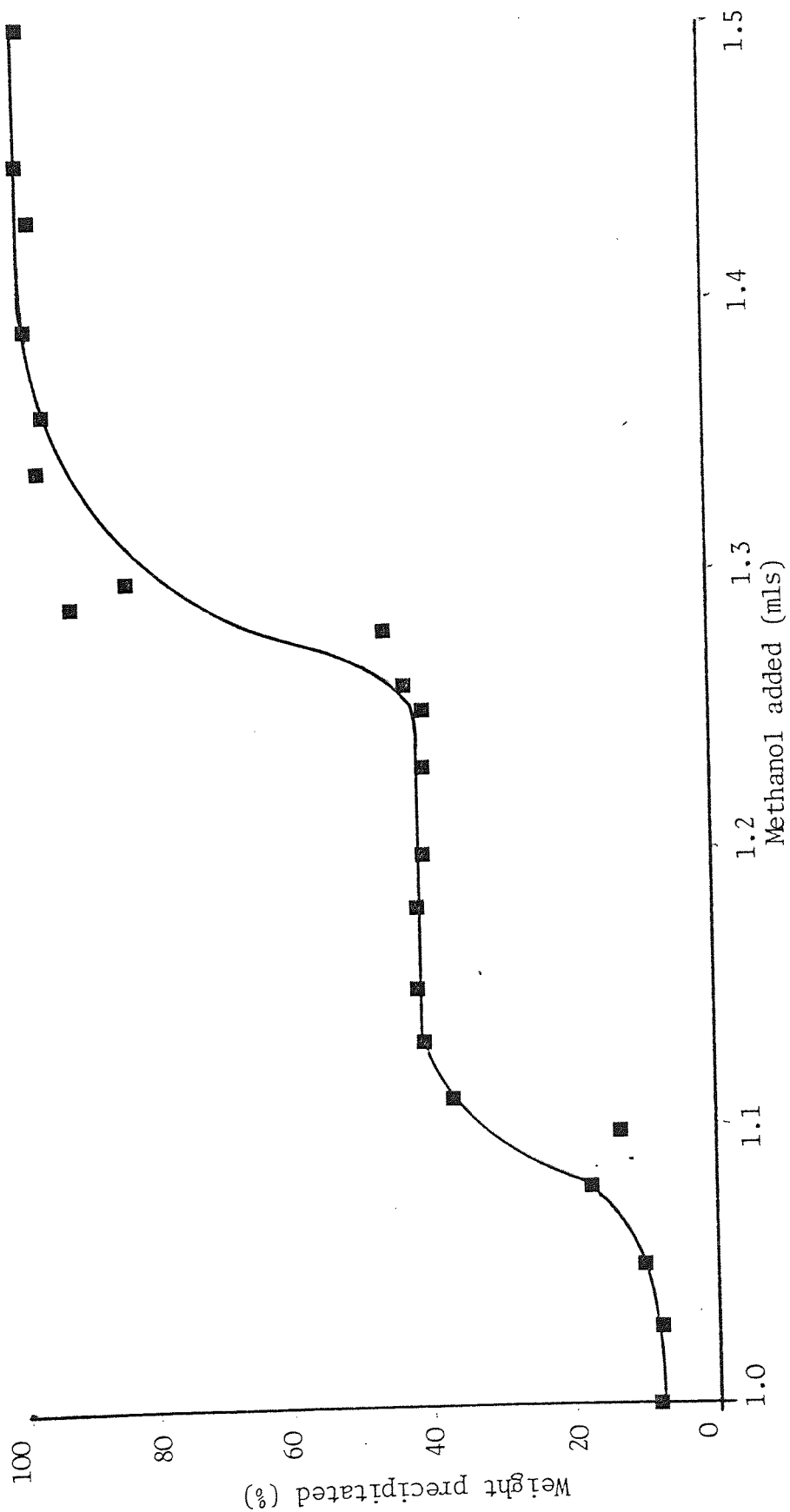


Fig 3.10 Determination of GS : NR interpolymer formation (formulation C, section 3.7.4)

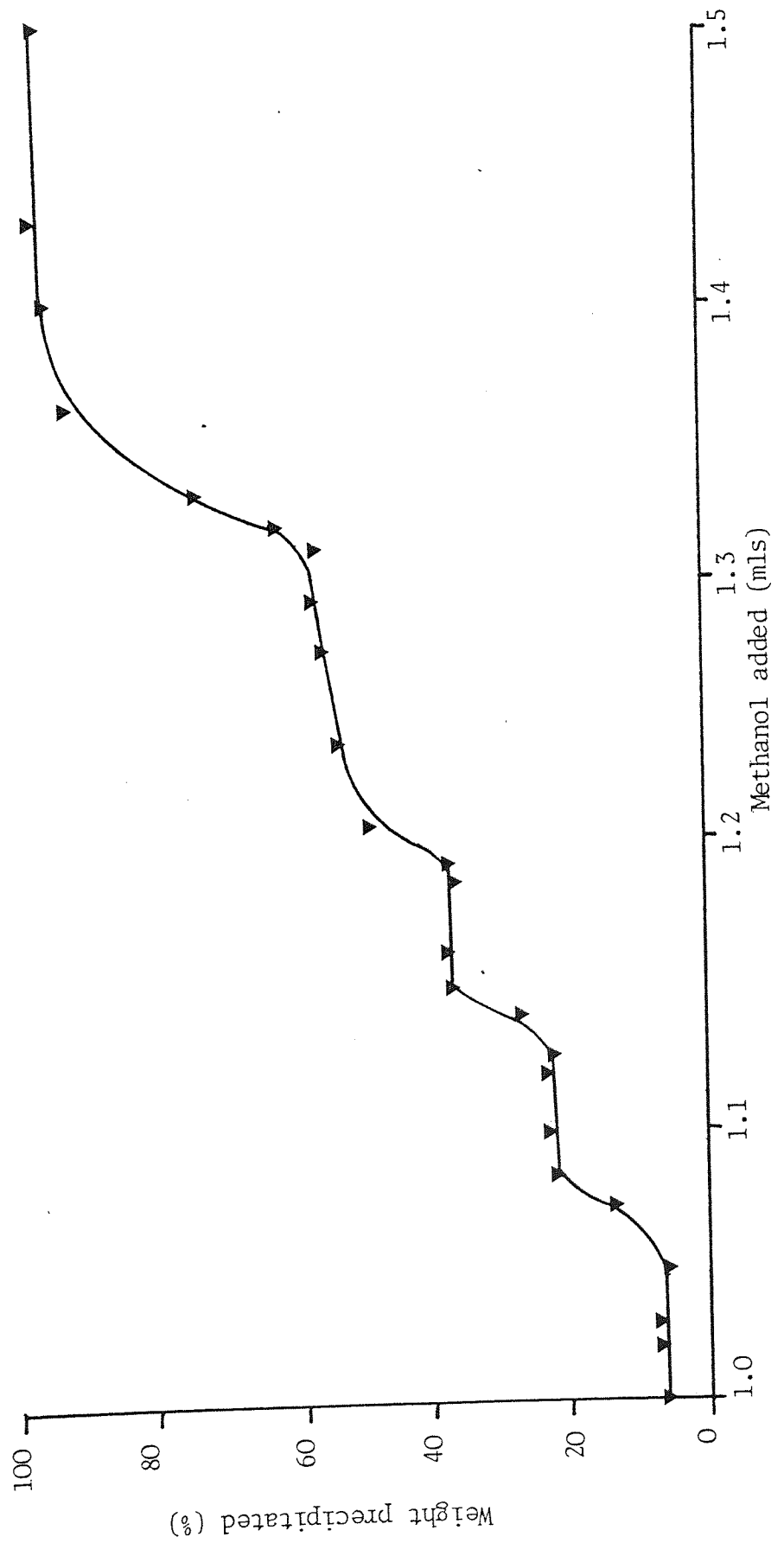


Fig 4.1 Effect of carbon black content on the fatigue behaviour of a 75 : 25 GS : W vulcanisate

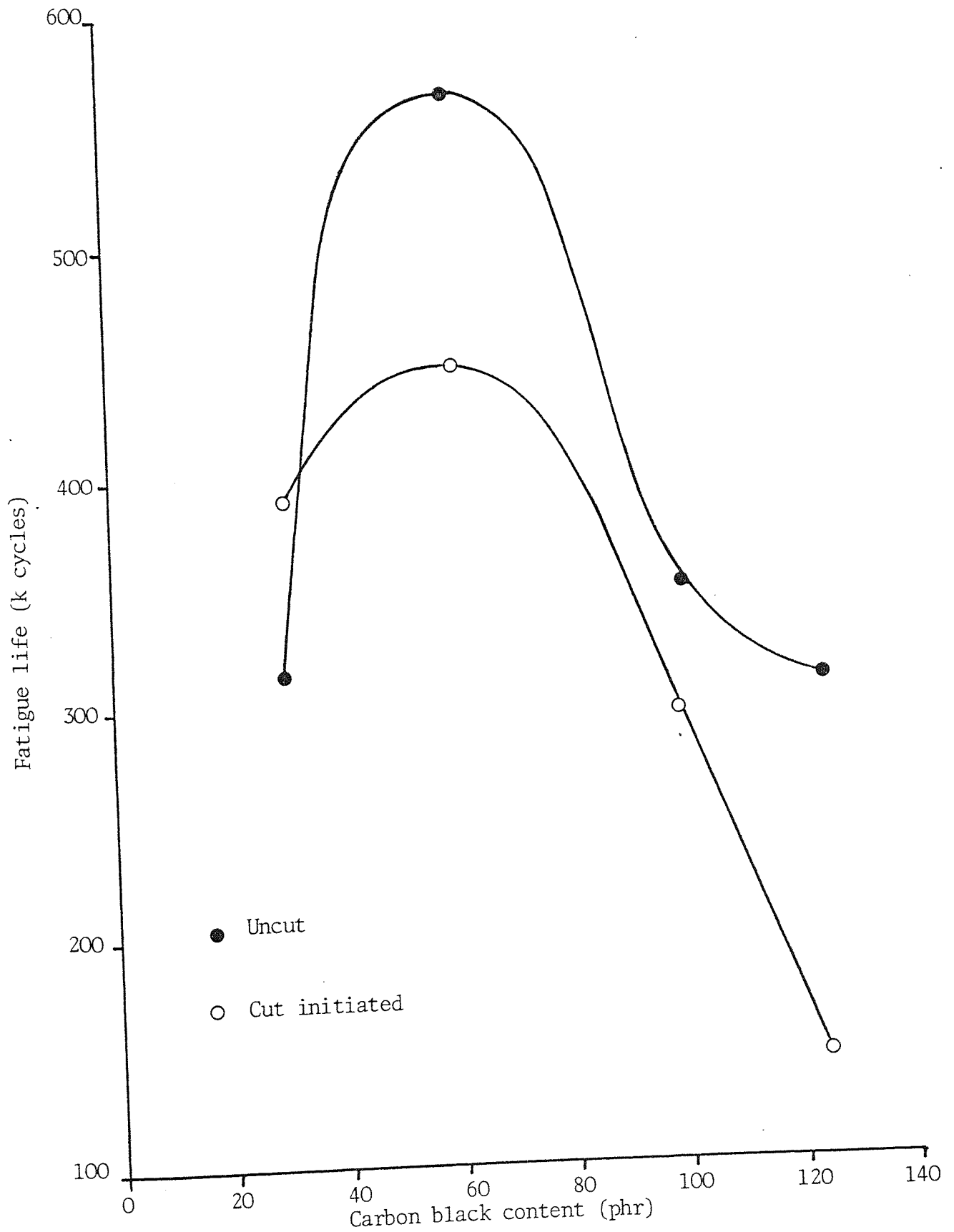


Fig 4.2 Effect of GW : W blend ratio on fatigue behaviour

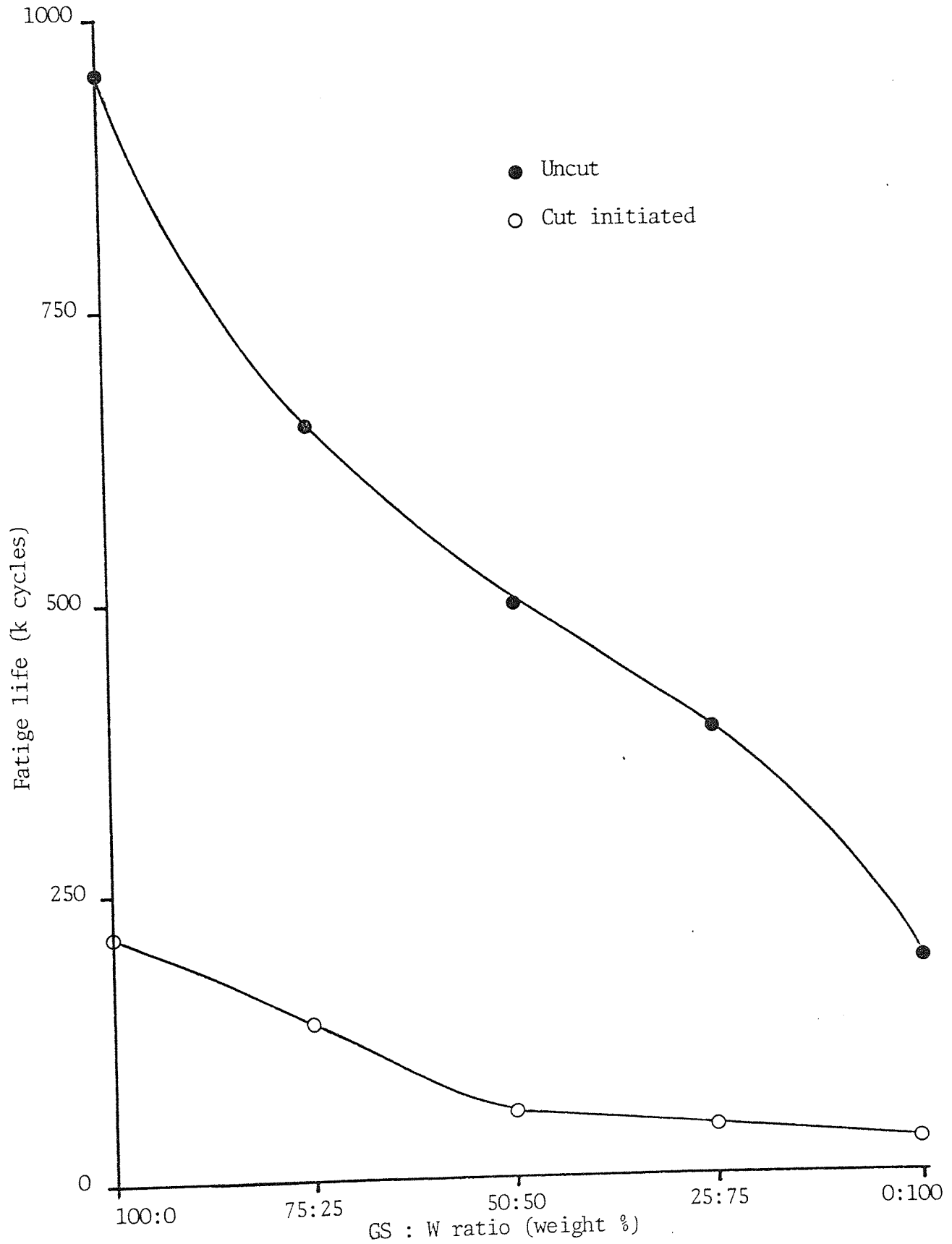


Fig 4.3 DSC thermograms of Neoprene GS and Neoprene W and 50 GS : W vulcanisates

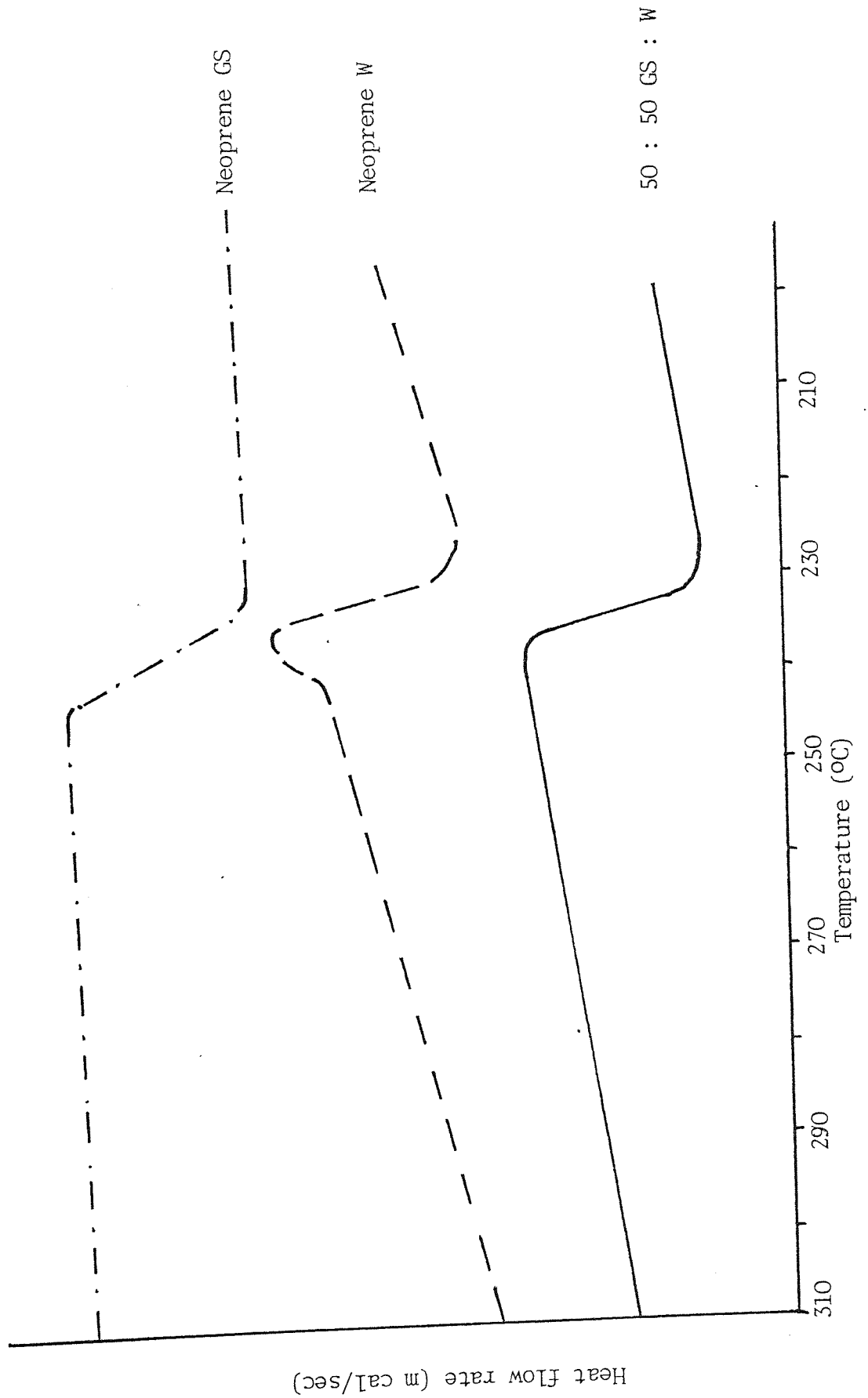


Fig 4.4 Effect of GS : W blend ratio on tear strength

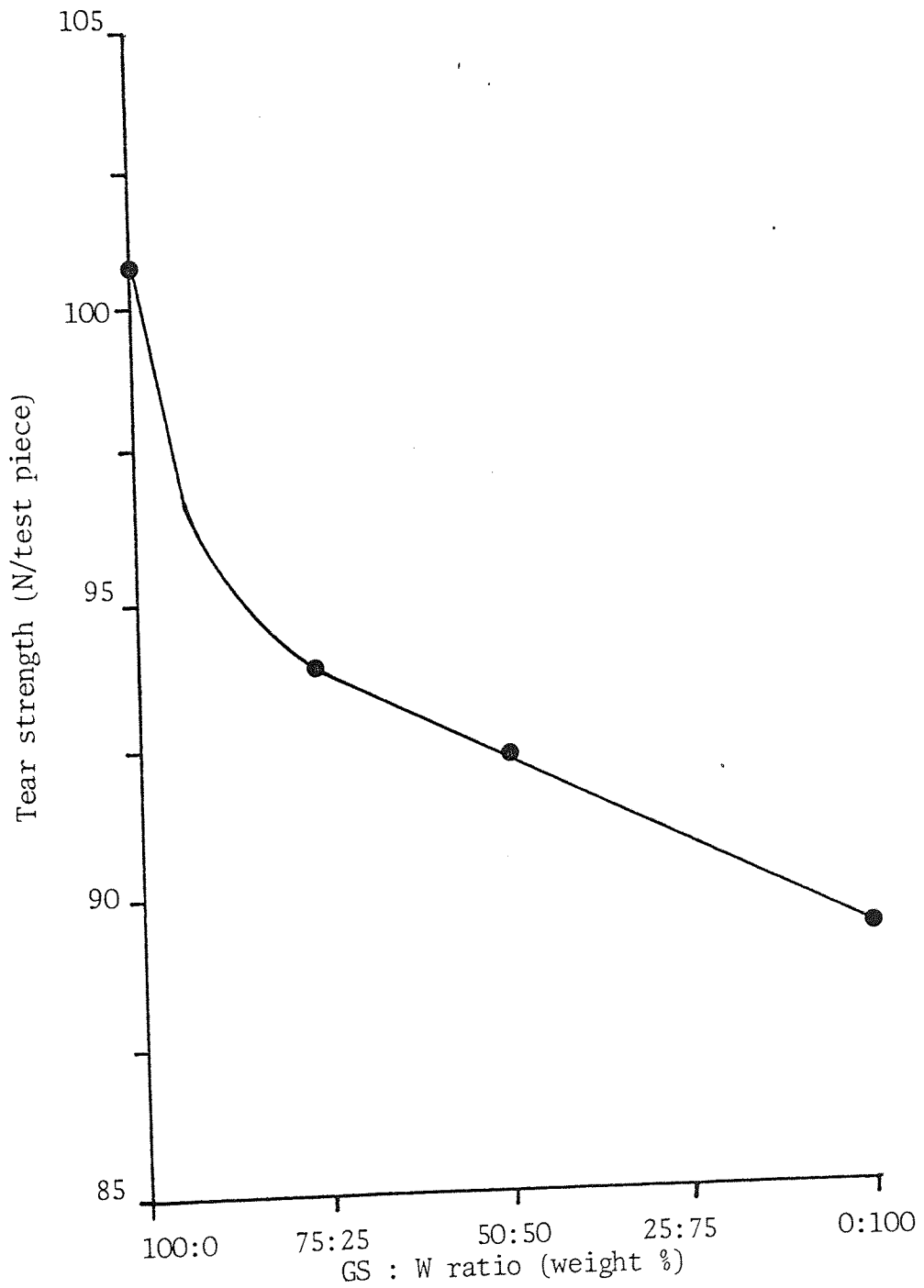


Fig 4.5 Effect of W : NR blend ratio on fatigue behaviour

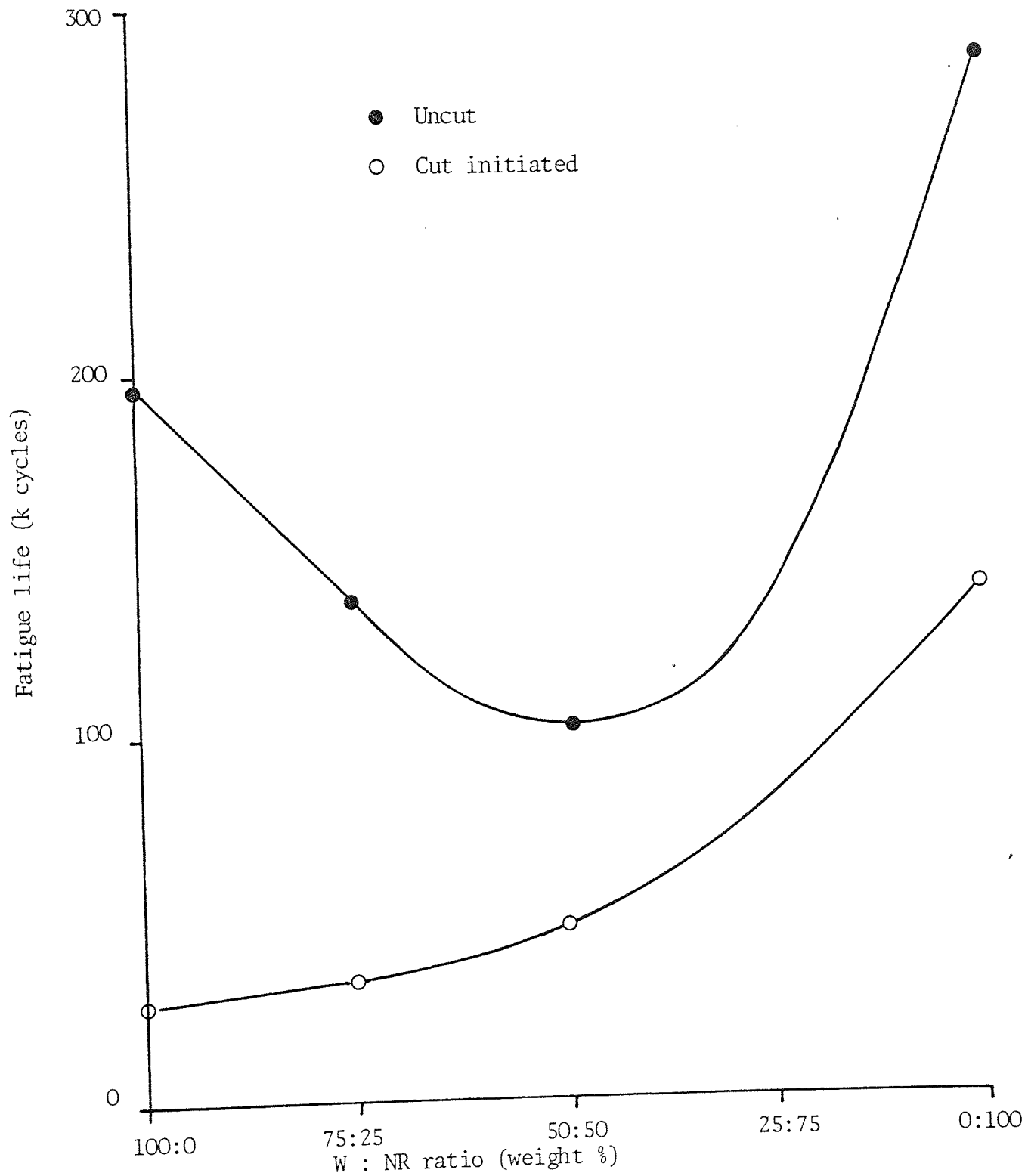


Fig 4.6 DSC thermograms of Neoprene W, natural rubber and 50 : 50 W : NR vulcanisates

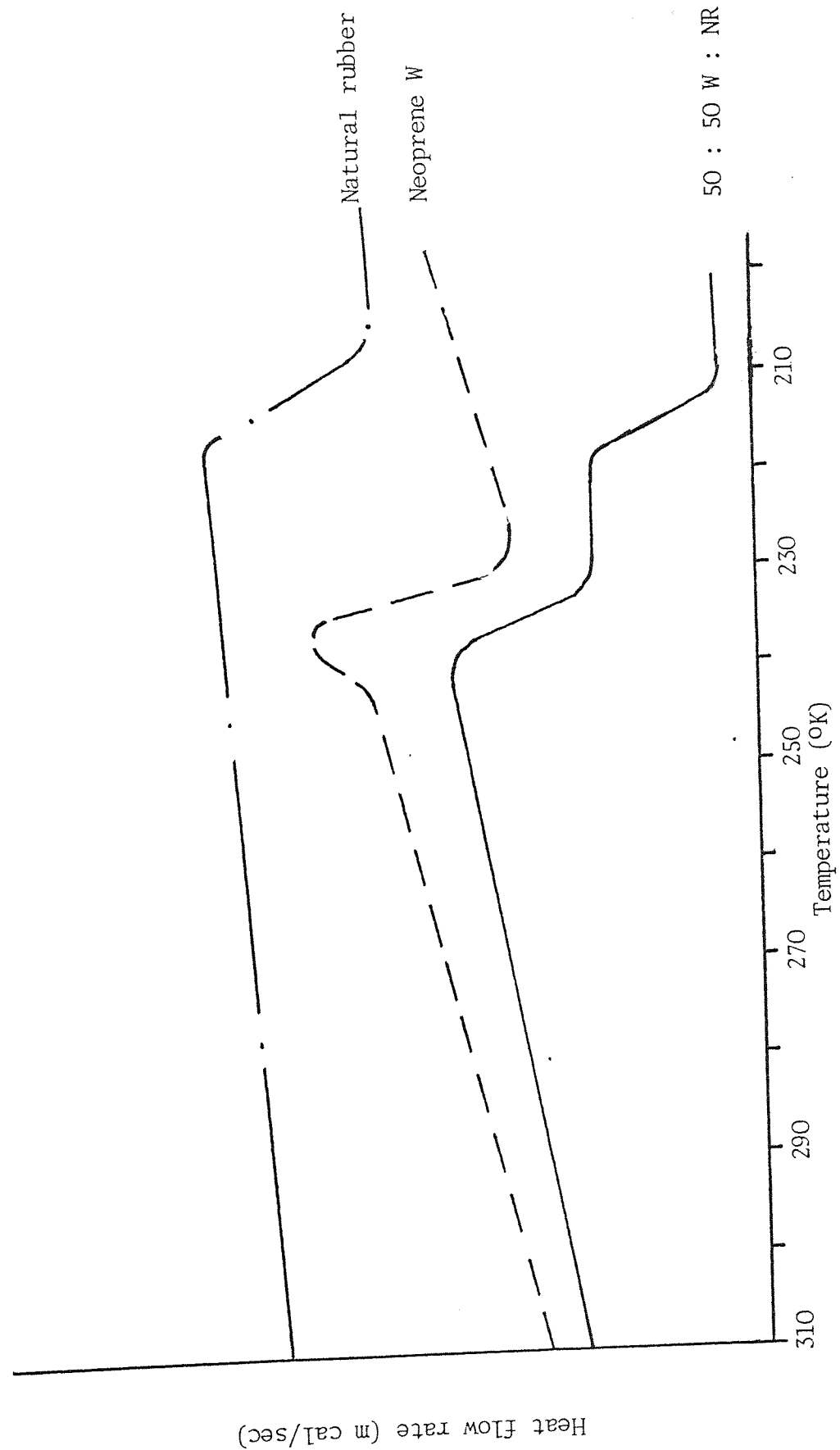


Fig 4.7 Effect of GS : NR blend ratio on fatigue behaviour

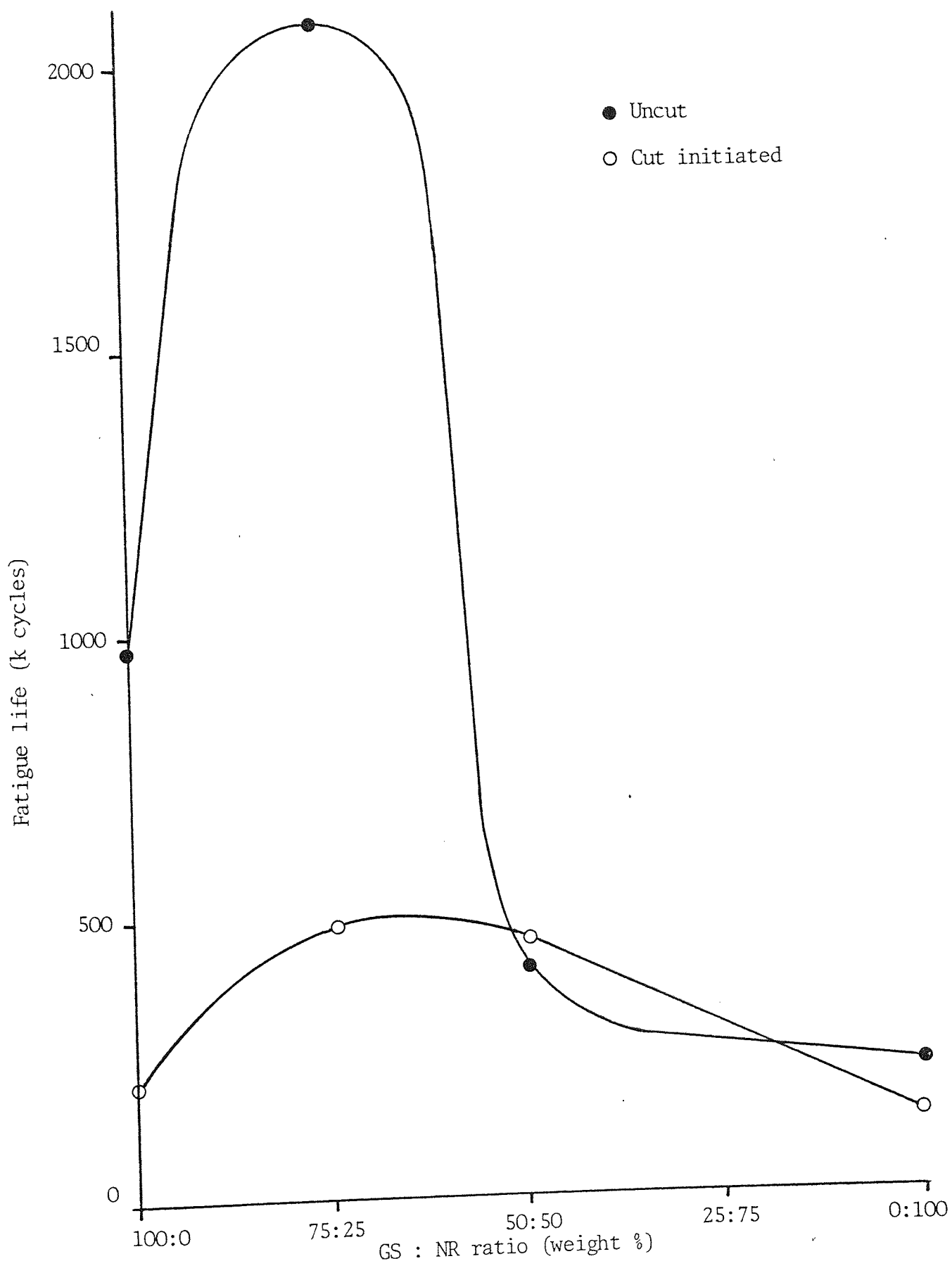


Fig 4.8 DSC thermograms of Neoprene GS, natural rubber and 50 : 50 GS : NR vulcanisates

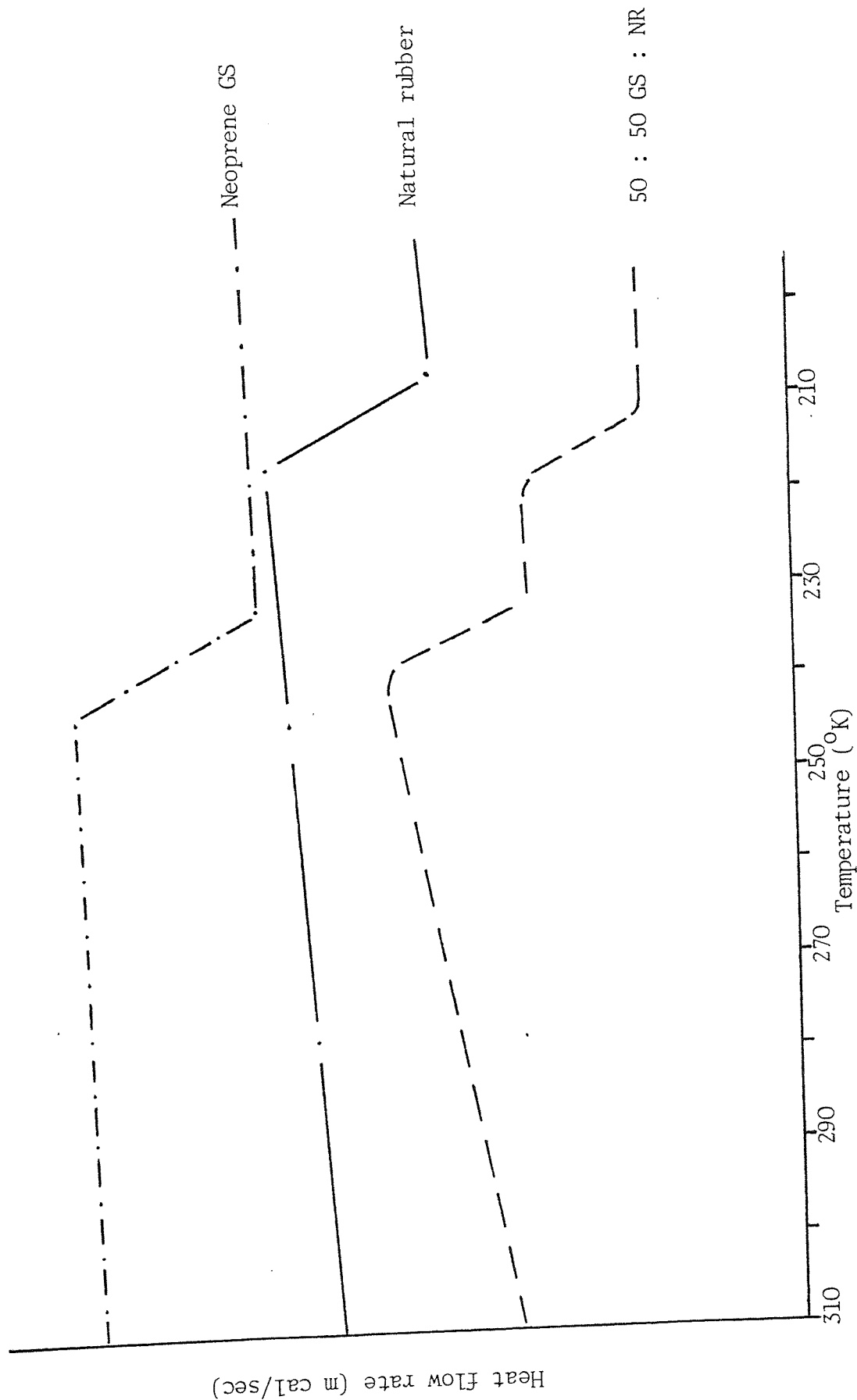


Fig 4.9 Effect of morphology on the uncut fatigue behaviour of GS : NR vulcanisates

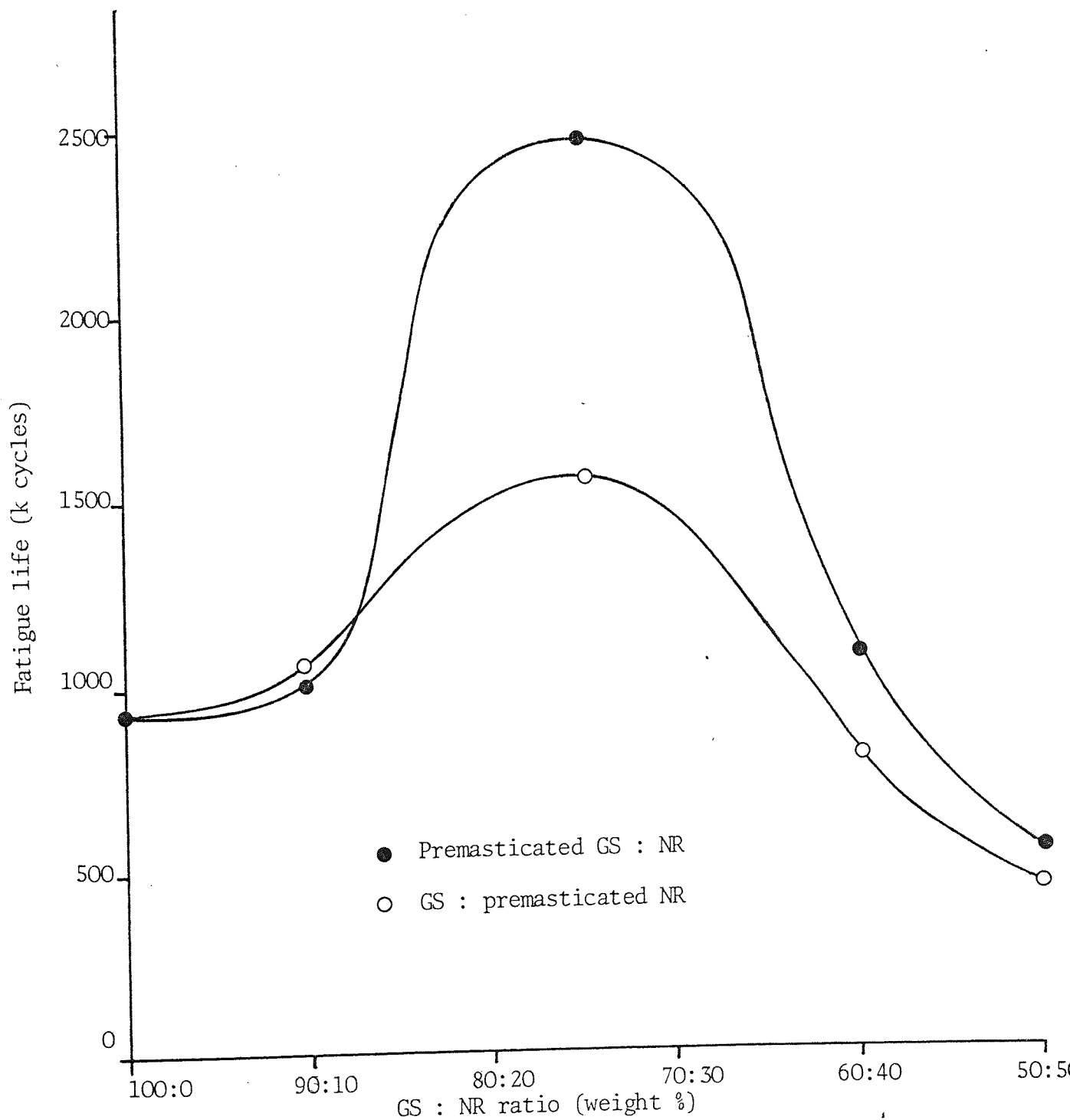


Fig 4.10 Effect of morphology on the cut initiated fatigue behaviour of GS : NR vulcanisates

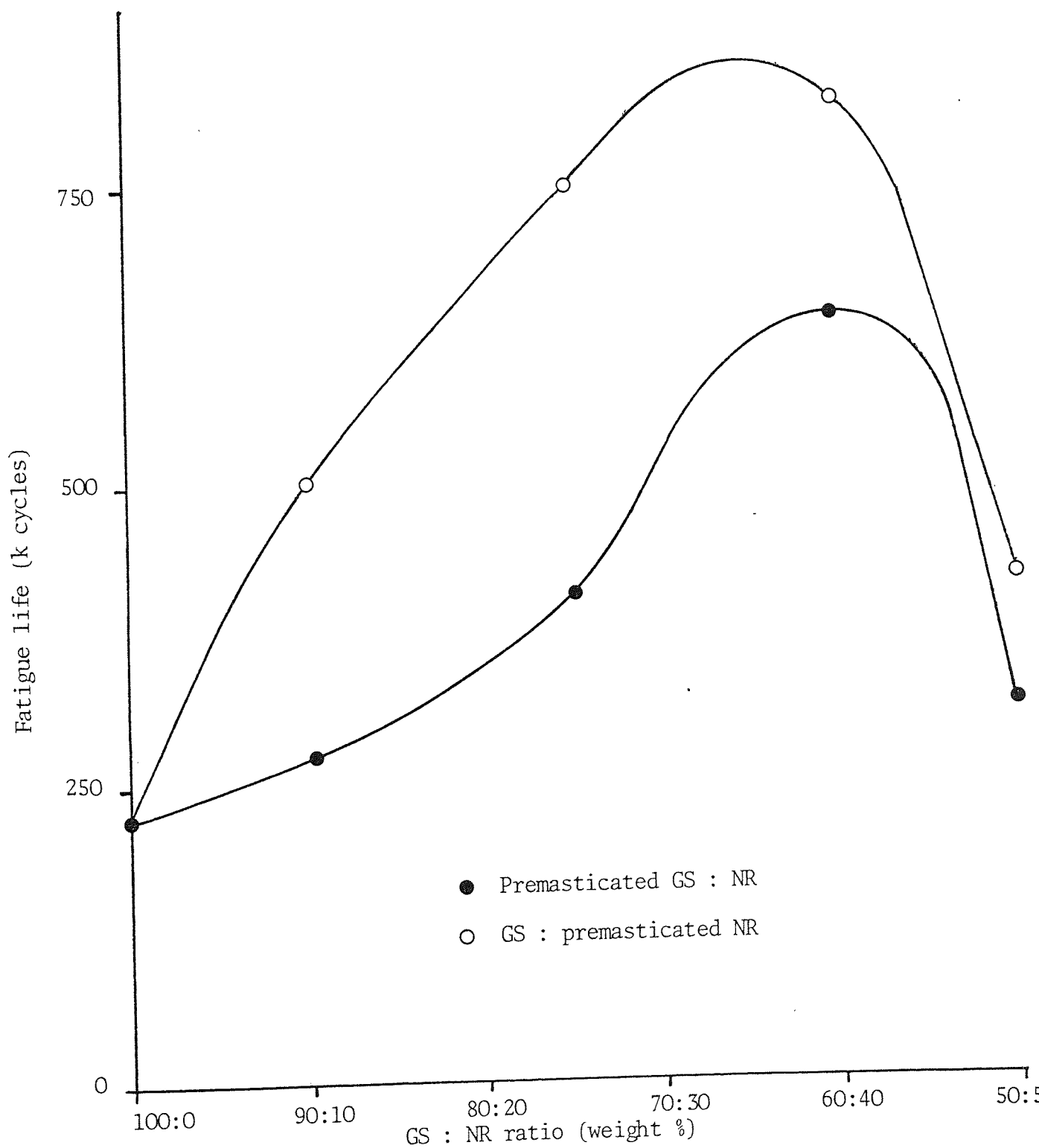


Fig 4.11 Effect of morphology on the tear strength of GS : NR vulcanisates

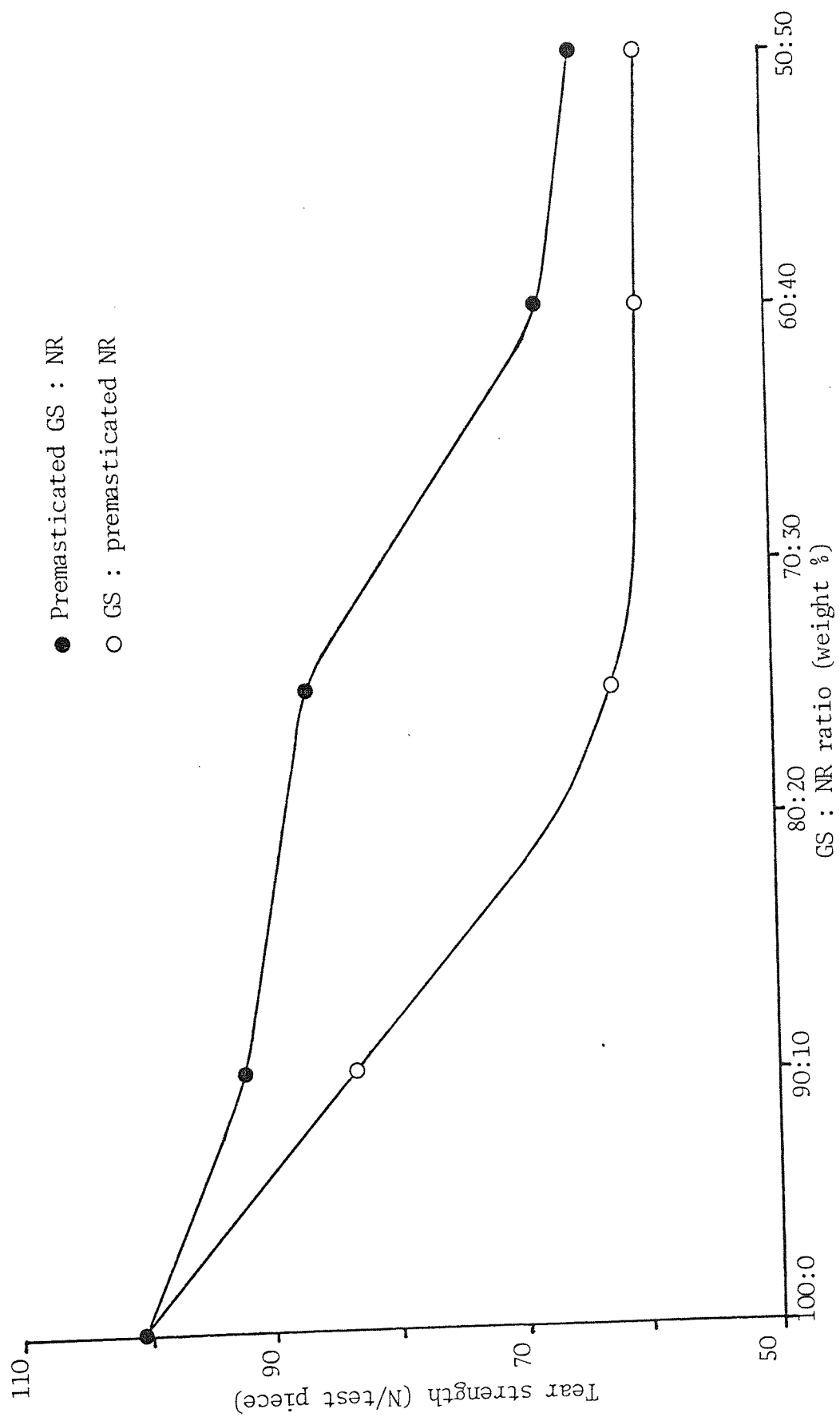


Fig 4.12 Effect of morphology on the uncut isostress fatigue behaviour of GS : NR vulcanisates

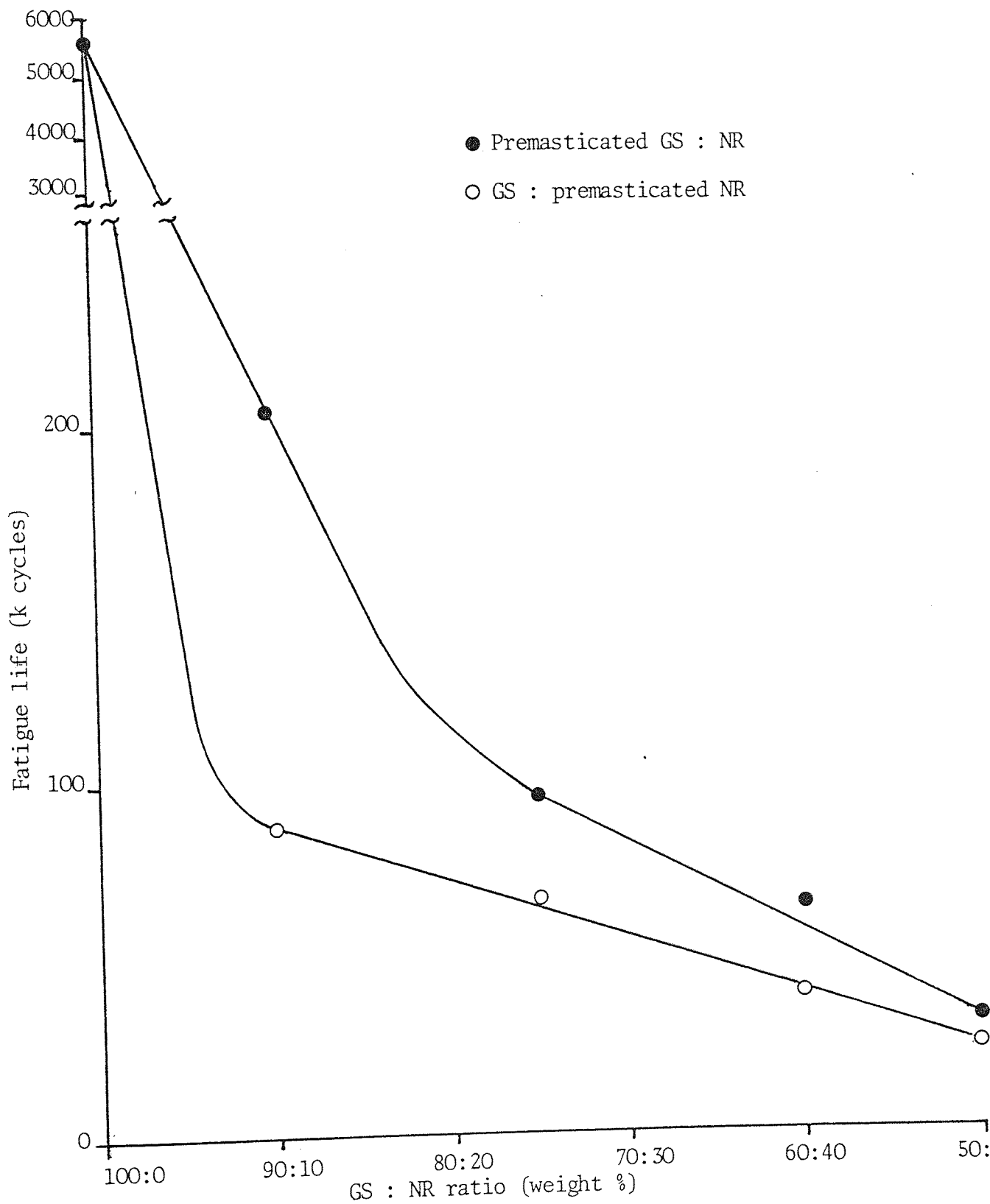


Fig 4.13 Effect of morphology on the cut initiated isostress fatigue behaviour of GS : NR vulcanisates

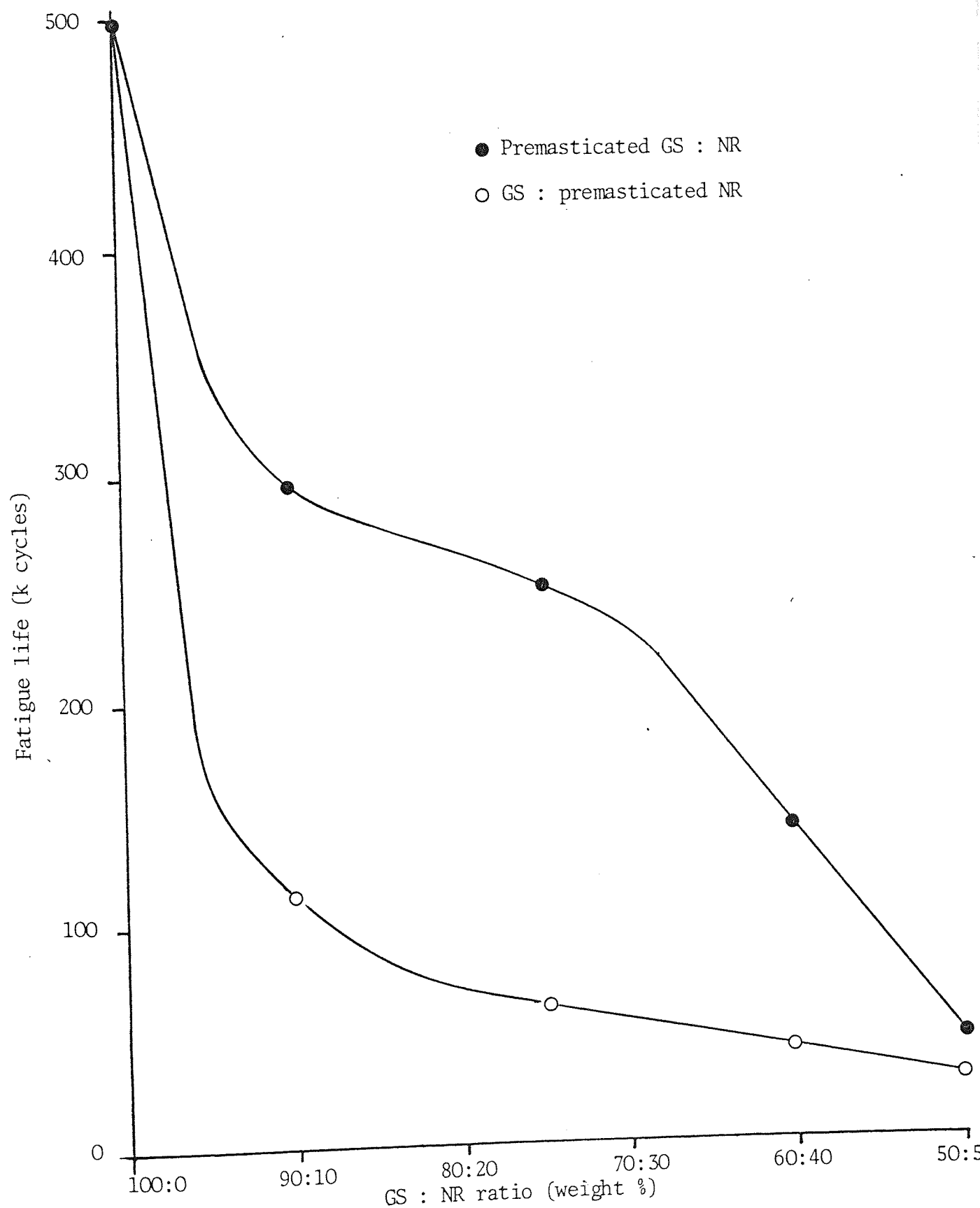


Fig 4.14 Effect of increasing interpolymer additions on the fatigue behaviour of a 50 : 50 GS : NR vulcanisate

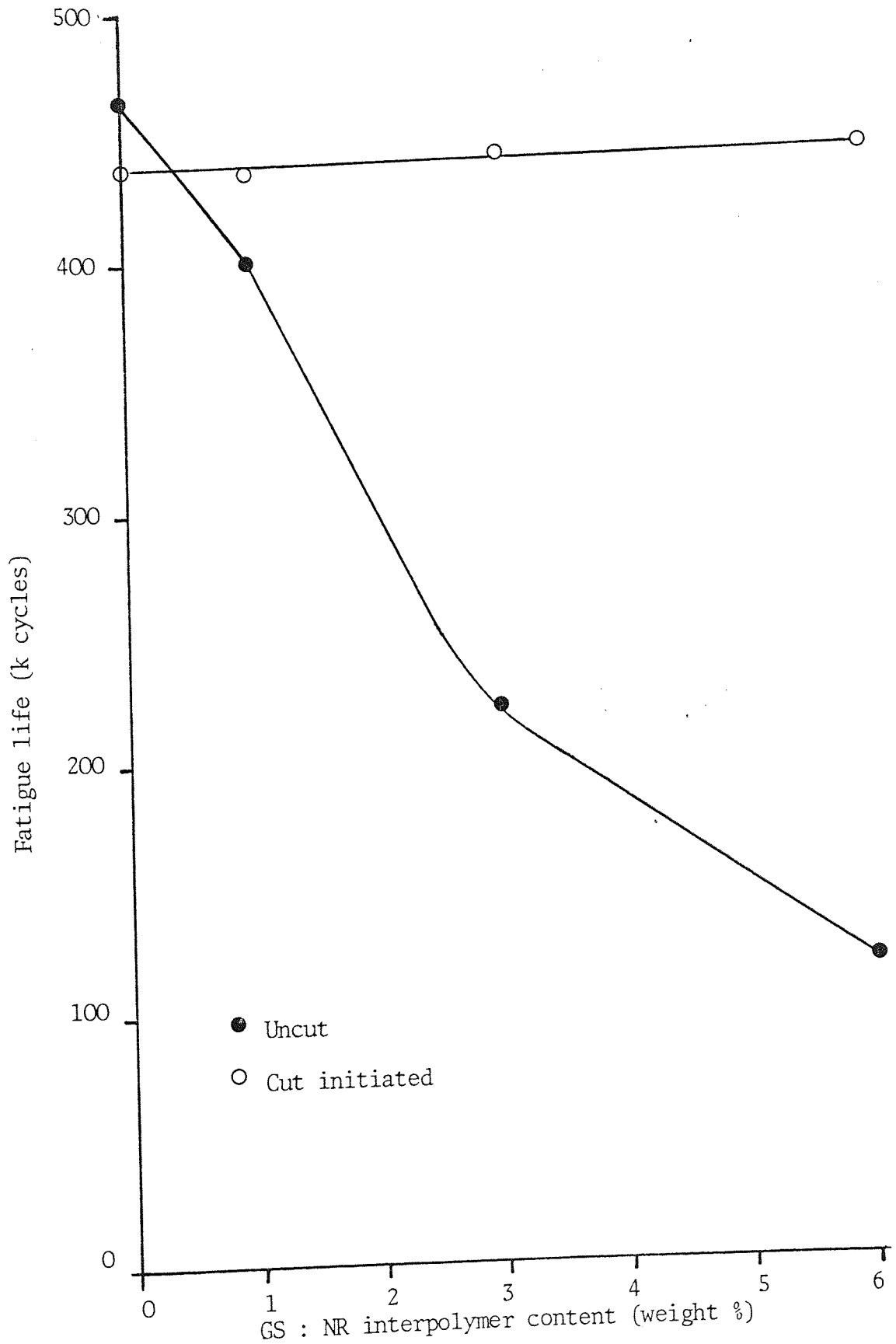


Fig 4.15 Effect of cure time on the CLD of NR and GS in a 50 : 50 GS : NR vulcanisate

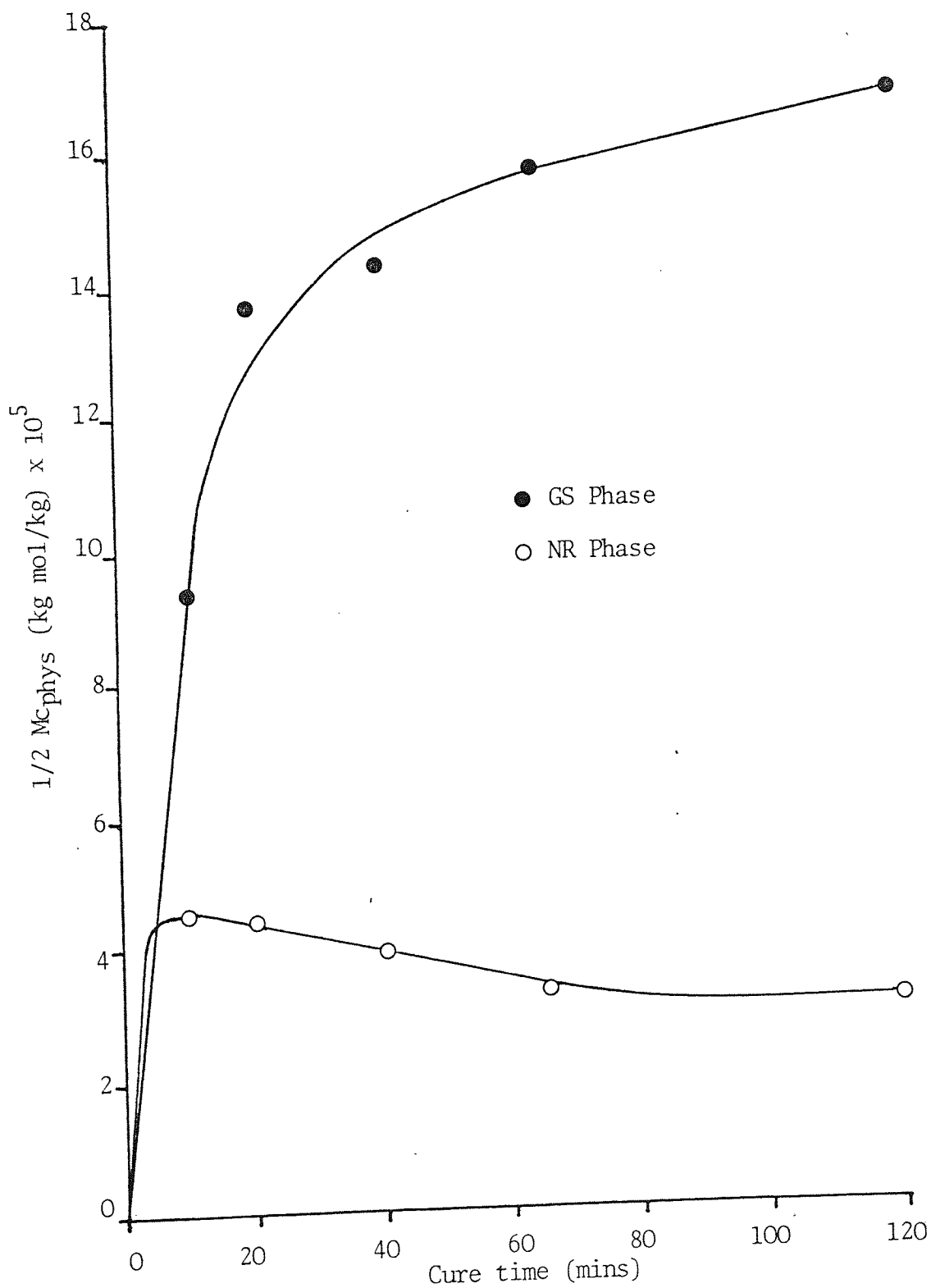


Fig 4.16 Effect of cure time on the network structure of a Neoprene GS vulcanisate

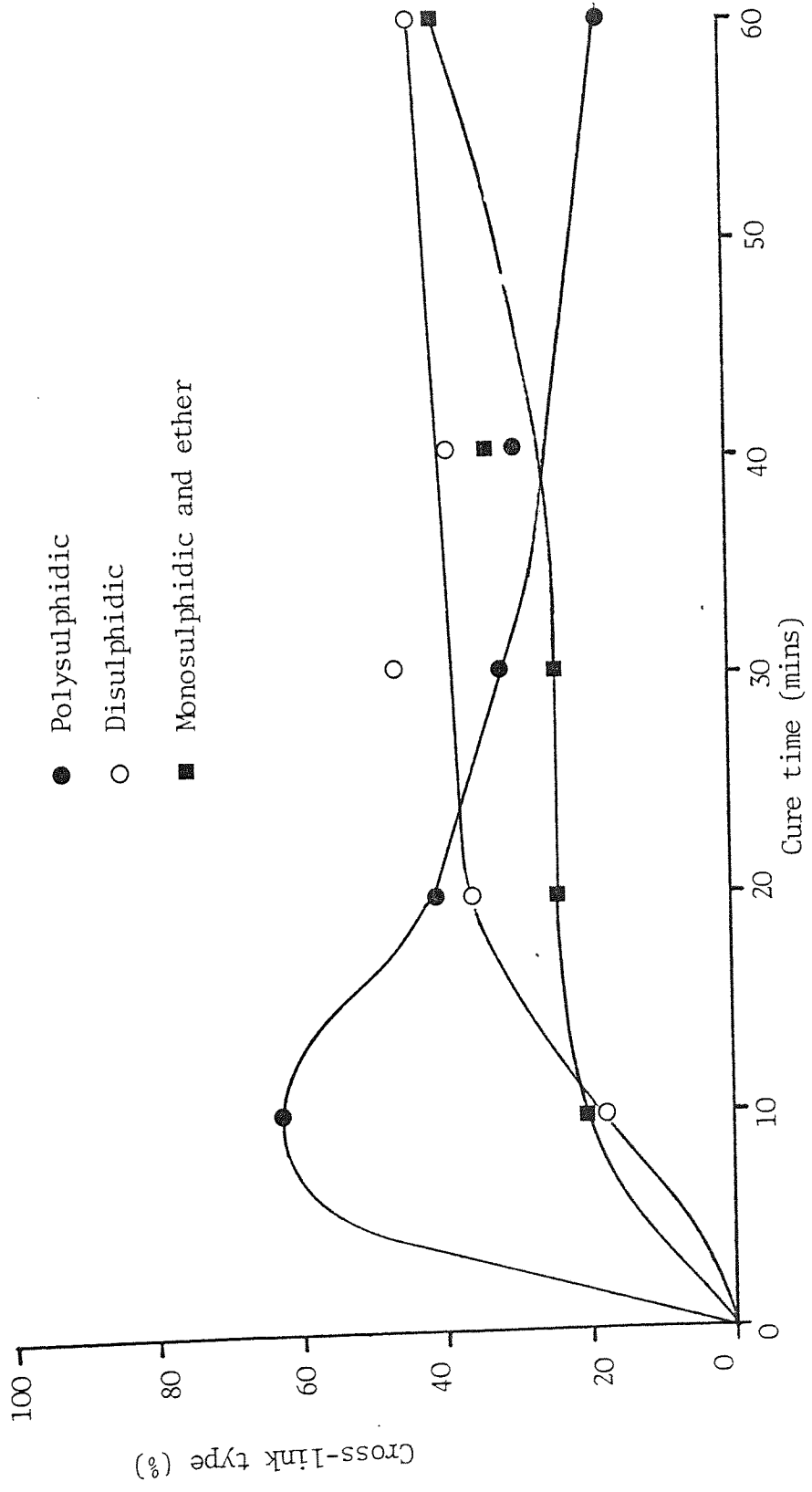


Fig 4.17 Effect of fatigue on the network structure of a natural rubber vulcanisate

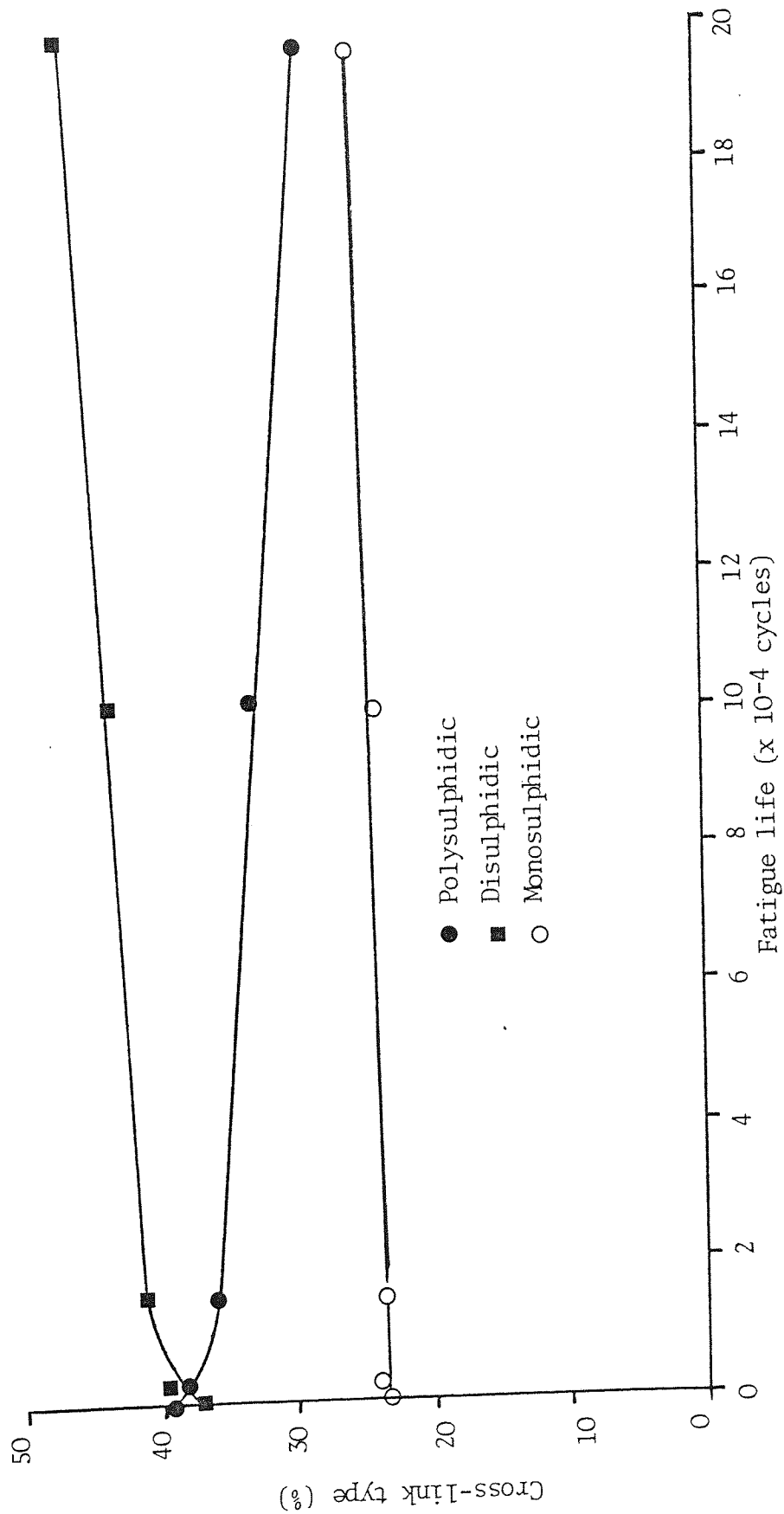


Fig 4.18 Effect of fatigue on the network structure of a Neoprene GS vulcanisate

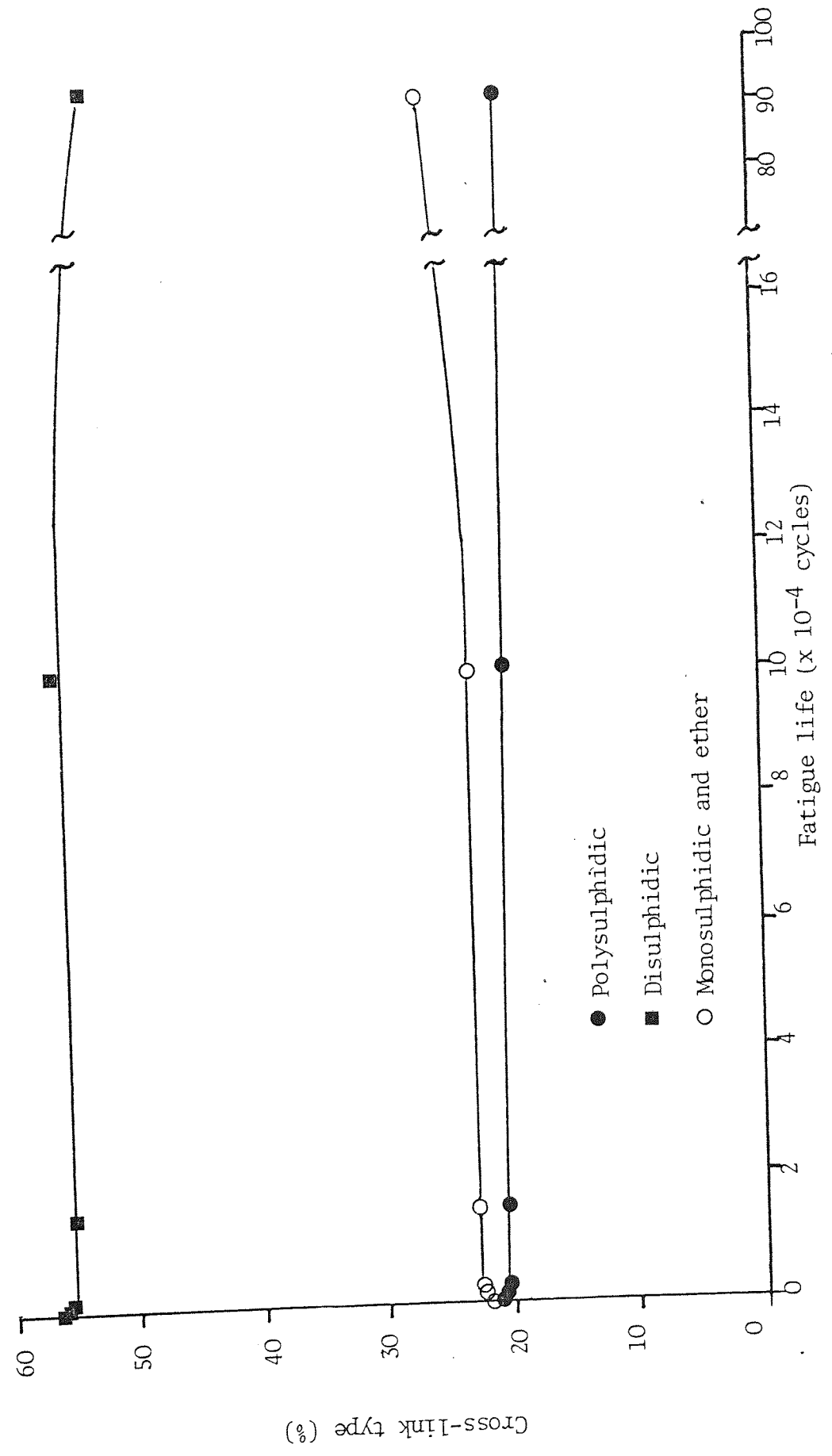


Fig 4.19 Effect of increasing sulphur additions on the fatigue behaviour of a 50 : 50 GS : NR vulcanisate

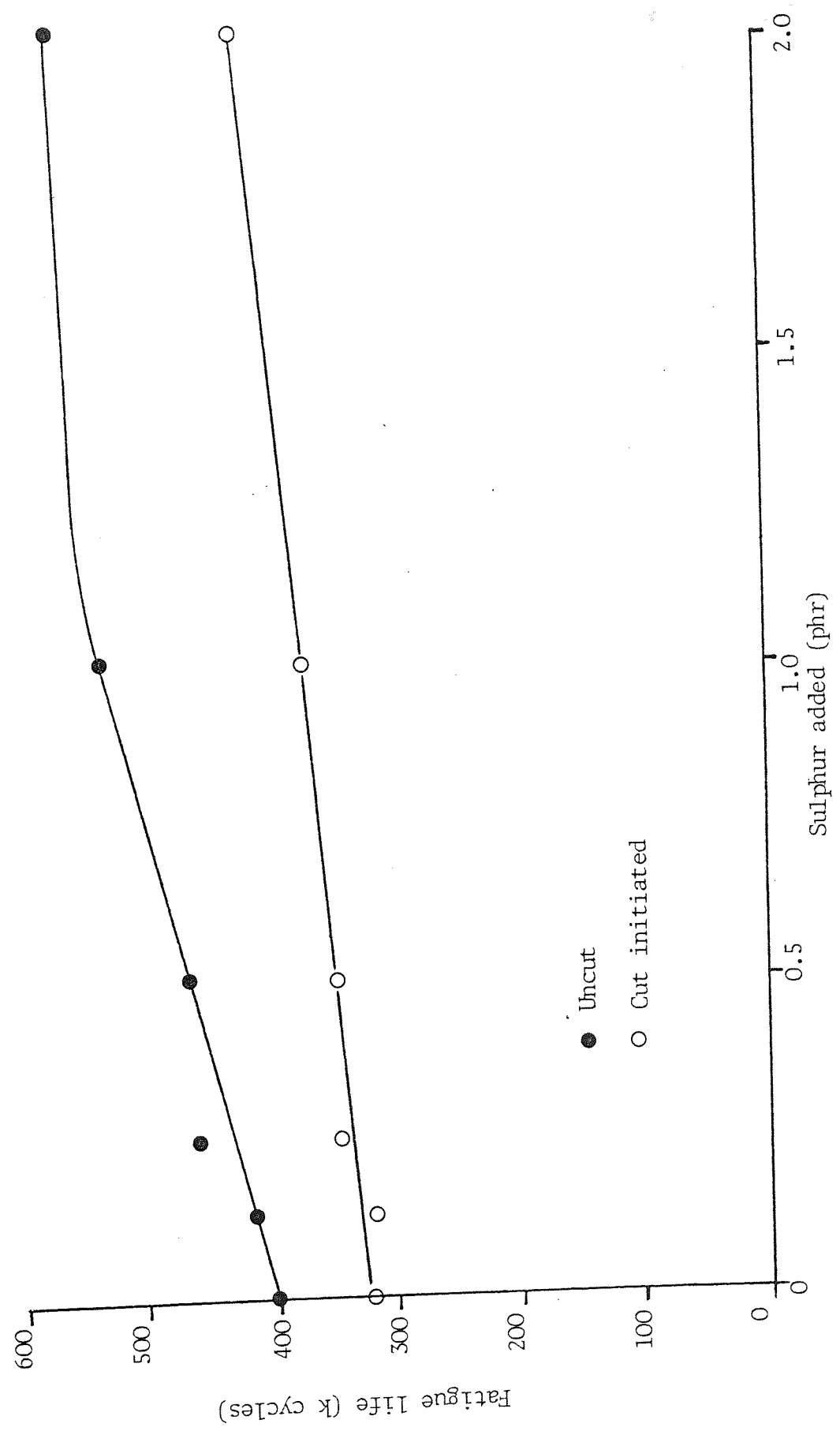


Fig 4.20 Effect of increasing CBS additions on the fatigue behaviour of a 50 : 50 GS : NR vulcanisate

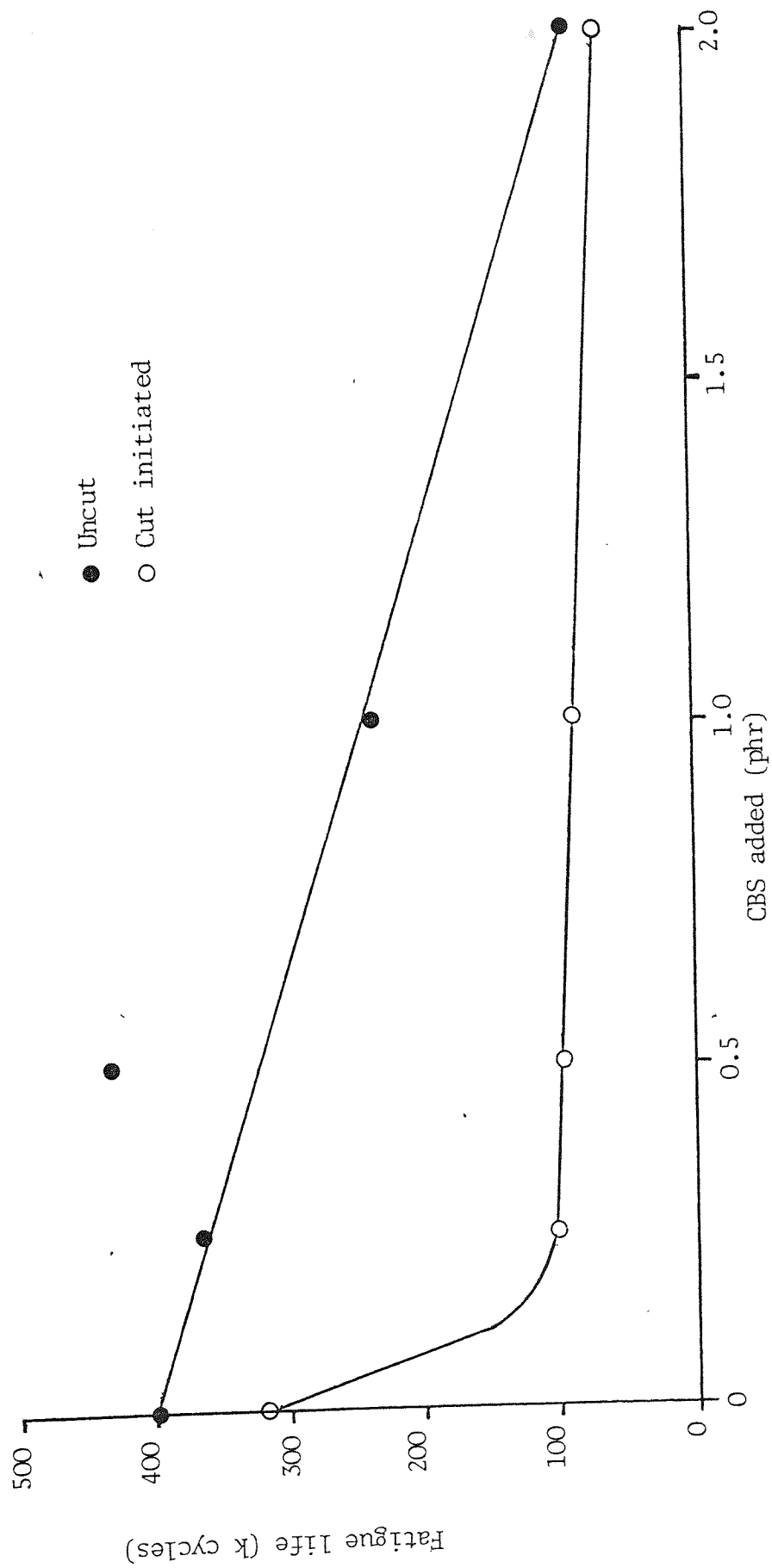
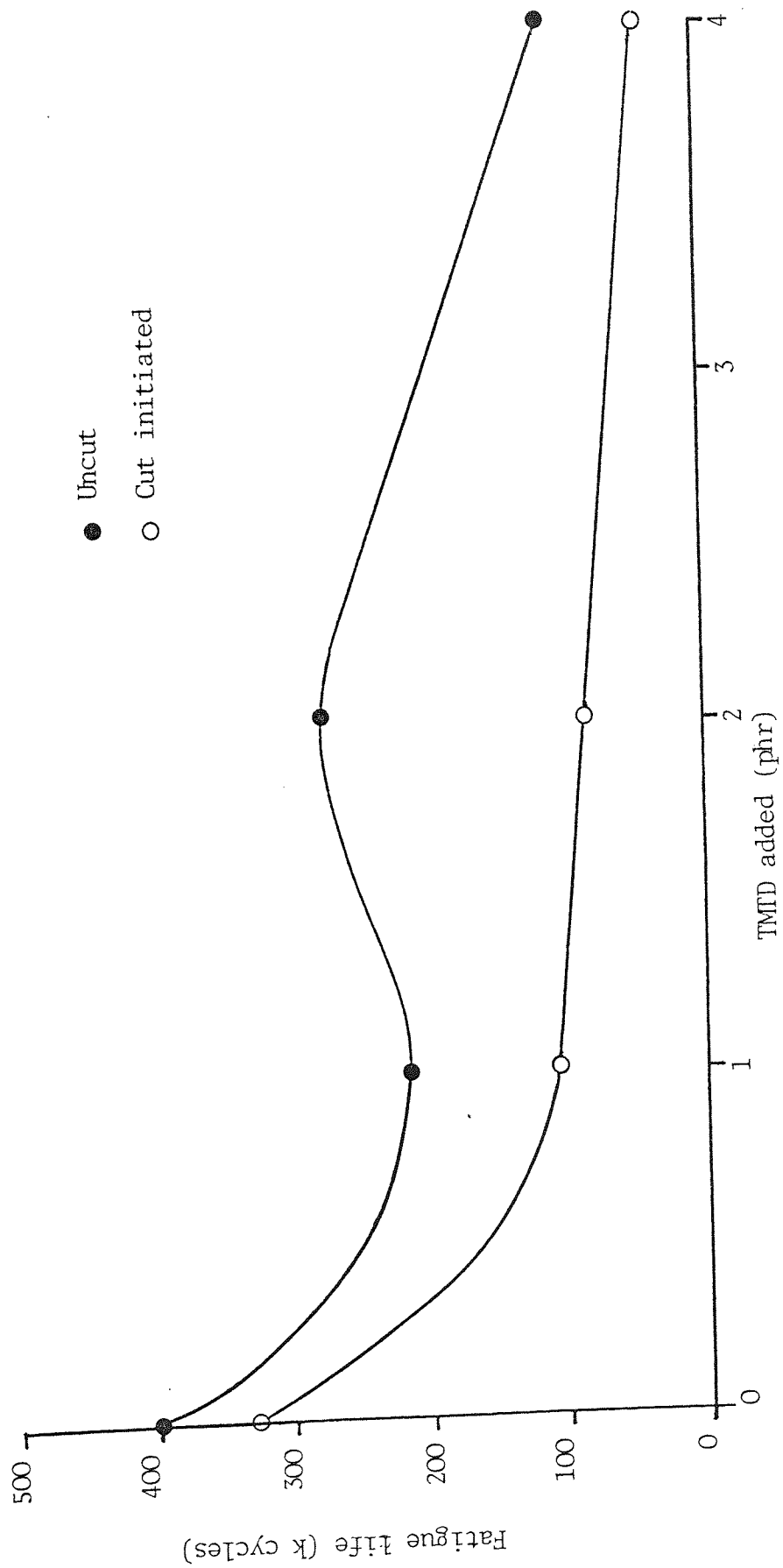


Fig 4.21 Effect of increasing TMD additions on the fatigue behaviour of a 50 : 50 GS : NR vulcanisate



APPENDIX THREE

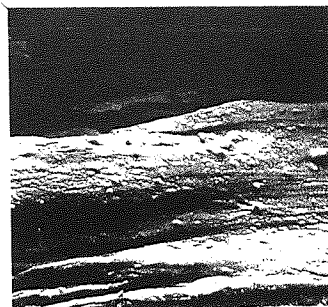
FRAMES

SEM micrographs of the fatigue failure surfaces of filled
75 : 25 GS : W and 50 : 50 GS : NR vulcanisates

Frame 5.1

75 : 25 GS : W

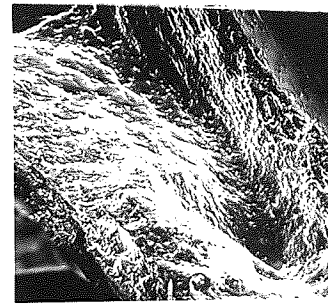
Magnification: 20X



Frame 5.2

50 : 50 GS : NR

Magnification: 20X

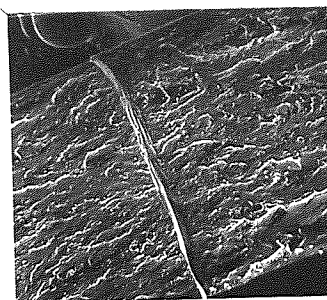


Effect of carbon black content on the fatigue failure surface
of 75 : 25 GS : W vulcanisates

Frame 5.3

125 phr of carbon black

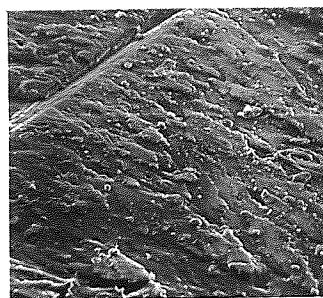
Magnification: 20X



Frame 5.4

100 phr of carbon black

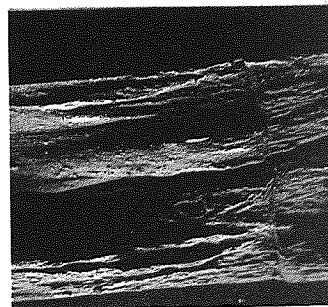
Magnification: 20X



Frame 5.5

60 phr of carbon black

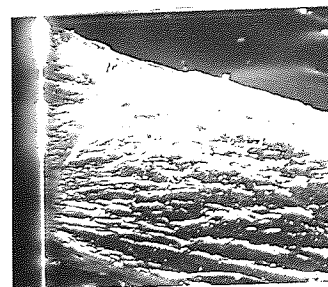
Magnification: 20X



Frame 5.6

30 phr of carbon black

Magnification: 20X

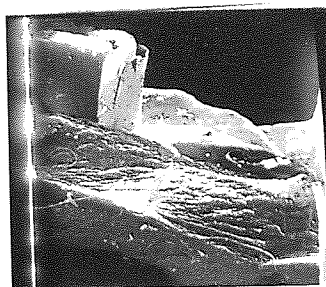


SEM micrographs of the fatigue failure surfaces of GS : W
vulcanisates containing increasing amounts of Neoprene W

Frame 5.7

100 : 0 GS : W

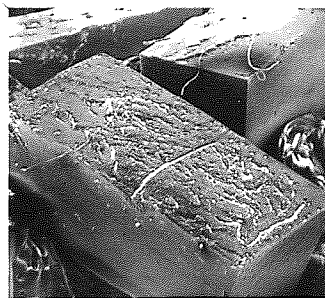
Magnification: 10X



Frame 5.8

75 : 25 GS : W

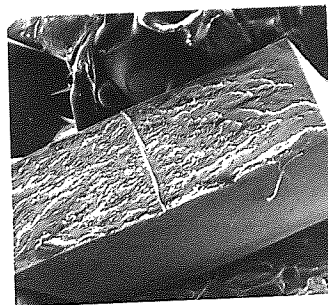
Magnification: 10X



Frame 5.9

50 : 50 GS : W

Magnification: 10X

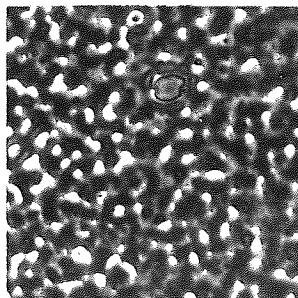


Phase contrast micrographs of W : NR gum vulcanisates containing increasing amounts of NR

Frame 5.10

75 : 25 W : NR

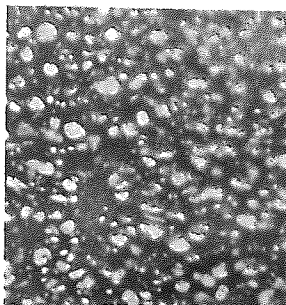
Magnification: 600X



Frame 5.11

50 : 50 W : NR

Magnification: 600X

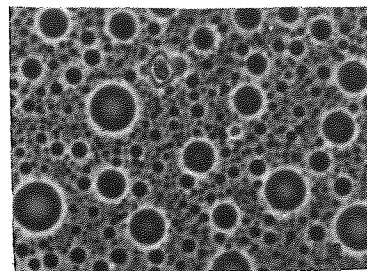


Phase contrast micrographs obtained from solutions of 50 : 50
GS : NR blends with and without 6% interpolymer

Frame 5.12

50 : 50 GS : NR no interpolymer

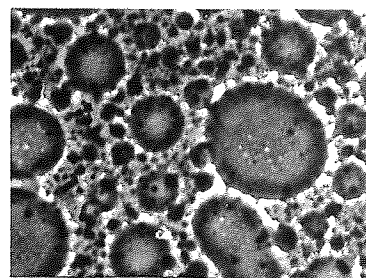
Magnification: 200X



Frame 5.13

50 : 50 GS : NR containing 6% interpolymer

Magnification: 200X



REFERENCES

- 1 W H Carothers and A M Collins, US Pat, 1,950,431 (1934)
- 2 W H Carothers and A M Collins, US Pat, 1,950,432 (1934)
- 3 I Williams, US Pat, 1,950,433 (1934)
- 4 W H Carothers, A M Collins and J E Kirby, US Pat,
1,950,436 (1934)
- 5 H W Starkweather, US Pat, 1,950,437 (1934)
- 6 W H Carothers and J E Kirby, US Pat, 1,950,439 (1934)
- 7 A M Collins, US Pat, 1,967,861 (1934)
- 8 W H Carothers, A M Collins and J E Kirby, US Pat,
1,967,860 (1934)
- 9 A M Collins, US Pat, 1,967,865 (1934)
- 10 D B Forman, 'Rubber Technology', M Morton (ed), 2nd Edn,
Chpt 13, p 322 (1973), Van Norstrand, NY (publ)
- 11 R M Murray and D C Thompson, 'The Neoprenes', Elast Chem
Div, E I Du Pont de Nemours and Co (1963)
- 12 N L Catton, 'The Neoprenes', Rubb Chem Div, E I Du Pont
de Nemours and Co (1953)
- 13 S Koch (ed), 'Manual for the Rubber Industry', Bayer (1972)
- 14 E Engelmann, J Inst Rubb Ind, 77, 3 (1969)
- 15 M Morton, J A Cala and M W Althier, J Polym Sci, 19,
547 (1956)
- 16 M Morton and I Piirma, J Polym Sci, 19, 563 (1956)
- 17 I Williams and H W Walker, Ind Eng Chem, 25, 199 (1933)
- 18 D E Andersen and R G Arnold, Ind Eng Chem, 45, 2727 (1953)
- 19 D Rosahl and H Esser, US Pat, 3,074,899 (1963)

- 20 P O Bare, US Pat, 2,426,854 (1947)
- 21 E J Lorand, US Pat, 2,569,480 (1951)
- 22 J T Maynard, US Pat, 2,707,180 (1955)
- 23 H Malz and D Rosahl, US Pat, 2,962,475 (1960)
- 24 G Jennes, H Sutter and K Nutzel, US Pat, 3,236,823 (1966)
- 25 H Walker, US Pat, 2,259,122 (1941)
- 26 A M Hutchinson, Can Pat, 661,997 (1963)
- 27 J R Goertz, US Pat, 2,576,009 (1951)
- 28 F P Demme, Ger Pat, 1,138,944 (1962)
- 29 L G Melkonyan, Arm Khim Zh, 21, 187 (1962)
- 30 L G Melkonyan, Arm Khim Zh, 22, 873 (1969)
- 31 L G Melkonyan, Arm Khim Zh, 22, 1062 (1969)
- 32 W E Mochel and J H Peterson, J Am Chem Soc, 71, 1426
(1949)
- 33 F Hrabak and J Zachoval, J Polym Sci, 52, 131 (1961)
- 34 W E Mochel, J Polym Sci, 8, 583 (1952)
- 35 A L Klebanskii, J Polym Sci, 30, 763 (1958)
- 36 W E Mochel, J R Nichols C J Mighton, J Am Chem Soc, 70,
2185 (1948)
- 37 N D Zakharov, N A Bogdanovich, Z D Tuyremnova and
U S Glavina, Vysokomol, Soed, 5, 910 (1963)
- 38 G W Scott, US Pat, 2,481,044 (1949)
- 39 G W Scott, US Pat, 2,518,573 (1950)
- 40 J E Kirby and W E Sharkey, US Pat, 2,477,338 (1949)
- 41 M A Youker, US Pat, 2,234,215 (1941)
- 42 W E Mochel and J R Nichols, Ind Eng Chem, 43, 154 (1951)
- 43 J T Maynard and W E Mochel, J Polym Sci, 13, 235 (1954)

- 44 J T Maynard and W E Mochel, J Polym Sci, 13, 251 (1954)
- 45 J T Maynard and W E Mochel, J Polym Sci, 18, 227 (1955)
- 46 R C Ferguson, J Polym Sci, A2, 4735 (1964)
- 47 C A Aufdermarsh and R Pariser, J Polym Sci, A2, 4727 (1964)
- 48 R R Garrett, C A Hargreaves and D N Robinson, J Macromol
Sci Chem, A4, 1679 (1970)
- 49 V A Kargin, T L Sogolova and T K Shaposhnikova,
Vysokomol Soedin, 6, 1022 (1964)
- 50 I Koessler and L Soob, J Polym Sci, 4, 77 (1961)
- 51 B Ya Teitelbaum and N P Anoshina, Vysokomol Soedin, 7,
978 (1965)
- 52 B Ya Teitelbaum, T A Yagfarova, N P Anoshina and V A Naumov,
Dokl USSR Phys Chem Sectn, 150, 463 (1963)
- 53 W R Krigbaum and R J Roe, J Polym Sci, A2, 4391 (1964)
- 54 W R Krigbaum et al, Polymer, 7, 61 (1966)
- 55 A N Gent, J Polym Sci, 3, 3787 (1965)
- 56 P Koviach, Ind Eng Chem, 47, 1090 (1955)
- 57 R Parisher, Kunststoff, 50, 623 (1960)
- 58 'The Chemistry and Physics of Rubber-like Substances',
L Bateman (ed), MacLaren (publ), London (1963)
- 59 B Saville and A D Watson, Rubb Chem Tech, 40, 100 (1967)
- 60 W Scheele, Rubb Chem Tech, 34, 1306 (1961)
- 61 A G Moore, J Polym Sci, 32, 503 (1958)
- 62 A N Gent, P B Lindley and A G Thomas, J App Polym Sci,
8, 465 (1964)
- 63 G J Lake and P B Lindley, J App Polym Sci, 8, 707 (1964)
- 64 R S Rivlin and A G Thomas, J Polym Sci, 10, 291 (1953)

- 65 A G Thomas, J App Polym Sci, 3, 163 (1960)
- 66 G J Lake, P B Lindley and A G Thomas, Proc 2nd Int Conf on Fracture, Brighton, p 493 (1969)
- 67 H W Greensmith, J App Polym Sci, 7, 993 (1963)
- 68 G J Lake and P B Lindley, Rubb J, 146, (10), 24 (1964)
- 69 G J Lake and P B Lindley, Rubb J, 146, (11), 30 (1964)
- 70 G J Lake and P B Lindley, J App Polym Sci, 10, 343 (1966)
- 71 A G James, PhD Thesis, University of Aston in Birmingham, (1970)
- 72 G J Lake and A G Thomas, Proc Roy Soc, A300, 208 (1967)
- 73 G J Lake and P B Lindley, J App Polym Sci, 9, 1233 (1965)
- 74 E H Andrews, J Mech Phys Solids, 11, 231 (1963)
- 75 J A C Harwood and A R Payne, J App Polym Sci, 12, 889 (1968)
- 76 J C Halpin, Rubb Chem Tech, 38, 1007 (1965)
- 77 K W Scott, Polym Eng Sci, 7, 158 (1967)
- 78 T L Smith, J Polym Sci, 32, 99 (1958)
- 79 L Mullins, Trans Inst Rubb Ind, 35, 213 (1959)
- 80 K A Grosch, J A C Harwood and A R Payne, 'Physical Basis of Yield and Fracture', Conf Proc, Oxford, p 144 (1966)
- 81 S M Caldwell, R A Merrill, C M Sloaman and F L Yost, Ind Eng Chem, Anal Ed, 12, 19 (1940)
- 82 G J Lake and P B Lindley, 'Physical Basis of Yield and Fracture', Conf Proc, Oxford, p 176 (1966)
- 83 R W Smith and A L Black, Rubb Chem Tech, 37, 338 (1964)
- 84 A N Gent, J App Polym Sci, 23, 497 (1962)

- 85 J R Beatty, *Rubb Chem Tech*, 37, 1341 (1964)
- 86 M K Khromov et al, *Int Polym Sci Technol*, 10, T/91 (1978)
- 87 M K Khromov et al, *Kauch i Rezina*, 5, 36 (1977)
- 88 M K Khromov and K N Lazareva, *Kauch i Rezina*, 5, 32 (1979)
- 89 G J Lake, *Rubb Chem Tech*, 45, 309 (1972)
- 90 G J Lake, *Rubb Developments*, 19, (2), 60 (1966)
- 91 M Braden and A N Gent, *J App Polym Sci*, 3, 100 (1960)
- 92 A N Gent and J E McGrath, *J Polym Sci*, A3, 1473 (1965)
- 93 A N Gent and H Hirakawa, *J Polym Sci*, A2, 5, 157 (1967)
- 94 G J Lake and P B Lindley, *J App Polym Sci*, 9, 2031 (1965)
- 95 G J Lake and A G Thomas, *Proc 4th Int Rubb Conf, Brighton*,
p 525 (1967)
- 96 A Dibbo, *Trans Int Rubb Inst*, 40, 202 (1964)
- 97 G J Lake, *Rubb Chem Tech*, 43, 1230 (1970)
- 98 P B Lindley, *J Strain Anal*, 6, 279 (1971)
- 99 P B Lindley, *Rubb Developments*, 19, (4), 168 (1966)
- 100 D G Lloyd and J Payne, *Rubb News*, June, p 26 (1967)
- 101 Monsanto Technical Bulletin, O/RC-5
- 102 S B Miller, *Rubb Age*, 98, (5), 60 (1966)
- 103 E S Dizon and A E Hicks, *Rubb Chem Tech*, 47, 231 (1974)
- 104 B A Dogadkin, *Rubb Chem Tech*, 27, 883 (1954)
- 105 W L Cox and C R Parks, *Rubb Chem Tech*, 39, 785 (1966)
- 106 A Dibbo and D G Lloyd, *Proc 4th Int Rubb Conf, Brighton*,
p 83 (1967)
- 107 A J Kuzminskii and L T Lyubchanskaya, *Rubb Chem Tech*, 29,
770 (1956)

- 108 J C Amberlang in 'Vulcanisation of Elastomers', Reinhold Publ, p 126 (1964)
- 109 E B McCall, J Rubb Res Inst, Malaya, 22, 354 (1969)
- 110 G M Bristow and R F Tiller, Kautschuk Gummi, 23, 55 (1970)
- 111 J Lal, Rubb Chem Tech, 43, 664 (1970)
- 112 R M Russell, Br Polym J, 1, 53 (1969)
- 113 J I Cunneen and R M Russell, J Rubb Res Inst, Malaya, 22, 300 (1969)
- 114 W Cooper, J Polym Sci, 28, 195 (1958)
- 115 H Pinner, Int J App Radn Isotopes, 5, 121 (1959)
- 116 B A Dogadkin, Z N Tarasova and I Goldberg, Proc 4th Int Rubb Tech Conf, London, p 65 (1962)
- 117 MSc Projects, University of Aston in Birmingham (1968-1976)
- 118 M H Walters and D N Keyte, Trans Int Rubb Ind, 38, 40 (1962); Rubb Chem Tech, 38, 62 (1965)
- 119 P J Flory, 'Principles of Polymer Chemistry', Cornell Univ Press, NY (1953)
- 120 T Pazonyi and M Dimitrov, Rubb Chem Tech, 40, 1119 (1967)
- 121 R L Scott, J Chem Phys, 17, 279 (1949)
- 122 G L Slonimskii, J Polym Sci, 30, 625 (1958)
- 123 J E Callan, B Topcik and F P Ford, Rubb World, 151, (6), 60 (1965)
- 124 W M Hess, L E Scott and J E Callan, Rubb Chem Tech, 40, 371 (1967)
- 125 B D W Powell, MSc Thesis, University of Loughborough (1970)
- 126 P A Marsh, A Voet and L D Price, Rubb Chem Tech, 41, 344 (1968)

- 127 J Rehner and P Wei, *Rubb Chem Tech*, 42, 985 (1969)
- 128 S M Hirshfield, US Pat, 3,281,289 (1966)
- 129 C W Snow, US Pat, 3,280,876 (1966)
- 130 E B Koldunovich et al, *Sov Rubb Tech*, 25, (12), 15 (1966)
- 131 S V Orekhov, N D Zakharov, M A Polak and V G Epshtein,
Sov Rubb Tech, 27, (6), 14 (1968)
- 132 ICI Technical Information Sheet, PC/R108
- 133 A Springer, *RAPRA Translation*, p 1170 (1964)
- 134 L M Glanville and P W Milner, *Rubb Plast Age*, 48, 1059
(1957)
- 135 J F Suetlik, E F Ross and D T Norman, Division Rubb Chem,
Amer Chem Soc, Chicago, Sept 2-4 (1964)
- 136 C A McCall and H K J De Decker, Fr Pat, 1,422,275 (1966)
- 137 Chemische Werke Huls AG, Fr Pat, 1,449,094 (1966)
- 138 A A Kortov, U N Reikh and N F Kovalev, *Sov Rubb Tech*,
25, (8), 5 (1966)
- 139 I A Levitin, Y G Kobalev and T A Kadyrov, *Sov Rubb Tech*,
26, (12), 18 (1967)
- 140 L Lcheal and N Odam, *Rev Gen Caout Plast*, 48, 509 (1971)
- 141 A H Speranzini and S J Drost, *Rubb Chem Tech*, 43, 48
(1970)
- 142 J M Willis and R L Denecour, *Rubb Age*, 100, (10), 61
(1968)
- 143 Z T Osserfort and W E Bergstrom, *Rubb Age*, 101, (9), 4
(1969)
- 144 L Spenadel and R L Sutphin, *Rubb Age*, 102, (12), 55 (1970)

- 145 H J Leib, S W Caywood and L H Knabeschuh, *Rubb World*,
165, (3), 52 (1971)
- 146 M S Sutton, *Rubb World*, 149, (5), 62 (1964)
- 147 K Satake, T Wada, T Sone and M Hamada, *J Inst Rubb Ind*,
4, 102 (1970)
- 148 D I Livingstone and R L Rongone, *Proc Int Rubb Tech Conf*,
Brighton, p 337 (1967)
- 149 E H Andrews, *Rubb Chem Tech*, 40, 635 (1967)
- 150 J B Gardiner, *Rubb Chem Tech*, 41, 1312 (1968)
- 151 J B Gardiner, *Rubb Chem Tech*, 42, 1058 (1969)
- 152 J B Gardiner, *Rubb Chem Tech*, 43, 370 (1970)
- 153 K Fujimoto and N Yoshimura, *Rubb Chem Tech*, 41, 669 (1968)
- 154 P J Corish, *Rubb Chem Tech*, 40, 324 (1967)
- 155 K Fujimoto and N Yoshimura, *Rubb Chem Tech*, 42, 1009 (1969)
- 156 K Hashimoto et al, *J Sol Rubb Ind, Japan*, 43, 652 (1970)
- 157 R L Zapp, *Rubb Chem Tech*, 46, 251 (1973)
- 158 M Z Rakhman, *Sov Rubb Tech*, 25, (9), 10 (1966)
- 159 D J Angier and W F Watson, *J Polym Sci*, 18, 129 (1955)
- 160 D J Angier and W F Watson, *Trans Inst Rubb Ind*, 33, 22
(1957)
- 161 M Pike and W F Watson, *J Polym Sci*, 9, 244 (1952)
- 162 G Scott, 'Atmospheric Oxidation and Antioxidants',
Elsevier Publ (1965)
- 163 G A Russell, *J Am Chem Soc*, 78, 1035 (1956)
- 164 G A Russell, *J Am Chem Soc*, 78, 1041 (1956)
- 165 R J Ceresa, *Rubb Chem Tech*, 33, 923 (1960)
- 166 G L Slonimskii and E V Reztsova, *Rubb Chem Tech*, 33, 457 (1960)

- 167 W J Burlant and A S Hoffman, 'Block and Graft Copolymers', Reinhold Publ, NY (1960)
- 168 D C Allport in 'Block Copolymers', App Sci Publ, London (1973)
- 169 H Staudinger, Hely Chim Acta, 8, 41 (1925)
- 170 K H Meyer, Von Susich and E Valko, Kolloidzeitschrift, 59, 208 (1932)
- 171 E Guth and T James, J Chem Phys, 11, 455 (1943)
- 172 F T Wall, J Chem Phys, 10, 485 (1942)
- 173 P J Flory and J Rehner, J Chem Phys, 11, 512 (1943)
- 174 A Ciferri, J Polym Sci, 54, 149 (1961)
- 175 L R G Treloar, 'The Physics of Rubber Elasticity', 2nd Edn, Clarendon Press, Oxford (1958)
- 176 E Guth, H M James and H Mark, 'Advances in Colloid Science', Interscience Publ, NY (1946)
- 177 G M Bartenev, J Tech Phys USSR, 20, 461 (1950)
- 178 M Morton, V R Allen and R D Gates, US Dept Com, Office Tech Serv, PB Rept 150491 (1959), Chem Abs, 56, 10345 (1962)
- 179 A V Tobolsky, D W Carlsson and N Indictor, J Polym Sci, 54, 175 (1961)
- 180 R S Rivlin and D W Saunders, Phil Trans Roy Soc, A243, 251 (1951)
- 181 M Mooney, J App Phys, 11, 582 (1940)
- 182 A N Gent and A G Thomas, J Polym Sci, 28, 625 (1958)
- 183 L Mullins, J Polym Sci, 19, 225 (1956)
- 184 L Mullins, J App Polym Sci, 2, 1 (1959)

- 185 L Mullins, S Grumbell and R Rivlin, *Trans Faraday Soc*,
49, 1495 (1953)
- 186 P J Flory, *Ind Eng Chem*, 38, 417 (1946)
- 187 L A Wood, *J Wash Acad Soc*, 47, 281 (1957)
- 188 L R G Treloar, *Trans Faraday Soc*, 50, 881 (1954)
- 189 W Kuhn and F Grun, *Kolloidzeitschrift*, 101, 248 (1942)
- 190 W Kuhn and H Kuhn, *Helv Chim Acta*, 29, 1095 (1946)
- 191 A Isihara, N Hashitsume and M Tatibana, *J Chem Phys*, 18,
108 (1951)
- 192 M C Wang and E Guth, *J Chem Phys*, 20, 1144 (1952)
- 193 G Gent, *Trans Faraday Soc*, 42, 585 (1946)
- 194 E Kay, B B Moore and D K Thomas, *RAF Establishment Rept*,
66388 (1966)
- 195 E Kay, B B Moore and D K Thomas, *Polymer*, 10, 55 (1969)
- 196 E F Cluff, E K Gladding and R Pariser, *J Polym Sci*, 45,
341 (1960)
- 197 A W Khadim and D A Smith, *Polymer*, 10, 711 (1969)
- 198 R E Melley and J E Stuckey, *J App Polym Sci*, 14, 2327
(1970)
- 199 P J Flory and J Rehner, *J Chem Phys*, 11, 521 (1943)
- 200 P J Flory, *J Chem Phys*, 18, 108 (1950)
- 201 L D Loan, *J App Polym Sci*, 7, 2259 (1963)
- 202 G M Bristow and W F Watson, *Trans Faraday Soc*, 54, 1567
(1958)
- 203 G Crespi and M Bruzzone, *Chim Ind (Milan)*, 41, 741 (1959)
- 204 W J Bobear, *Ind Eng Chem, Prod Res Dev*, 3, 277 (1964)
- 205 C G Moore and B R Trego, *J App Polym Sci*, 8, 1957 (1964)

- 206 G Buttenuth, *Rubb Age*, 94, (5), 737 (1964); *Rubb Chem Tech*, 37, 326 (1964)
- 207 E Guth and O Gold, *Phys Rev*, 53, 322 (1938)
- 208 K H Meyer and W Møhenemser, *Helv Chim Acta*, 18, 1061 (1935); *Rubb Chem Tech*, 9, 201 (1936)
- 209 J R Brown and E A Hauser, *Ind Eng Chem*, 30, 1291 (1938)
- 210 M L Selker and A R Kemp, *Ind Eng Chem*, 36, 16 (1944)
- 211 M L Selker and A R Kemp, *Ind Eng Chem*, 36, 20 (1944)
- 212 M L Selker, *Ind Eng Chem*, 40, 1467 (1948)
- 213 T P Hilditch and S Smiles, *J Chem Soc*, 91, 1394 (1907)
- 214 W Steinkopf and S Müller, *Ber*, 56B, 1926 (1923)
- 215 H Klinger and A Maason, *Ann*, 252, 241 (1898)
- 216 A Brjuchonenko, *Ber*, 31, 3176 (1899)
- 217 W Steinkopf and R Bessaritch, *J Prakt Chem*, 2, 109, 230 (1925)
- 218 P G Stevens, *J Am Chem Soc*, 67, 407 (1945)
- 219 R F Naylor, *J Chem Soc*, p 1106 (1947)
- 220 R F Naylor, *J Chem Soc*, p 2749 (1949)
- 221 B R Trego, PhD Thesis, University of London (1965)
- 222 F E Ray and I Levine, *J Org Chem*, 2, 267 (1937)
- 223 C G Moore, B Saville and B R Trego, Unpublished Paper
- 224 M B Evans and B Saville, *Proc Chem Soc*, p 18 (1962)
- 225 D S Campbell and B Saville, *Proc Int Rubb Conf, Brighton*, 1 (1967)
- 226 D S Campbell, *J App Polym Sci*, 13, 1201 (1969)
- 227 G Gorin, G Doughty and R Gideon, *J Chem Soc*, B, 729 (1967)
- 228 De Mattia, *Rubb Age*, 25, 218 (1929)

- 229 ASTM Designation, D813-57T
- 230 A Ross, Vanderbilt Rubber Handbook, p 438 (1948)
- 231 ASTM Designation, D1052-55
- 232 D G Lloyd, 'Fatigue Failure and its Reduction in Natural Rubber', Monsanto Technical Bulletin, LA24/1
- 233 Monsanto Fatigue to Failure Tester Handbook
- 234 F Zernike, Physica, 1, 689 (1934)
- 235 F Zernike, Z Techn Physik, 16, 454 (1935)
- 236 F Zernike, Physica, 9, 686 (1942)
- 237 F Zernike, Physica, 9, 974 (1942)
- 238 P J Corish and B D W Powell, Rubb Chem Tech, 47, 481 (1974)
- 239 J E Callan, W M Hess and C E Scott, Rubb Chem Tech, 44, 814 (1971)
- 240 A H Bennett, 'Phase Microscopy', John Wiley Publ, NY (1951)
- 241 R Barer, 'Phase Contrast, Interference Contrast and Polarising Microscopy', R C Mellors (ed), 'Analytical Cytology', McGraw-Hill Publ, NY (1955)
- 242 Decker, R W Wise and Gueray, Rubb Chem Tech, 36, 451 (1963)
- 243 C G Moore, J Polym Sci, 32, 503 (1958)
- 244 C G Moore and W F Watson, J Polym Sci, 19, 237 (1956)
- 245 A Y Coran, Rubb Chem Tech, 37, 668-689 (1964)
- 246 A Y Coran, Rubb Chem Tech, 38, 1 (1965)
- 247 J Haslam, H A Willis and D C M Squirrel, 'Identification and Analysis of Plastics', Butterworth Publ, London (1972)
- 248 A I Vogel, 'Quantitative Inorganic Analysis', Longmans Publ, London (1961)